Final Report of Subsidence Investigations at the Galatia Site, Saline County, Illinois

Danny J. Van Roosendaal
Brenda B. Mehnert
Nelson Kawamura
Philip J. DeMaris

Illinois Mine Subsidence Research Program

IMSRP XI 1997

Cooperating agencies

ILLINOIS STATE GEOLOGICAL SURVEY
Department of Natural Resources

BUREAU OF MINES
United States Department of the Interior

Final Report of Subsidence Investigations at the Galatia Site, Saline County, Illinois

Danny J. Van Roosendaal
Brenda B. Mehnert
Nelson Kawamura
Philip J. DeMaris

Illinois Mine Subsidence Research Program

IMSRP XI 1997

ILLINOIS STATE GEOLOGICAL SURVEY
William W. Shilts, Chief
Natural Resources Building
615 East Peabody Drive
Champaign, IL 61820-6964

The **Illinois Mine Subsidence Research Program** (IMSRP) was established in 1985 to investigate methods and develop guidelines for underground mining operations that aim to maximize coal extraction yet preserve the productivity of prime farmland. The research program was initiated by the Illinois Coal Association and the Illinois Farm Bureau.

The Illinois State Geological Survey, a division of the Illinois Department of Natural Resources, directed the IMSRP. Participating research institutions included Southern Illinois University at Carbondale, the University of Illinois at Urbana-Champaign, Northern Illinois University, and the Illinois State Geological Survey. A five-year Memorandum of Agreement, signed by the State of Illinois and the Bureau of Mines, U.S. Department of the Interior, ensured collaboration, cooperation, and financial support through 1991. Major funding was also provided by the Illinois Coal Development Board.

This publication is one in a series printed and distributed by the Illinois State Geological Survey as a service to the IMSRP.

Appendixes to this volume are available upon request as Open File Series 1997-9

Printed with soybean ink on recycled paper
Printed by authority of the State of Illinois/1997/500

CONTENTS

FIGURES

TABLES

ABSTRACT

The purpose of this investigation was to study the amount, extent, and location of overburden fracturing leading to surface expression of coal-mine subsidence and to examine the effects of bedrock deformation on local hydrogeology. Two longwall panels in Saline County, Illinois, were characterized before and after subsidence by using core drilling, geotechnical instrumentation, and in situ testing. Geotechnical instruments, including surface monuments, piezometers, a pump well, two multiple-position borehole extensometers, and a time-domain reflectometry cable, were used to monitor overburden and ground-surface response.

The ratio of subsidence to mined-out height at the centerline of panel 1 was 70.5% when the mine face advanced to a distance of 500 feet past the monitoring station; 18 months later, this ratio increased slightly to 71.8%. Over panel 2, a ratio of 66.3% was determined when the face had reached a distance of about 1,900 feet past; additional time-dependent subsidence over the following 6 months increased this ratio to 68.1%. Maximum dynamic horizontal tensile strains of about 0.018 foot/foot were generated at the ground surface at a distance of 50 feet behind the panel face. Net increases in bedrock hydraulic conductivity due to mining of multiple panels are estimated to be on the order of 300% to 400%, but they may be somewhat higher.

INTRODUCTION

Scope and Purpose of Work

High-extraction mining techniques are being used more frequently in Illinois to maximize coal mining productivity and to decrease the cost of the delivered product. Underground coal extraction by these techniques causes rapid collapse of the overburden and subsidence of the ground surface. Farmland and water resources may be affected by this surface subsidence. The Illinois Mine Subsidence Research Program (IMSRP) was created to address these concerns. This study is one of several projects performed under the IMSRP with funding from the U.S. Bureau of Mines (USBM), Illinois Department of Natural Resources Coal Development Board, and the Office of Surface Mining Reclamation and Enforcement.

The purpose of this investigation was to study the amount, extent, and location of overburden fracturing leading to the surface expression of coal-mine subsidence and to examine the effects of the bedrock deformation on the local hydrogeology. Two longwall panels in Saline County, Illinois, were characterized before and after subsidence by using core drilling, geotechnical instrumentation, and in situ testing. Geotechnical instruments, including surface monuments, drift and bedrock piezometers, a pump well, two multiple-position borehole extensometers (MPBX), and one time-domain reflectometry (TDR) cable, were used to monitor overburden and ground-surface response. A grid of monuments was established on the edge of one panel to monitor deformation in the predicted tensile zone. Four inclinometers were installed at the corners of the grid, along with tiltplates at each corner. The Illinois State Geological Survey (ISGS) monitored the instruments before, during, and after subsidence. Northern Illinois University (NIU) assisted the ISGS in characterizing the hydrologic changes in the overburden. This report summarizes the geotechnical monitoring program and the results from monitoring from November 1989 through July 1993.

Background and Previous Studies

Natural resources affected by mine subsidence Coal and farmland are both important to the state's economy. Illinois is the second largest producer of agricultural commodities and the fifth largest producer of coal in the United States. Problems sometimes exist in ensuring that both farmland and coal resources are used to their maximum potential. Depending on the original topography of the land, subsidence-induced ground movements can modify surface drainage, possibly affecting crop yields of gently rolling farmland. Mine operators need to understand the impact of underground mining on near-surface hydrology and surface-drainage patterns.

Method of mining The modern longwall mining system has been used in Illinois since 1976 (Janes 1983). Longwall mining produces immediate planned subsidence over each longwall panel. The longwall panels are laid out using traditional room-and-pillar methods to form entryways. When panel layout is complete, specialized longwall equipment is moved in, set up, and mining of the defined block of coal begins (fig. 1). Gradually advancing under movable hydraulic shields, the longwall shearer removes all of the coal across a wide working face. The room-and-pillar entryways, which are used for ventilation and transportation, are left in place between the panels. As the mine face advances, the overburden behind the shields is left unsupported and

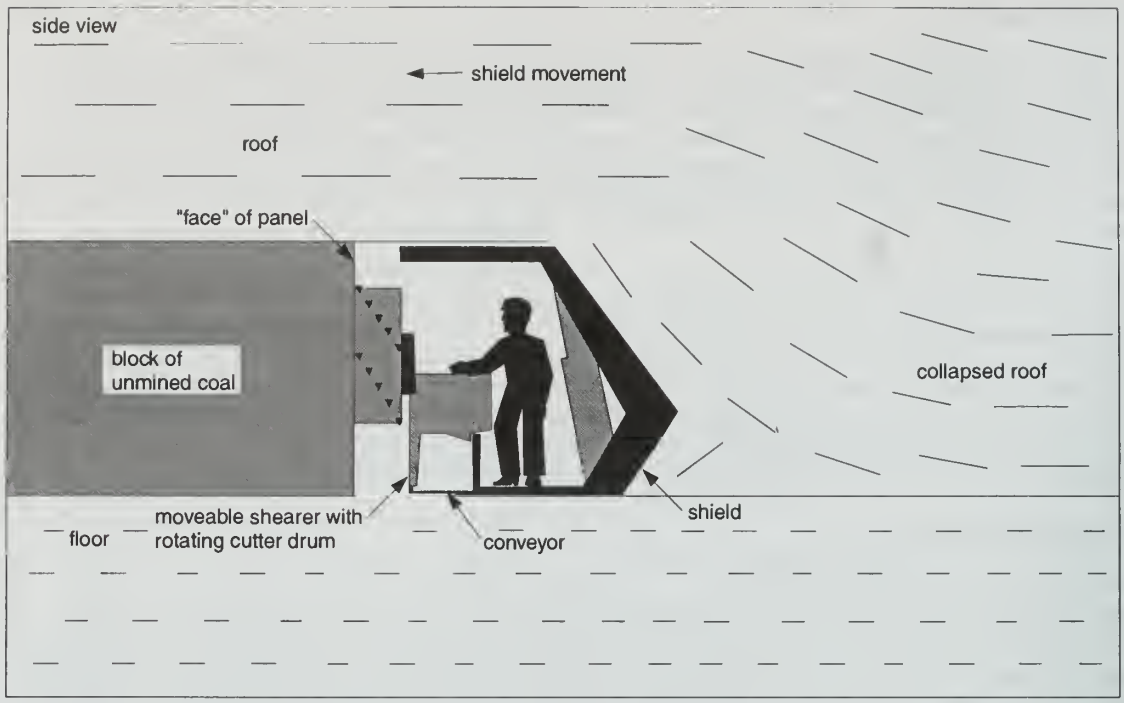

Figure 1 Diagram of the longwall mining technique.

collapses into the void. Vertical and horizontal movements are propagated by gravity up through the bedrock and surficial materials; thus, surface subsidence quickly follows this collapse. A general model for this process is shown in figure 2.

Overburden fracturing Coe and Stowe (1984), Ming-Gao (1982), and Whitworth (1982) investigated the location and amount of fracturing in subsided bedrock over longwall operations in Ohio (U.S.A.), Jiangsu Province (China), and South Staffordshire Coalfield (United Kingdom), respectively. Before the IMSRP began, Conroy (1980) conducted the only study concerning fracturing above a high-extraction mining operation in Illinois. He grouted two TDR cables into boreholes that extended from the ground surface into a 625-foot-deep longwall mine and found that the bedrock movements severed one of the cables to within 100 to 150 feet of the surface.

More recently, Bauer et al. (1991) investigated fracturing using a TDR cable and an MPBX over a high-extraction mine in Williamson County, Illinois. They found that differential movements were associated with interfaces between materials of contrasting strength, such as bedrock and drift, or near the boundaries of a fragipan within the soil where the TDR cable was sheared.

Hydrogeologic effects Fracturing of the overburden may affect water-bearing formations by creating voids and increasing secondary permeability, as found in the Appalachian Plateau of Pennsylvania by Booth (1986). In a study in England, Garritty (1982) suggested that fracturing of the bedrock up to the surface may hydrologically connect an aquifer or surface water body with the mine. In Illinois, Cartwright and Hunt (1978) observed localized, open, vertical joints due to faulting in a mine roof; they speculated that these joints could provide a direct passage for water from higher strata in the immediate roof. These fractures were discontinuous, however, and did not provide any hydrologic connection to the surface. In another study in Illinois, Nieto (1979) found no leakage into mines with faults located 600 feet under the Rend Lake reservoir. Subsequent studies in Illinois, including this one, also have shown that discontinuous, localized fracturing caused by strains in the bedrock occurs without any hydrologic connections to the surface.

Before this study was initiated, the hydrogeological effects of subsidence on aquifers had been investigated by several researchers, including Coe and Stowe (1984), Duigon and Smigaj (1985), Garritty (1982), Owili-Eger (1983), Pennington et al. (1984), and Sloan and Warner (1984). In studies of the Appalachian Plateau, Coe and Stowe (1984), Booth (1986), and Pennington et al. (1984) observed water level drops in wells that were undermined by the longwall mining method.

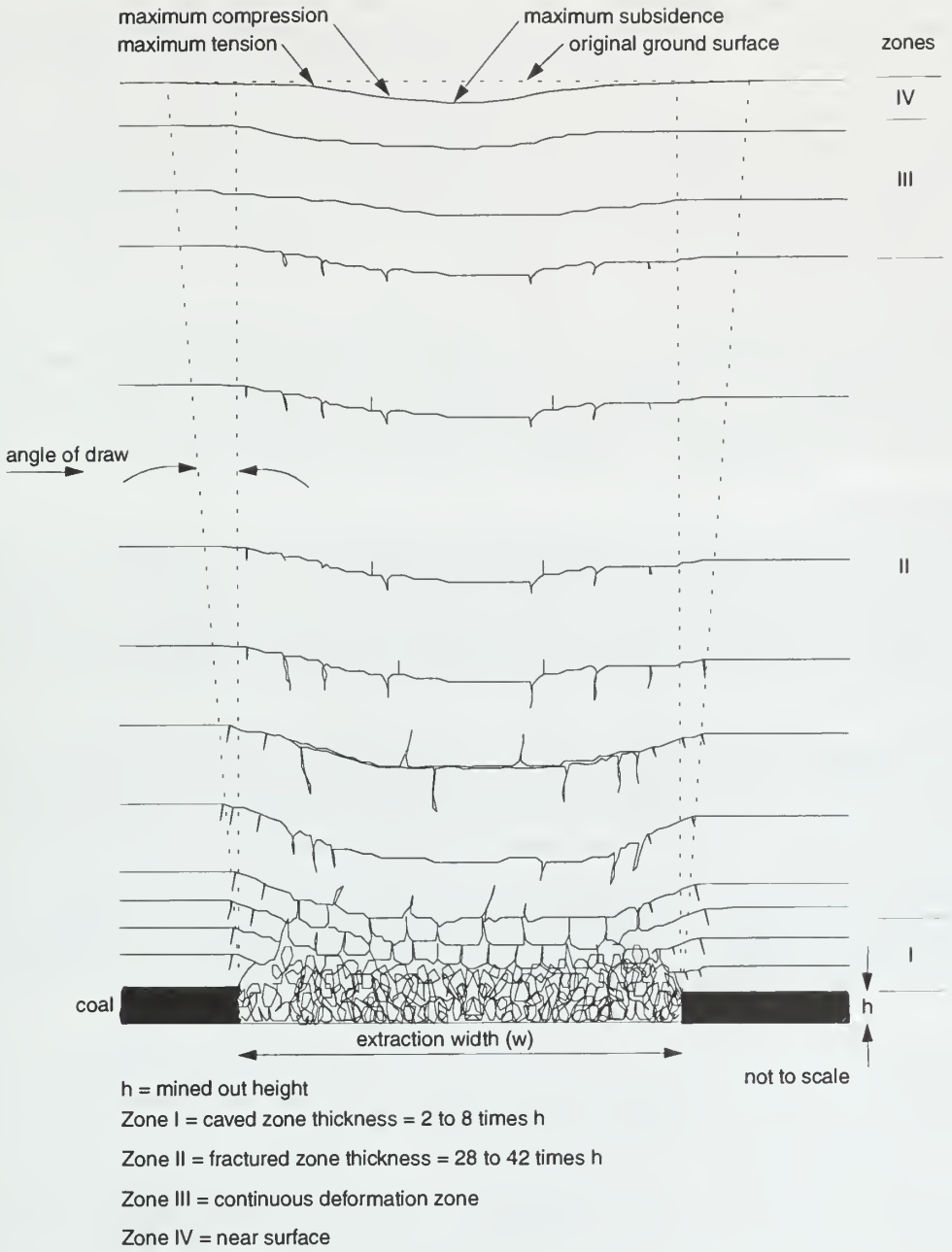

Figure 2 Strata deformation associated with longwall mining. Modified from Peng and Chiang (1984) and New South Wales Coal Association (1989).

Water levels partially or completely recovered, however, several months after being undermined by the longwall method in the Appalachian Plateau (Owili-Eger 1983). Subsequent studies in Illinois by Pauvlik and Esling (1987) have also observed a similar response of wells to mining.

Surface subsidence characteristics The longwall method of mining produces planned subsidence. As the longwall face advances, a subsidence trough develops at the surface; it is both longer and wider than the area of total coal extraction at the mine level. The face advance at mine level produces a dynamic traveling wave at the surface directly above and slightly behind the face position. The subsidence trough is typically characterized by two types of profiles: static and dynamic.

Static profiles are generally measured transverse to the panel to show the final shape of the subsidence trough. In general, a "maximum possible subsidence" cannot exceed the thickness of the

mined-out height. For geological conditions prevailing in Illinois, the maximum subsidence is approximately 60% to 70% of the mined-out height. Three conditions of the subsidence trough's final shape were defined by a width-to-depth ratio (W/D) (Whittaker and Reddish 1989) for the United Kingdom coal field. Subcritical extraction would correspond to a W/D <1.4; critical extraction would correspond to a W/D = 1.4; and super-critical extraction would correspond to a subsidence W/D >1.4. These conditions are dependent on the overburden's strength characteristics and its bridging ability; therefore, these ratios may not hold true for the Illinois Basin or the Appalachian area. The vertical movements are also accompanied by horizontal displacements that act toward the area of maximum subsidence. The magnitude of the horizontal displacements is a function of the gradient of the subsidence profile (Whittaker and Reddish 1989, Tandanand and Triplett 1987).

Dynamic profiles are documented as surface subsidence occurs. A longitudinal survey line over the length of the panel is used to document the dynamic traveling subsidence wave that develops on the ground surface behind the advancing face. At the sides of the trough, the progression from dynamic to static subsidence occurs rapidly and produces a complex pattern of surface cracks (Van Roosendaal et al. 1990, 1991). Both types of profiles are presented in this report.

Physical Setting

Site selection Several factors were considered during the site selection process. First, a longwall mine had to be available for study within a reasonable time frame. It was essential that instruments be installed well before the site was undermined so that site characterization and baseline data collection could take place. Next, the full cooperation of the mine operators and surface owners was required. Formal agreements with these parties were negotiated prior to initiation of work. Finally, the site had to be accessible and well suited for both instrument installation and long-term monitoring.

The above criteria were used to select two longwall panels located in northwestern Saline County, Illinois (fig. 3). The panels are located about 7 miles north-northwest of Harrisburg in Sections 16, 17, and 18 of T8S, R6E. The study area lies in the NW quarter of Section 17. The instrumented study site is 1/4 mile south of Illinois State Route 34 and 2 miles east of the town of Galatia.

Physiography The study site is located in the Mount Vernon Hill Country physiographic division of Illinois. The geomorphology of the area is characteristic of a maturely dissected, sandstone-shale plain of low relief under a thin mantle of Illinoian drift. Restricted uplands and broad alluviated valleys occur along the larger streams (Leighton et al. 1948).

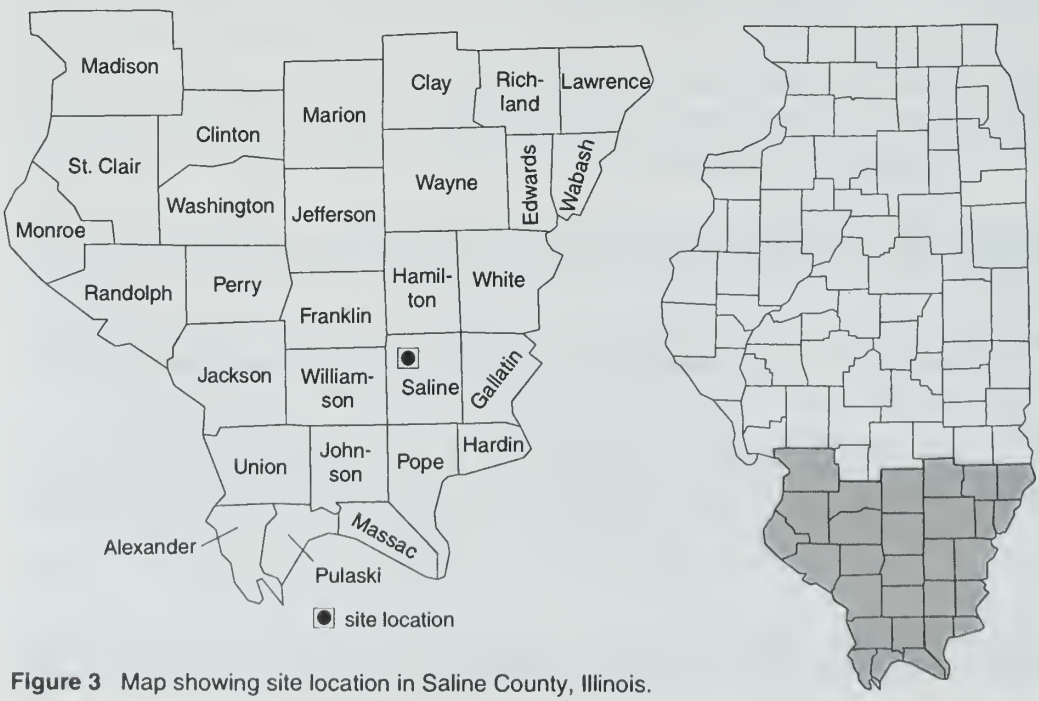

Figure 3 Map showing site location in Saline County, Illinois.

Surface topography above the panels is gently rolling with elevations between 390 to 440 feet above mean sea level. The topography in the area is primarily bedrock-controlled (Horberg 1950). Bedrock features are modified, however, by glacial action and somewhat subdued by a mantle of deeply eroded drift that covers the region (Leighton et al. 1948).

Dendritic drainage is predominantly bedrock-controlled in the vicinity of the panel site (MacClintock 1929). The panels are located in the drainage basin of the Saline River and are adjacent to the Harrisburg Reservoir. Any surface water over the panels generally drains south into the Middle Fork of the Saline River.

Surficial geology The Bluford and Wynoose silt loams are the predominant modern soils developed over the study area (Seils et al. 1992), which is a somewhat poorly drained upland sloping gently to the south. Slopes range from 1% to 2% over most of the area and reach 4% in the shallow drainageways. On these low slopes, erosion of the original 2 to 4 feet of Peoria Loess in which the modern soil developed has been minimal. The Bluford and Wynoose silt loam soils were originally forested and are generally well suited to corn, soybeans, small grains, hay, and pasture (Soil Conservation Service 1978, 1988). A weakly expressed fragipan in the B horizon inhibits water and root penetration and may become brittle in the dry season.

In the study area, there is as much as 80 feet of drift over bedrock below the modern soil, and even on the upland areas there seems to be at least 20 feet of drift. Most of this material appears to be Illinoian till (Frye et al. 1972) derived from Pennsylvanian bedrock, capped by the Sangamon paleosol, and overlain by several feet of Peoria loess. The till is poorly sorted throughout but generally has two sections: a clay-rich upper section that is locally silty with thin pebbly or sandy intervals; and a lower portion with more sand and silt than above, often containing wood fragments and weathered pieces of bedrock. A proposed boundary of glacial Lake Saline is located a short distance to the south (Frye et al. 1972), but most of the study site is well above the proposed maximum lake level, and no lacustrine sediments were reported during drilling. It appears that Illinoian deposits blanketed the original bedrock topography before the development of Lake Saline (A.M. Curtiss, Northern Illinois University, personal communication 1994).

Bedrock stratigraphy and structure Only the Herrin and Springfield Coals are considered suitable for underground mining in this township. The study mine operated in both the Springfield seam at a depth of about 570 feet and the Herrin seam at a depth of about 440 feet. The Springfield Coal was mined previously using the room-and-pillar method. This operation was subjacent and near the development of the longwall panels in the Herrin Coal. All bedrock above the mined coal seams is of Pennsylvanian age.

The Herrin Coal is 5 to 7 feet thick in much of the mine and may have Energy Shale, Anna Shale, Brereton Limestone or, rarely, Anvil Rock Sandstone as immediate roof. The immediate roof sequence is 4 or more feet of Brereton Limestone separated from the Herrin Coal by several feet of black Anna Shale. Figure 4 shows a representative roof sequence above the mine.

In this area, the bedrock above the Herrin Coal is dominated by thick shale intervals with a few thin interspersed beds of coal, impure limestone, and siltstone. The only possible bedrock aquifers are the sandstones at 180 and 280 feet deep. The lower sandstone, which may be the Gimlet Sandstone, is generally thin and of less interest as an aquifer. The upper sandstone is the Trivoli, which is very persistent, ranges from 2 to 55 feet thick over the south side of the mine, and occurs as both a sheet as much as 35 feet thick and a channel facies from 35 to 55 feet thick (A.M. Curtiss, NIU, pers. comm. 1994). The Trivoli Sandstone is present in the study area only as the sheet facies (fig. 5), and it is both laterally continuous and of variable thickness (A.M. Curtiss, NIU, pers. comm. 1994). The Trivoli Sandstone is a local water source, and several piezometers were placed within this unit for monitoring.

Directly below the study area, the Herrin Coal and overlying strata are relatively undeformed and level; but to the south, the strata rise 90 feet in elevation over 4,000 feet horizontally (A.M. Curtiss, NIU, pers. comm. 1994). This change suggests that an anticline or fault might be present to the south, perhaps related to the Cottage Grove Fault System. The study site is 4 miles north of the master fault of the Cottage Grove Fault System, and subsidiary faults and folds have been seen at this distance from the master fault (Nelson and Krausse 1981).

Hydrogeology Groundwater resources are limited and are primarily used for domestic and household needs. Surface water reservoirs, such as Harrisburg Reservoir and smaller impoundments,

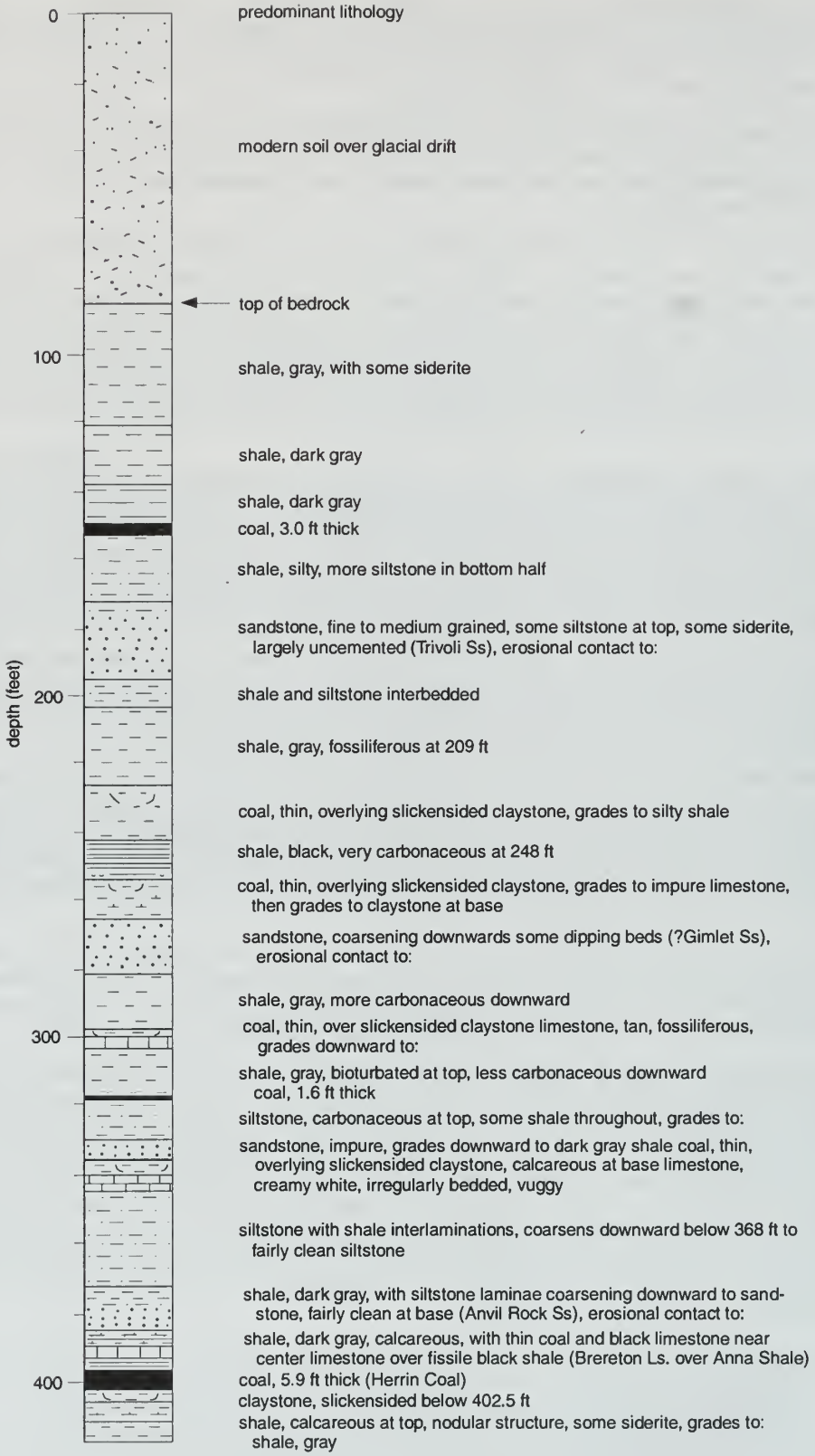

Figure 4 Bedrock lithology above the Herrin Coal at panel 1. Data are from the TDR drill hole and are corrected for tilt.

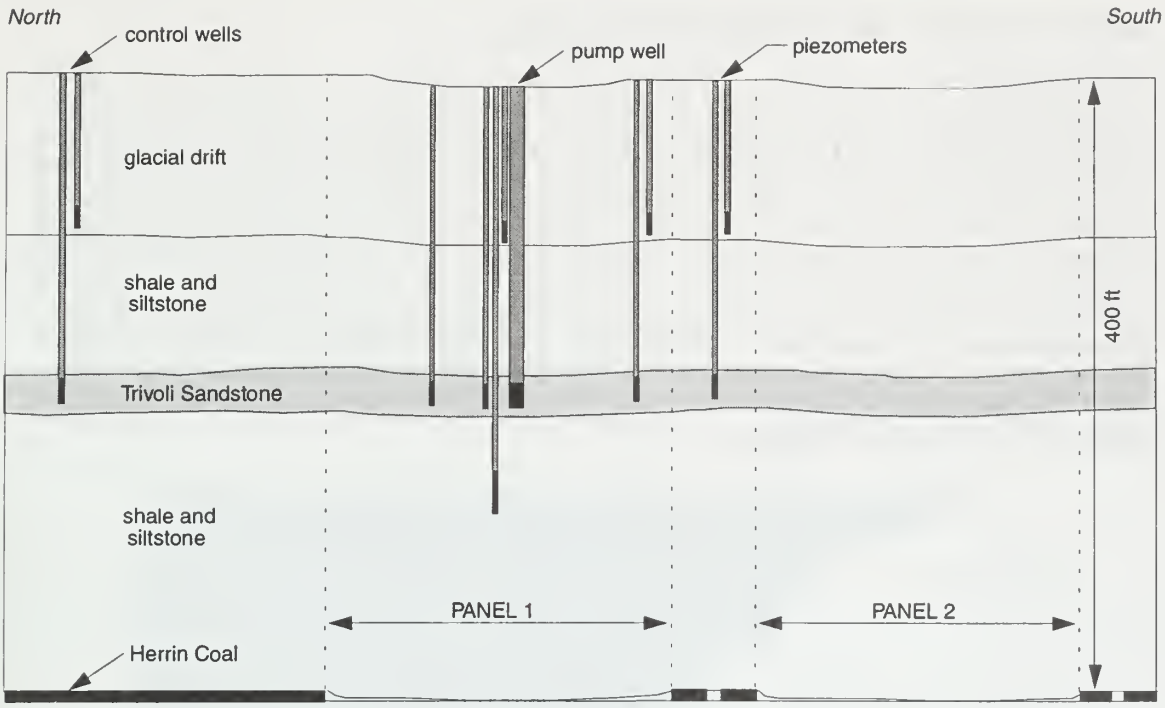

Figure 5 North–south diagrammatic cross section through the study area.

supply water to the larger communities. Water for livestock, minor irrigation, and other farming purposes is usually obtained from small ponds.

Groundwater is pumped from large-diameter (typically 3–6 ft) dug wells that provide water for domestic purposes. These wells are 15 to 35 feet deep, ending above or near the top of bedrock. These wells access the thin sand and gravel lenses in the glacial drift overlying the bedrock surface. Most domestic wells in the area have capacities of less than 5 gallons per minute (Illinois State Water Survey 1957). Smaller diameter modern wells also obtain groundwater from the glacial drift, but yields are generally low.

Bedrock aquifers of the Pennsylvanian Series in the study area are limited primarily to sandstone units; some fractured limestone aquifers, however, were also reported (Pryor 1956). A limited number of wells were driven to bedrock aquifers near the study area; most access the Trivoli Sandstone, and only a few reach the deeper Gimlet Sandstone. In the study area, the Trivoli Sandstone is about 170 to 200 feet deep, consistently present, and typically 15 to 25 feet thick. The less persistent Gimlet Sandstone is not consistently seen on logs, but it is about 12 feet thick and 280 feet deep over panel 1.

Study area mining activity The mine has been using the modern longwall system since 1987. The study area consisted of segments of longwall panels 1 and 2, their adjacent entries, and the ground surface above them. Both panels extend approximately 1 mile from east to west, and both were mined from east to west. Panel 1 had a total unsupported panel width of 668 feet, resulting in a panel width versus mine depth (W/D) ratio of 1.67 (fig. 6). Panel 2 had a total unsupported panel width of 618 feet, resulting in a W/D ratio of 1.62.

Longwall mining of panel 1 began on May 3, 1989. The north half of the transverse monument line and associated piezometers were undermined December 15, 1989, and the south end and associated piezometers were undermined December 18, 1989. Mining of the first panel was completed on March 18, 1990. Longwall mining of panel 2 began in April 1990. The transverse monument line was undermined September 2, 1990, and the mining of the second panel was completed on November 27, 1990. The south end of the extended transverse line was undermined by the third panel on April 21, 1991.

GEOTECHNICAL MONITORING PROGRAM

Introduction

The instrumentation for this study was selected to measure the geotechnical and hydrological effects of subsidence on the overburden. The ISGS proposed an instrumentation plan that was reviewed and accepted by the USBM Twin Cities Research Center and the mine company. The ISGS was responsible for subcontracting the drilling and installation of instruments. The drilling contract was awarded to Raimonde Drilling, Inc. (RDI) of Chicago, Illinois. RDI was responsible for installation of four drift piezometers, six bedrock piezometers, one pump-test well, one TDR cable, and two MPBX assemblies. One angled, cored borehole was geotechnically and geophysically logged and used for the installation of a TDR cable. ISGS personnel assisted RDI in the installation of the TDR cable and the MPBX assemblies. Initial drilling and installation was done between mid-July 1989 and October 1989. ISGS staff installed about 115 survey monuments, seven tilt plates, and four inclinometer casings; they also installed two bedrock piezometers in wells drilled by the coal company.

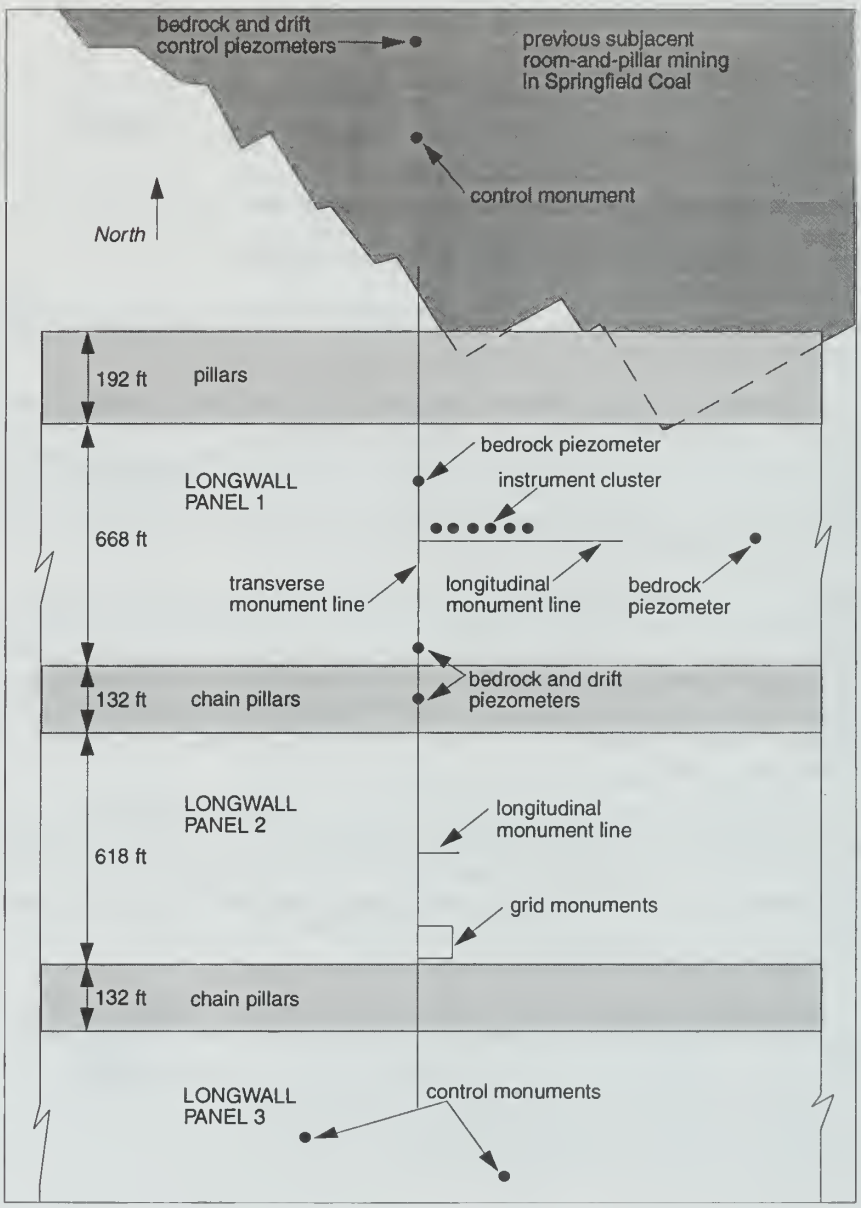

Figure 6 Instrumentation and monument locations for the study area.

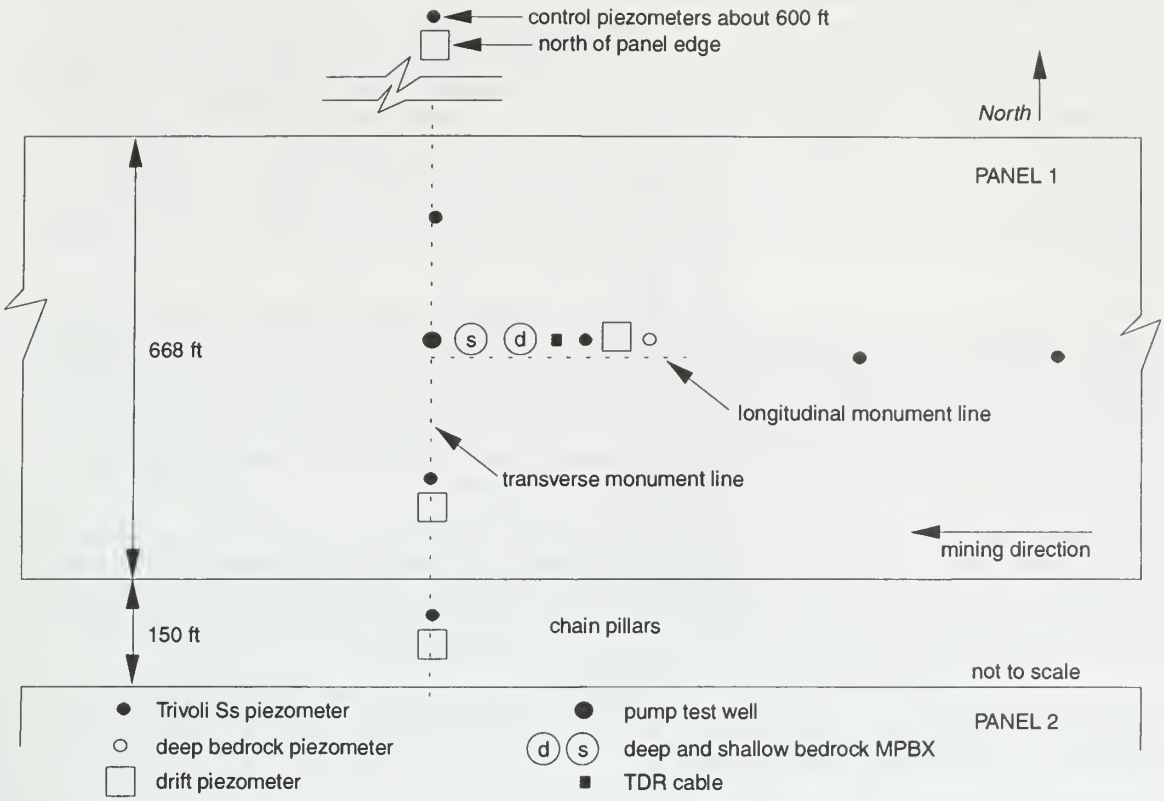

Figure 7 Instrumentation plan over longwall panel 1.

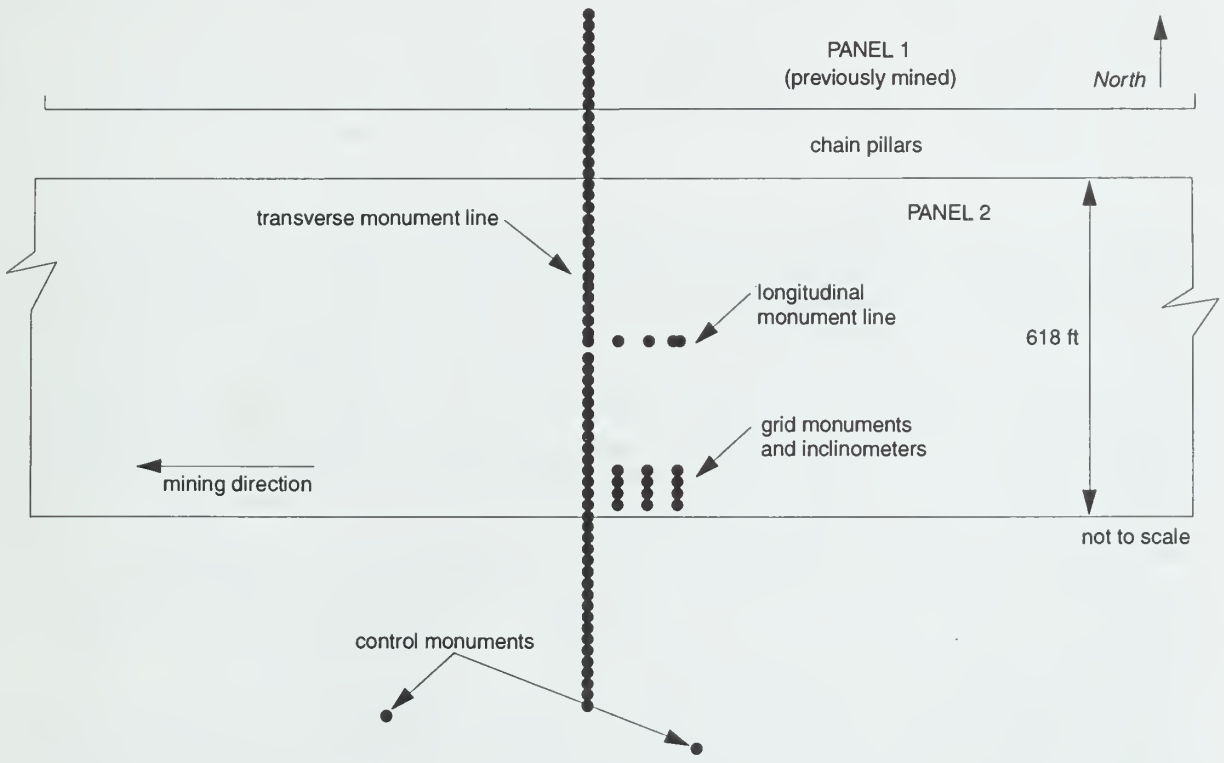

Figure 8 Instrumentation plan over longwall panel 2.

Instrument layout Mine coordinates were initially used to stake out the panel 1 centerline on the surface. The instrumentation layout was designed to measure the different responses of the overburden to mining of the panel. The instruments were placed over the chain pillars, the edge, and the centerline of the panel. The instrumentation plan called for one TDR cable at the centerline of the panel; two MPBX assemblies at the center of the panel; bedrock and drift piezometers over the chain pillars, as well as the edge, centerline, and north of the panel; and one pump well on the centerline. The monitoring plans also called for transverse and longitudinal monument lines, as well as control monuments north of the panel. Postsubsidence drilling was also done to reestablish the pump well, add a bedrock piezometer, and characterize fracturing and rock mass changes.

Panel 2 instrumentation was located directly south of the panel 1 instrumentation (figs. 7, 8). The transverse monument line was extended south to the centerline of panel 3, and a shorter longitudinal monument line was developed on the centerline of panel 2. Control monuments were established farther south, away from the influence of mining. In addition, a grid of 16 monuments was established parallel to the transverse line near the south edge of panel 2 to monitor deformation in the predicted tensile zone. Four inclinometer casings, each 20 feet long, were installed at the corners of the grid; tiltplates were also installed at each corner.

Mine operations In the vicinity of the transverse line and instrument cluster, the average advance of the longwall face of panel 1 was about 35 feet per working day. The average longwall face advance in the vicinity of the transverse line for panel 2 was about 45 feet per working day. Mining heights for both panels generally ranged from 5.5 to 7.5 feet; typical mining height was about 6.5 feet, which generally included about 0.5 foot of roof shale.

Mining of panel 3 started on December 13, 1990, and it was completed on July 3, 1991. The transverse line, located between the north edge and centerline of panel 3 as an extension from panel 2, was undermined on April 21, 1991.

Surface Subsidence and Deformation Monitoring

Surveying *Monument design and installation* Subsidence monuments are used to monitor vertical and horizontal movements of the land surface as it subsides. The design and configuration of subsidence monuments can compensate for movements due to frost and moisture changes in the soil—movements that commonly cause sources of error in subsidence surveys (Bauer and Van Roosendaal 1992). Individual monuments (fig. 9) were designed to eliminate the effects of frost-induced soil movements. The lower portion of the rebar monument was anchored in the soil below the frost line. The upper section, which extended through the frost zone to the ground surface, was jacketed with closed-cell foam insulation and PVC pipe to isolate the rebar from shallow soil movements.

The procedure for installing a surface monument included augering a small-diameter hole to a depth of 3 feet. The hole diameter had to be large enough to accept the 2-inch inner diameter (I.D.) PVC casing but as small as possible to minimize backfilling. A 3.25-foot-long piece of 2-inch I.D. PVC, with Armaflex or some other closed-cell foam insulation of equal length inside of the PVC, was lowered into the augered hole. A piece of rebar (no. 8), 5 feet long and 1 inch in diameter, was lowered through the center of the PVC/Armaflex assembly. The closed-cell insulation filled the annular gap between the rebar and the PVC pipe (i.e., I.D. about 1 in., O.D. about 2 in.). A lubricant such as graphite, silicon spray, or oil was needed to slip the foam inside the PVC pipe and over the rebar. The rebar was driven into the ground until nearly flush with the top of the PVC casing (fig. 9). The rebar was usually left sticking up slightly higher than the PVC casing so that a flat-bottomed surveying rod could rest only on the rebar.

A single, prominent indentation was made in the top center of the rebar with a metal punch and hammer. The indentation was for the tip of the surveying rod and for strain measurement between monuments. A 2-inch I.D. PVC cap was placed over the top of the 2-inch I.D. PVC pipe, and any annular space around the pipe was backfilled. The monument designation number was written on the inside and outside of the PVC cap.

Surveying methods and frequency The ISGS began baseline monitoring in November 1989. A Lietz SET3 total station equipped with a SDR2 electronic notebook was used to set control monuments and the longitudinal and transverse survey monument lines over panels 1 and 2, and a half width of panel 3. Several baseline surveys were initially performed using the mine's control

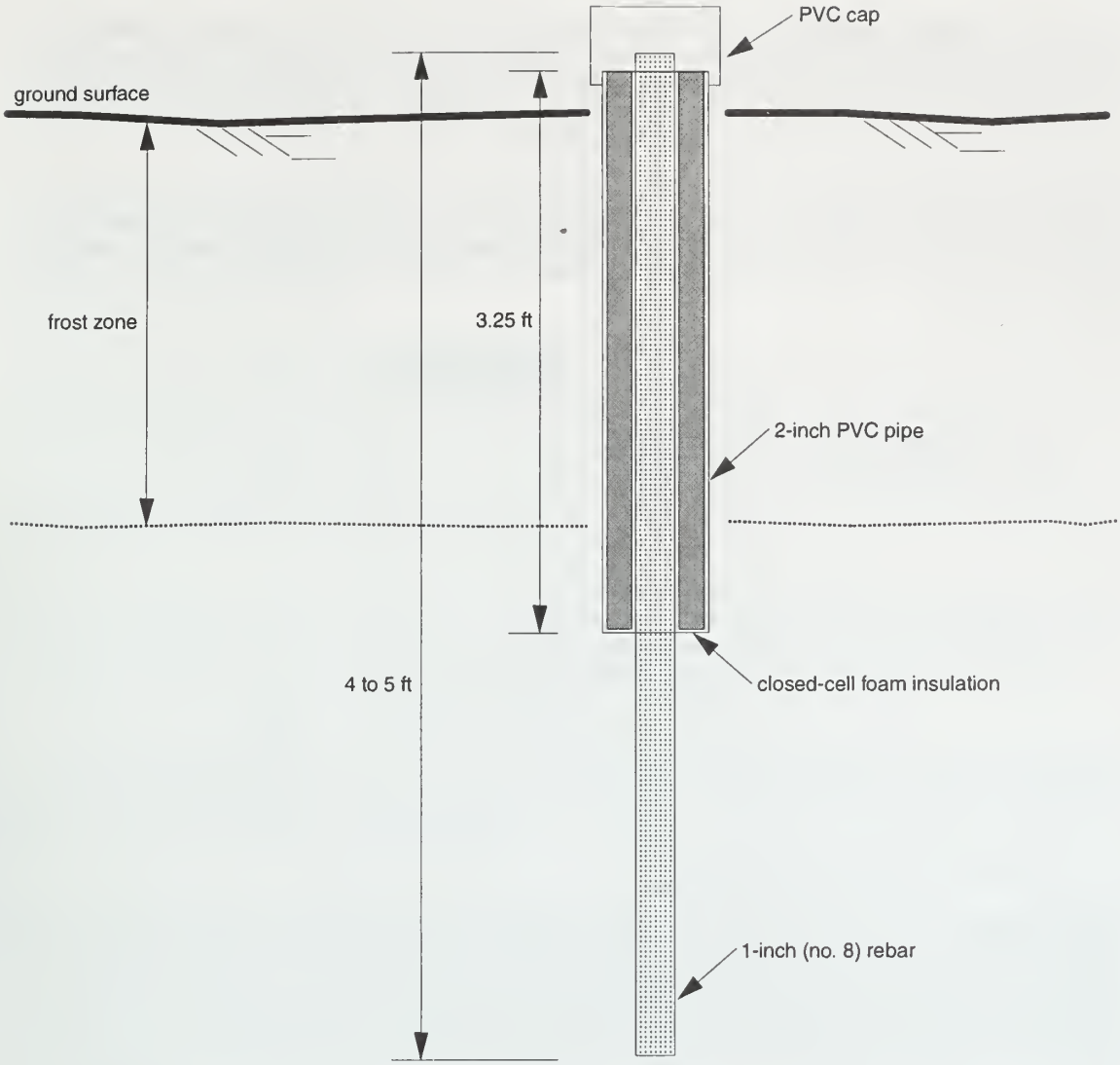

Figure 9 Frost-isolated monument design.

monuments to determine the coordinates and elevations of the controls. The mine's monuments consisted of a rebar anchor 2 to 3 feet in length hammered into the ground and a spike on a telephone pole. Once the elevation and coordinates for the ISGS monuments were established, the mine's monuments were no longer used. This procedure ensured greater survey accuracy by using all monuments of similar construction.

ISGS monuments were used as controls for installing survey monuments 20 feet apart (5% of depth of mining) in transverse and longitudinal lines over panel 1 to document dynamic and static surface subsidence and strain. Level surveys were performed using a WILD NA-2 with a micrometer and a wooden sectional rod. When proper procedures are used, the NA-2 instrument is able to achieve First-Order, Class II, results according to the Federal Geodetic Control Committee (1984). The transverse monument line was later extended over panel 2 to the centerline of panel 3 to determine the subsidence effects between panels and any long-term subsidence over panels 1 and 2, and a half width of panel 3.

Information provided by mine personnel was used to track the mining progress and to determine the frequency of monitoring. Monitoring surveys to document time-related effects were most frequent during the early, most active stage of subsidence. The frequency of monitoring decreased with the decrease in the rate of movement. Long-term monitoring through December 1991 continued to document residual movement of the overburden.

Horizontal displacements Horizontal displacement between monuments was measured using a steel tape. The accuracy of the readings was ± 0.005 feet. Horizontal measurements were performed in the transverse line of panel 1 and along 16 monuments on the longitudinal line located at the centerline of panel 1. Measurements were taken throughout the active subsidence period, as well as for 20 months after mining was completed.

Tiltplates Tiltplates were used to record changes in slope as the subsidence wave passed. Tiltplate installation is illustrated in figure 10. The plates were set into mortar beneath the frost zone (12–15 in. deep) and inside of 6-inch I.D. PVC casings with caps. The tiltplates were placed next to four frost-isolated longitudinal survey monuments. Tiltplates were monitored during the most active subsidence.

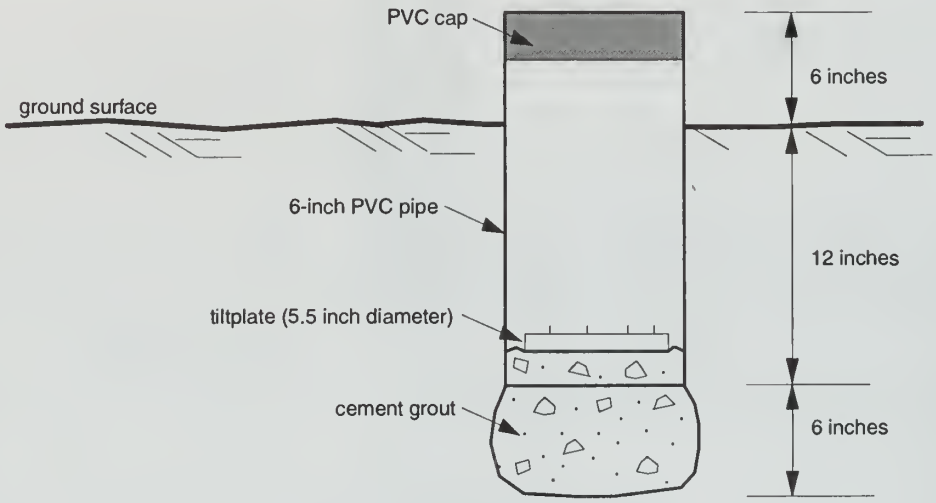

Figure 10 General tiltplate installation.

Inclinometers Four short inclinometers were installed at the corners of a 60-by-60-foot grid. The grid was over a predicted tension zone on the south side of panel 2. The 3.34-inch I.D. ABS plastic inclinometer casings (manufactured by SINCO, Inc.) were placed in 6.5-inch diameter boreholes augered by the ISGS drilling rig. The purpose of these inclinometers was to measure horizontal displacements within the upper portion of the drift as a function of depth. The annulus was filled with sand; the inclinometers were not anchored at the top or bottom. The inclinometers were read each time the grid was surveyed. The readout unit used was a Geokon, Inc. Model GK-601, which has an accuracy of 0.1% full scale and a resolution of 1 in 20,000. In addition, a movable inclinometer sensor was used; it was accurate to within 0.025 foot in deflection measurements of the top of a 100-foot hole and had a sensitivity of 1 in 10,000. The standard range of inclination measured by this sensor was 30° from vertical.

Overburden Characterization

Exploratory drilling *Geotechnical core logs* Core was obtained before and after subsidence from holes drilled at a 10° angle from vertical, dipping to the north, near the center of panel 1. The coring was performed at an angle in order to sample vertical fractures. Core description, core recovery, fractures, and rock quality designation (RQD) were logged in the field by ISGS personnel. The presubsidence borehole was drilled to a depth of 423.8 feet. Postsubsidence drilling was difficult because of subsidence-induced fracturing in the overburden. Problems associated with loss of circulation prevented drilling below 265.6 feet.

A stratigraphic section developed from the presubsidence core log is presented in figure 4. The bedrock is all of Pennsylvanian age, and a total of about 87 feet of glacial deposits of Pleistocene age overlies it. The bedrock is composed of 14% sandstone, 14% siltstone, 56% shale, 4% limestone, and 12% claystone and coal.

Split-spoon sampling of glacial material was performed before and after subsidence, allowing comparisons between the samples. Atterberg limits were performed on the samples. Standard penetration tests were performed over panel 2 following ASTM 1586-84.

• Rock quality designation (RQD) Rock quality designation is a standard parameter for evaluating the degree of fracturing of a rock core. RQD is used as an index property to indicate rock-mass quality. The RQD value, expressed as a percent, is the quotient of the sum of the length of all core segments longer than 4 inches to the drilled length of the core run. Fractures caused by drilling or handling are not included in the RQD determination.

• Fracture frequency (FF) Total fracture frequency per core run, in units of fractures per foot, is determined by counting the number of natural fractures per core run and dividing by the length of the core run. All natural discontinuities are counted, including separations along weak bedding planes and joints. As with RQD, drilling- and handling-induced breaks are not included in the fracture frequency determination.

Geophysical logging Geophysical logs, including gamma ray, density, and sonic velocity, were run in the open, angled boreholes. A correlation of rock and fluid properties can be made by simultaneously running these logs. The elastic properties of the rock were computed using the sonic and the density logs. BPB Instruments, Inc. was subcontracted by the ISGS to run these logs.

• Caliper log The caliper log is a mechanically measured profile of the borehole wall. A single-arm electro-mechanical device was held closed for entry into the borehole and activated during the logging run (BPB Instruments, Inc. 1982).

• Gamma ray log The gamma ray log is used to measure the naturally occurring radioactivity in the rock. Radioisotopes normally found in rocks are potassium (^{40}K), thorium, and uranium. Clay minerals usually have high concentrations of ^{40}K, so shales generally exhibit high gamma ray intensity. Sandstones and carbonates generally produce lower gamma ray counts because of their relatively low concentration of highly radioactive constituents (Lynch 1962).

• Density log The density log is a measure of the electron density of the formation. Gamma rays are first scattered in the formation. These rays then collide with the electrons in the formation; the rays reaching a detector are then counted as an indication of formation density. Density logs are primarily used as porosity logs (Lynch 1962).

• Sonic log The sonic log is generally used to determine the porosity of the formation. The sonic device measures the transit time of a sound pulse, or compression wave, through a given length of rock; in this case, the receivers produced 20- and 60-cm transit times. Measurement of the time taken for the wave to pass between receiver pairs enables the calculation of the velocity, normally known as the sonic velocity. The rate of propagation of the compression wave through the rock depends on the elastic properties of the rock matrix and its contained fluids. The multi-channel sonic sonde measures the compressional 'P' wave velocity (V_p) (Lynch 1962, BPB Instruments 1982).

• Computed composite moduli analysis The use of borehole geophysical logging techniques presumes that there are relationships between the geophysical and the geotechnical properties of the geological strata. Although there is a scale effect associated with this presumption, borehole geophysical logging techniques are used to provide in situ geotechnical parameters. The shear wave velocity was calculated, using the density log and the sonic log, by Christiansen's equation:

$$V_s = V_p \left[1 - 1.15 \frac{\frac{1}{\rho} + \frac{1}{\rho^3}}{e^{\frac{1}{\rho}}}\right]^{\frac{3}{2}}$$

where V_s = shear wave velocity (ft/s)
V_p = compression wave velocity (ft/s)
ρ = mass specific gravity of rock, defined as γ/γ_w, where γ and γ_w are the unit weights of rock and water (lb/in.^{3}), respectively.

Forster and McCann (1979) determined that these computed shear wave velocities were in error by as much as 25% as a result of low readings of the density tool in sections of boreholes where excessive caving had occurred.

Poisson's ratio is calculated using the following equation (BPB Instruments 1982):

$$\sigma = \frac{[R^2-2]}{2[R^2-1]} \qquad \text{where} \quad R = \frac{V_p}{V_s}$$

Young's modulus was calculated by this equation (BPB Instruments 1982):

$$E = \frac{\gamma}{g} V_p^2 \; \frac{(1+\sigma)\,(1-2\sigma)}{(1-\sigma)}$$

where E = Young's modulus (psi)
g = acceleration of gravity (in./s^2)
V_p = compression wave velocity (in./s)

Shear modulus was calculated by this equation (BPB Instruments 1982):

$$\mu = \frac{\gamma}{g} V_s^2$$

where μ = shear modulus (psi)
V_s = shear wave velocity (in./s)

Bulk modulus was calculated by this equation (BPB Instruments 1982):

$$B = \frac{\gamma}{g} V_p^2 - \frac{4}{3}\mu$$

where B = bulk modulus (psi)
V_p = compression wave velocity (in./s)

The computed elastic moduli may be found in appendixes G and H.

Laboratory testing for intact rock properties Rock characterization was performed in the ISGS laboratory. Core samples were tested for unconfined compressive strength, modulus of elasticity, indirect tensile strength, specific gravity, Shore hardness, and point-load index by following standards and suggested methods of the American Society for Testing and Materials (1988) and International Society for Rock Mechanics (1985).

Unconfined strength and elastic modulus Samples were cut with a saw to nearly the allowable tolerance before they were lapped. Additional preparation of the sample consisted of lapping to a height-to-diameter ratio of 2 to 2.5 with a tolerance for nonparallelism of less than 0.0025 inch, according to ASTM D 4543-85. The 2:1 height-to-diameter ratio requirement was not always maintained, especially within a section of core that was quite fractured. Sample loading was under constant strain conditions, as allowed by ASTM D 2938-86. The sample ends were not capped, following the ISRM Suggested Methods for Determining Uniaxial Compressive Strength and Deformability of Rock Material (Brown 1981).

The elastic modulus was obtained directly from the plot of load versus deformation. The elastic modulus represents the slope of the line tangent to the elastic portion of the stress/strain curve and at 50% of the ultimate compressive strength. The ultimate compressive strength was found by dividing the ultimate axial force by the area of core perpendicular to its axis, as suggested by the ISRM (Brown 1981).

Indirect tensile strength Discs 1 inch thick were compressed diametrically between high modulus (steel) platens. The values of indirect tensile strength, σ_t, are calculated by the following equation (Brown 1981):

$$\sigma_t = \frac{2P}{\pi Dt}$$

where P = axial load (lbs)
D = diameter (in.)
t = thickness (in.)

Axial point-load index The method suggested for the axial point-load index by the ISRM Commission on Testing Methods (1985) was used. Samples with a height-to-diameter ratio of 0.3 to 1.0 were tested. The samples were placed between two spherically truncated, conical platens of the standard geometry (60° cone). The load was steadily increased to produce failure within 10 to 60 seconds, and the failure load, P, was recorded. The point-load index is calculated using the following equation:

$$I_s = \frac{P}{t^2}$$

where I_s = uncorrected point-load strength (psi)

This equation does not take into account variable sample thicknesses; therefore, a size correction is required. The size correction for the axial point-load index, T_{500}, of a rock specimen or sample is defined as the value that would have been measured by a diametral test with $D = 50$ mm (Brook 1980). The corrected axial point-load index is calculated by the following equation:

$$T_{500} = 211.47\frac{P}{A^{0.75}}$$

where T_{500} = corrected point-load index (MPa)
P = load (kN)
A = diameter x thickness (mm^2)

Moisture content A center portion of the samples tested for unconfined strength was used to determine moisture content. Moisture content was calculated as a percentage of the dry weight of the sample, as specified in ASTM D 2216-80.

Shore hardness A model D schleroscope, manufactured by Shore Instrument and Manufacturing Company, was used for hardness determination of compressive strength specimens. Each of the values in the summary tables is an average of the highest 10 tests from a total of 20 tests performed on the lapped ends of the uniaxial compressive strength test specimen, as described in Brown (1981).

Overburden Deformation Monitoring

Time-domain reflectometry The TDR technique was used to document fracture development caused by subsidence in the overburden. This technique was developed by the power and communications industries to locate breaks in transmission cables. A TDR tester sends ultra-fast rise time voltage pulses down the coaxial cable. Reflections appear as a distinct signature versus distance on a cathode-ray tube (CRT) or strip-chart recorder. Changes in the distance between the inner and outer conductors of the cable, breaks in either conductor, or touching of the inner and outer conductors will produce changes in the induced voltage signature. These changes in the cable geometry reflect signals back to the cable tester; these signals can be viewed on the CRT screen and preserved on paper by a strip-chart recorder. Researchers at Northwestern University (Dowding et al. 1988, 1989) determined the optimum cable size, bonding strength, and grout

composition; they also characterized the signatures caused by different modes of deformation (e.g., tension vs. shear). The TDR installation and monitoring was part of an ongoing contract with the Office of Surface Mining to test the application of TDR to monitor overburden fractures. Results of several studies over both active and abandoned mines using the TDR technique may be found in Bauer et al. (1991).

The entire cable was laid out on the ground and reference crimps were placed at intervals of 20 feet. Without reference crimps along the cable, location accuracy is on the order of 2% of the distance from the tester to the cable defect. Crimps at known distances allow for much more accurate measurements. The reflected signal is attenuated as a function of distance along the cable. Therefore, a wider crimp, consisting of adjacent individual plier crimps, was required at greater depths to produce the desired signal amplitude of 40 mρ.

Shear deformation of the TDR cable causes an easily detectable TDR reflection spike that increases in magnitude in direct response to shear deformation of the cable. Consequently, it is possible to monitor the rate of shear deformation by obtaining a series of TDR records over a period of time. Extension deformation of the TDR cable causes a subtle, trough-like TDR reflection that increases in length as the cable is deformed. Cable failure caused by extension can be distinguished from that caused by shearing by the absence of a shear reflection spike at the point of failure.

The TDR cable installed at panel 1 (fig. 11) was a 0.50-inch-diameter, unjacketed Cablewave System FXA 12-50. It was placed on the panel centerline near the MPBXs. The cable was installed in an angled, 3-inch diameter, cored borehole. The cable was about 426 feet long and required six plier crimps every 20 feet from a depth of 4.5 to 44.5 feet, eight plier crimps from 64.5 to 344.5 feet, 10 plier crimps from 364.5 to 384.5 feet, and 12 plier crimps from 404.5 feet to the bottom of the cable. The large number of crimps made the reflected signals very flat and wide. The resultant signal at the deeper portion of the cable was therefore poorly defined in comparison with the narrower sharp signal peaks of the upper portion of the cable. The cable was lowered down by hand with a 5-foot long, 0.75-inch-diameter black steel pipe used as the anchor/weight. The borehole was backfilled to the top of the bedrock with grout having a 65% water-to-cement ratio. High early strength Type III cement (7.6 gallons/94 lb sack cement) and 2% additive (Intrusion-Prepakt, Inc.) were used, as recommended by Dowding et al. (1989). A bentonite grout was used up through the glacial material in order to avoid shear failure of the cable.

Multiple-position borehole extensometers Two 6-anchor MPBXs were installed at panel 1 as shown in figure 12. The anchors of the shallow MPBX were grouted at depths of 120, 140, 160, 180, 200, and 220 feet below the ground surface; those of the deep MPBX were grouted at depths of 280, 300, 320, 340, 360, and 380 feet. The extensometers mechanically monitor vertical overburden movements at each of the six levels. Anchor displacements are transmitted by the fiberglass rods to the surface, where movement of the rod tips is measured relative to a reference plate. Displacements of the anchors relative to each other and to the reference plate indicate the magnitude of the vertical component of the differential and total ground displacements. Elevation control was maintained by surveying the reference plates to establish absolute anchor movements.

Hydrogeologic Investigations

Open-standpipe piezometers of 1-inch-diameter PVC (fig. 13) were installed to monitor the hydrogeologic effects of subsidence in the glacial drift, the Trivoli Sandstone aquifer, and a deep sandstone unit. Drift and Trivoli Sandstone piezometers were positioned over the chain pillars, on the centerline, near the edge of the longwall panel, and at the control site to the north. The piezometers monitoring the deep sandstone unit and the pump well were located near the centerline of panel 1. Piezometric levels were monitored hourly using pressure transducers and data recorders during the most active subsidence and with a drop line after water levels were deemed more stable.

Drift piezometers Piezometers in the glacial drift ranged from 53 to 78 feet deep, with a 10-foot screened section at the bottom of the hole. Screens were placed in the lower part of the drift just above the bedrock.

Bedrock piezometers All but one of the bedrock piezometers were placed in the Trivoli Sandstone, which is typically 15 to 25 feet thick. All bedrock piezometers were installed with 10-foot screened sections, with the exception of BP1, the easternmost piezometer, which had a 5-foot screened section. The deep bedrock piezometer was placed at a depth of 275 feet within a

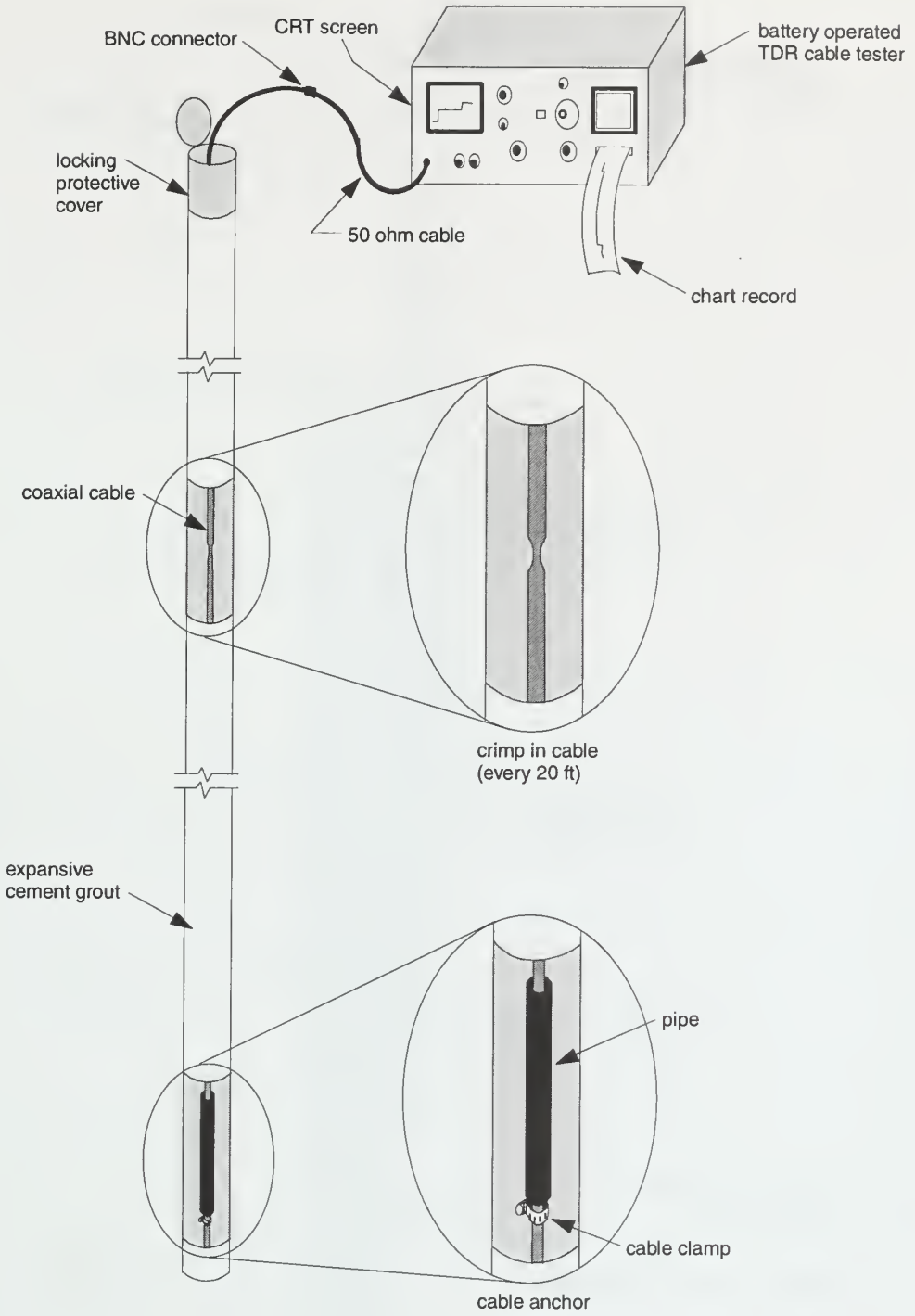

Figure 11 TDR installation.

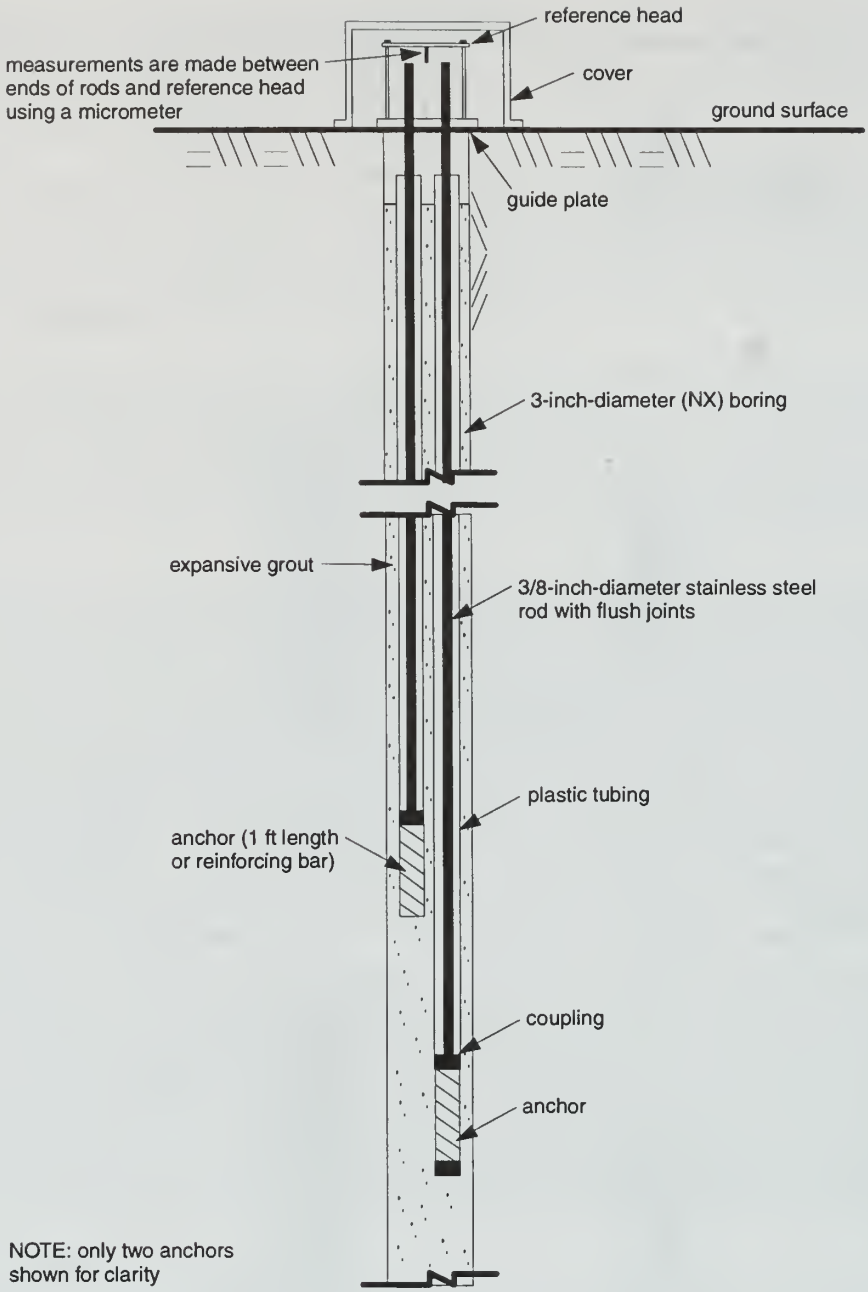

Figure 12 MPBX installation.

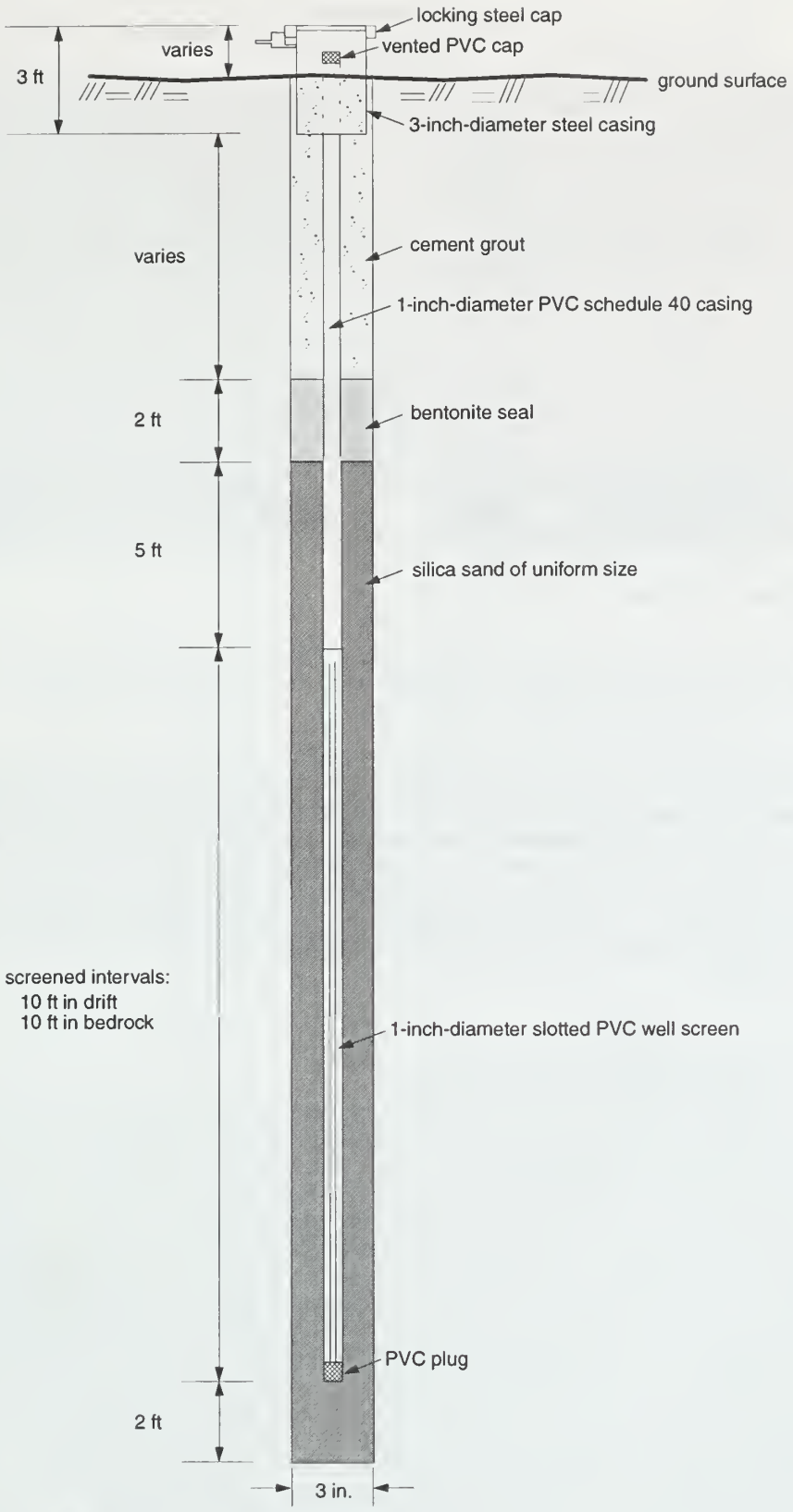

Figure 13 Design and installation of the drift and bedrock piezometers.

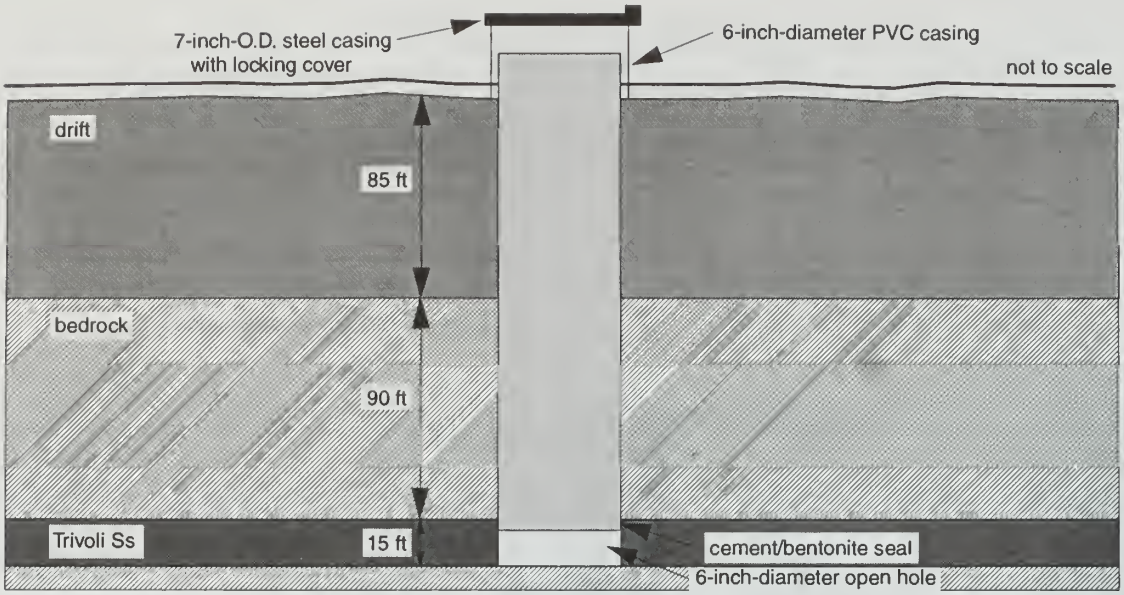

Figure 14 Design and installation of the pump well.

sandstone unit that may have been the Gimlet Sandstone. A 6-inch-diameter, 190-foot well was installed over the center of panel 1. The well was cased (with PVC) down to the Trivoli Sandstone (fig. 14) and was used to perform pump tests.

Aquifer characterization Premining hydraulic properties over panel 1 were determined using slug tests in piezometers, aquifer pumping tests in the 6-inch well, and hydraulic injection tests (packer tests) in the deep inclined borehole (GT1) near the centerline. Subsidence damage to piezometers inside the panel prevented their further use; however, postsubsidence hydraulic properties were determined by packer tests in the postsubsidence cored borehole (GT2), which was also near the centerline. A piezometer was installed in 1990 over panel 1 to determine the postsubsidence water levels and hydraulic conductivity of the Trivoli Sandstone aquifer. Aquifer characterization was performed by NIU researchers assisted by ISGS personnel (Booth and Spande 1991, Booth 1992).

RESULTS

Surface Subsidence Characteristics

Subsidence profiles Panel 1 was surveyed for 19 months, starting on November 21, 1989, when the panel face was located approximately 400 feet from the transverse line. The face reached the transverse line on December 18, 1989, and had an average face advance of 33.5 feet/day for the last 200 feet (fig. 15). Panel 1 was 668 feet wide by 7,893 feet long; its average mined-out height was 6 feet. The panel roof was located at a depth of 402 feet. The panel face progressed from east to west. The survey monuments began to show elevation changes when the longwall face approached to within 250 feet of the monument position as projected to mine level (fig. 16). An elevation change of 0.03 foot was measured as the panel face advanced to 120 feet from the transverse line. The monuments continued to register substantial changes in elevations until the face was 500 feet past the transverse line at the mine level. At this time (January 20, 1990), subsidence of 4.44 feet was measured at the panel centerline. The mined-out height below the transverse line was 6 feet. A more representative value of subsidence of 4.73 feet was obtained by averaging the readings taken on January 11, 1990, from six survey monuments located along the panel centerline. These monuments were located at distances of 140, 180, 200, 220, 260, and 280 feet from the transverse line. The average mined-out height below these monuments was 6.72 feet. The resulting ratio of subsidence to mined-out height was 70.5%. Figure 16 indicates that about 7.5% of the subsidence occurred before the face reached the monitoring line and that most of the subsidence (75%) took place when the face was located 50 to 250 feet past the monitoring line.

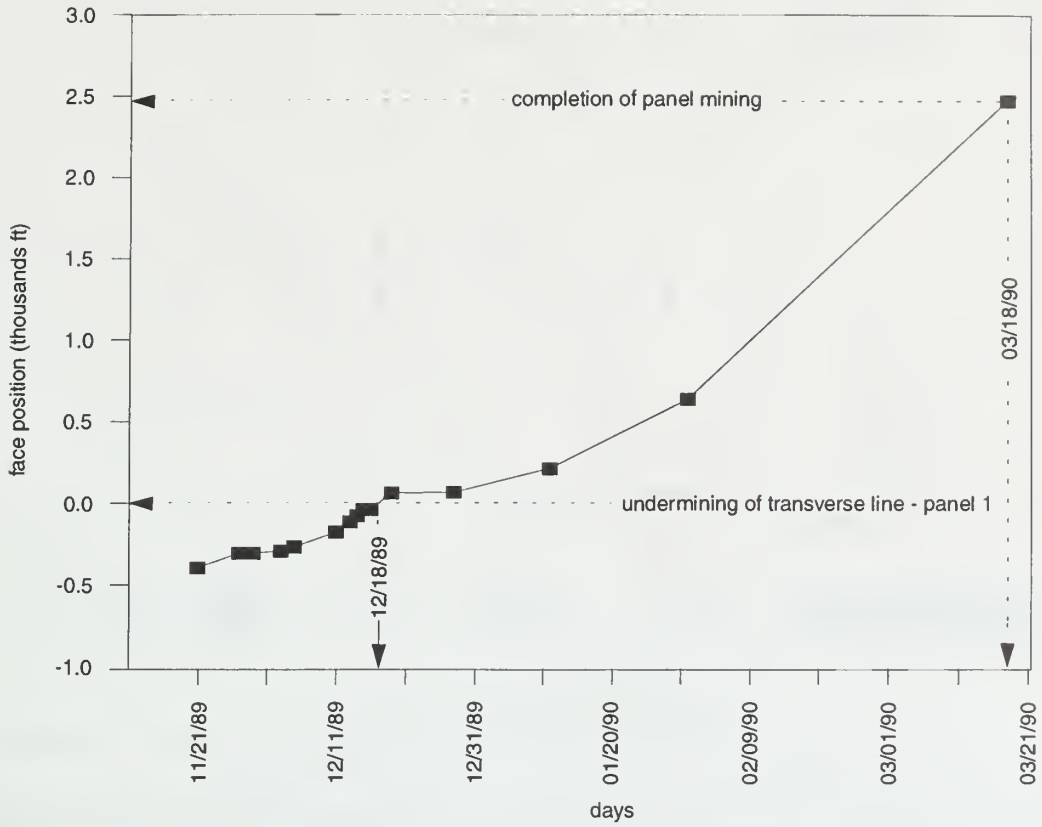

Figure 15 Face position with respect to time in relation to transverse line (panel 1). Note the slow advance rate at the time of the undermining of the transverse line.

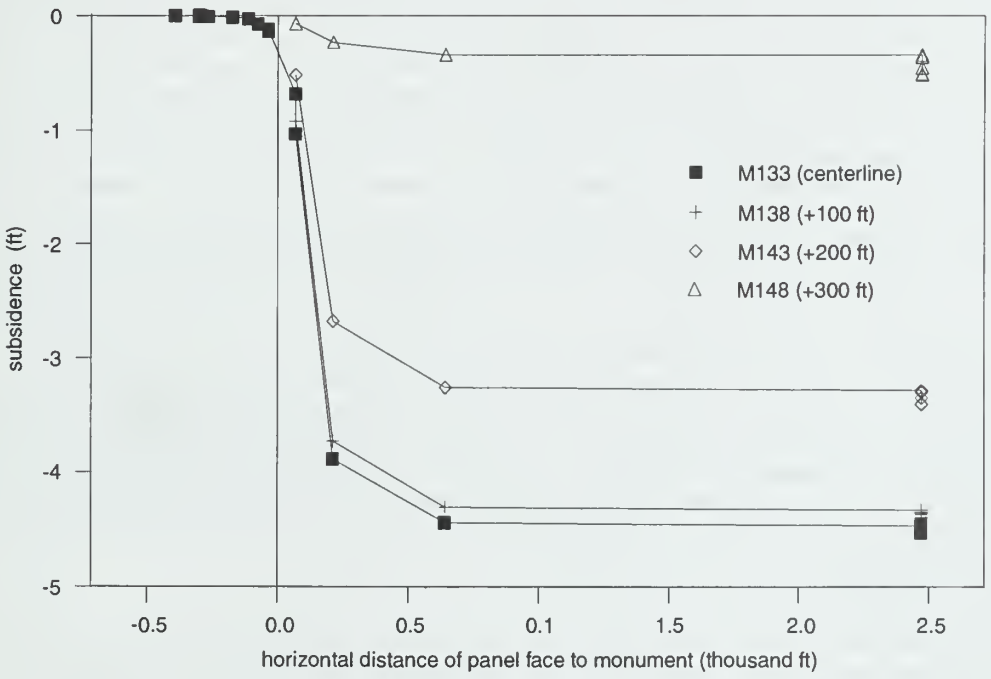

Figure 16 Development of subsidence with face advance for panel 1.

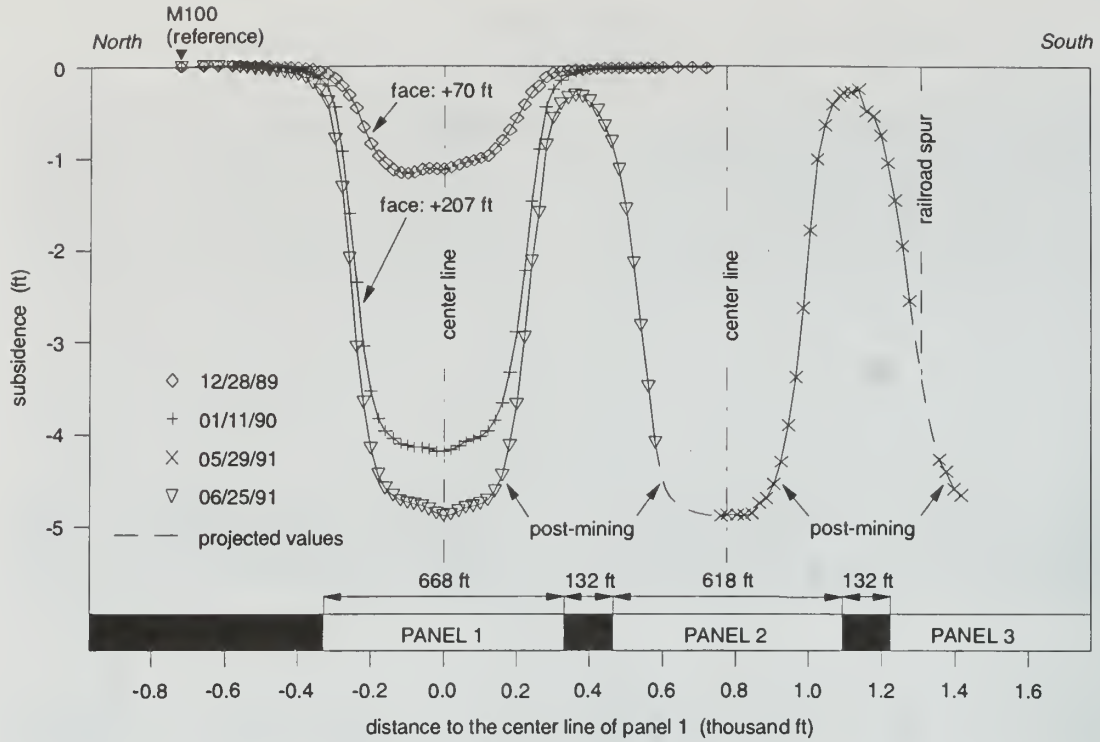

Figure 17 Transverse subsidence profile development. Coal height is exaggerated.

During the 18 months after undermining, total subsidence averaged 4.84 feet at the panel centerline (i.e., a small increase of 2.3% relative to the amount recorded at the end of active mining). This increase primarily reflected the effect of time-dependent displacements developed within the overburden rock mass. This average value of total subsidence was also determined using readings taken in six monuments located along the longitudinal line at distances of 140, 180, 200, 220, 260, and 280 feet from the transverse line. The corresponding ratio of subsidence to mined-out height increased to 72%. The angle of draw for the static transverse subsidence profile at panel 1 was consistently 20°; there was no indication that the angle of draw changed with time. The angle of draw was determined for surface subsidence of 0.03 ft, which was located abut 150 ft outside the edge of the panel. This value was taken as the lower limit of surface subsidence because readings smaller than 0.03 ft may be affected by natural ground movements (Bauer and Van Roosendaal 1992).

Subsidence at the centerline of panel 1 generated by the mining of panel 2 was negligible. At the south edge of panel 1, however, about 0.11 foot of subsidence was recorded at the completion of panel 2. The distance between panels 1 and 2 was 132 feet, representing two rows of chain pillars between the panels. Additional subsidence of 0.07 foot was measured at the south edge during the following 7 months of readings; thus, a total subsidence of 0.18 foot was recorded at the south edge. This amount corresponded to 57% of the 0.31 foot of overall subsidence measured during the period of readings. Subsidence of 0.13 foot had initially occurred at this location when panel 1 was completed. At the centerline of the chain pillar located 66 feet south of the south edge of panel 1, an increase in subsidence of 0.13 foot was measured over a previous subsidence of 0.09 foot, which had been induced by the mining of panel 1. After the completion of panel 2, additional subsidence over the chain pillar was 0.07 foot. These two components of vertical settlements generated a total subsidence of 0.20 foot, which represented 69% of the overall subsidence of 0.29 foot over the chain pillars.

Panel 2 was located 132 feet south of panel 1, edge to edge. It ran east–west, was 618 feet wide, and had an average mined-out height of 6.6 feet. Mining of panel 2 started as soon as panel 1 was completed. Its transverse line was located in the same alignment as that of panel 1. Subsidence of 4.40 feet was measured at the panel centerline on November 13, 1990, at the time of completion of the panel. The transverse line was undermined previously on September 2, 1990. The resulting ratio of subsidence to mined-out height was equal to 66.3%, less than the 70.5%

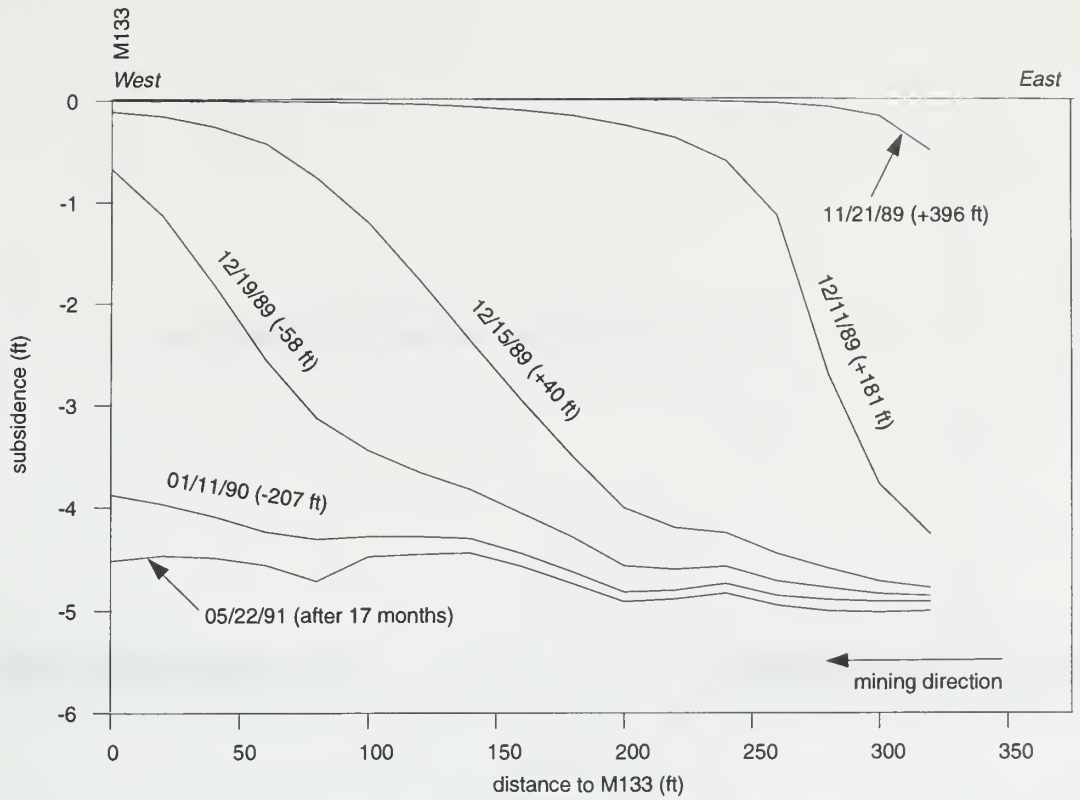

Figure 18 Panel 1 longitudinal subsidence profile development (+ approaching, - past).

induced at panel 1. About 6 months later, an increase in subsidence of 0.12 foot was measured at the centerline of panel 2; the resulting ratio of subsidence to mined-out height was 68%.

Subsidence at the south edge of panel 2 increased 0.18 foot on May 29, 1991, about 40 days after the face of panel 3 passed the transverse line. At the centerline of the chain pillars between panels 2 and 3, there was an increase in subsidence of 0.20 foot during the same period. On November 13, 1990 (53 days after the completion of panel 2), initial subsidences equal to 0.11 and 0.03 foot were recorded at the south edge and centerline of the chain pillars, respectively. These subsidence values are comparable with those measured at the south edge of panel 1, as well as at the centerline of the chain pillars located between panels 1 and 2. The angle of draw determined at panel 2 for the static transverse subsidence profile was similar to that obtained for panel 1—about 20°. Figure 17 presents the transverse subsidence profile, including panels 1 and 2 and part of panel 3. The transverse subsidence profile reflected the effect of rapid progressive subsidence by showing an asymmetric shape with respect to the panel centerline; this asymmetric subsidence is caused by ongoing subsidence that occurred during the 3-hour survey of the transverse line.

A 320-foot longitudinal line over the centerline of panel 1 was used to monitor the advance of the dynamic subsidence wave. The wave started about 250 feet ahead of the panel face and extended behind it to 500 feet, totaling a length of 750 feet. Subsidence of 0.15 to 0.30 foot was measured when the panel face reached the survey monuments (fig. 18). The rate of wave advance was closely controlled by the rate of face advance. The effect of the rate of face advance on the longitudinal subsidence profile was not clearly detected. Total station data are presented in appendix A; longitudinal and transverse surveys and subsidence calculations are presented in appendix B.

Strain profile Five sets of horizontal displacement readings taken at panel 1 provided the change in static transverse strain profile with face advance. The static transverse strain profile shows the distribution of the permanent changes in surface horizontal strains along the transverse line for a given face position. The first set of readings was obtained when the face approached to a distance of 302 feet from the transverse line. The other four sets were obtained when the face was 67, 211, 682, and 2,471 feet past the transverse line. The last set of readings was taken 17 days after the completion of the panel and 108 days after the face passed the transverse line. Horizontal strain calculations are presented in appendix C.

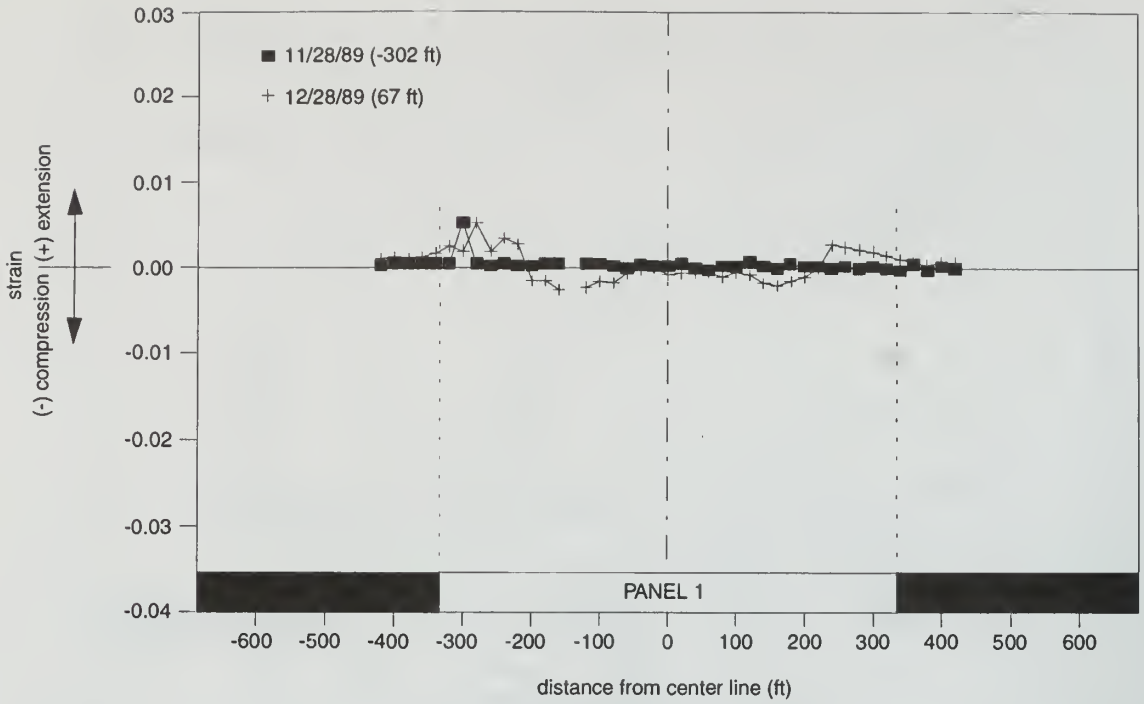

Figure 19 Panel 1 transverse strain profile for 11/28/1989 and 12/28/1989.

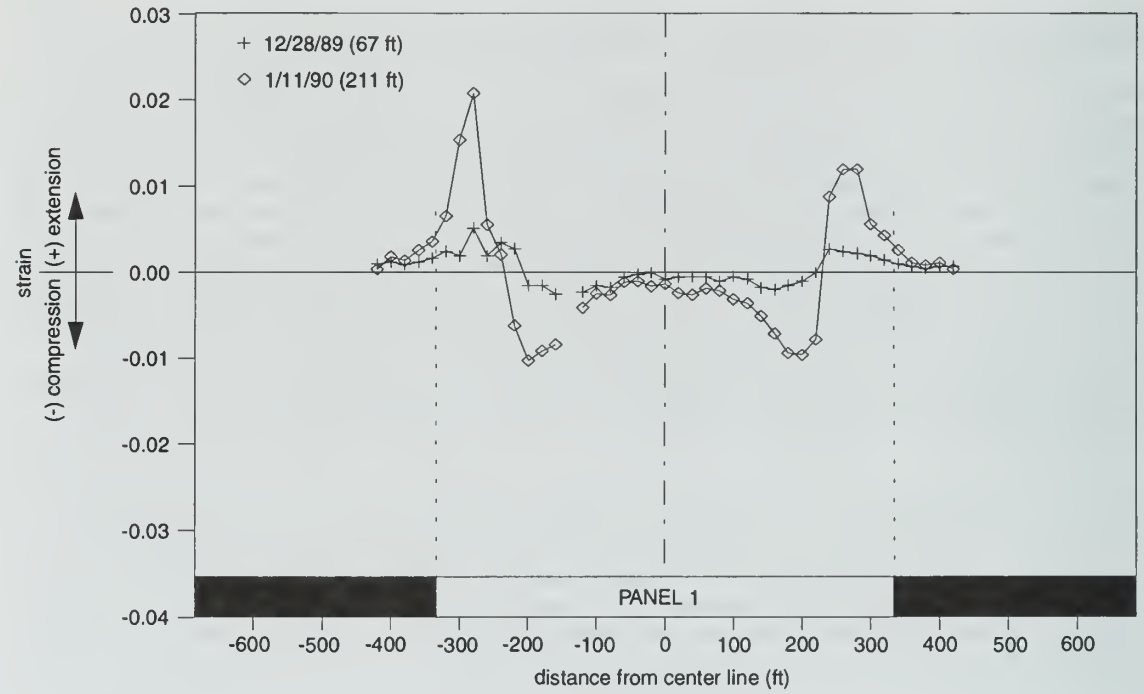

Figure 20 Panel 1 transverse strain profile for 12/28/1989 and 1/11/1990.

Because of the limited number of readings, the exact start and end of the change in horizontal surface displacements induced in the transverse direction by the effect of active mining were not documented. These two events, however, should have coincided with the development of vertical surface displacements, starting with the face about 250 feet away and ending with the face 500 feet past the transverse line. The monitoring data confirmed that horizontal displacements started when the panel face was somewhere between 302 feet from and 67 feet past the monitoring

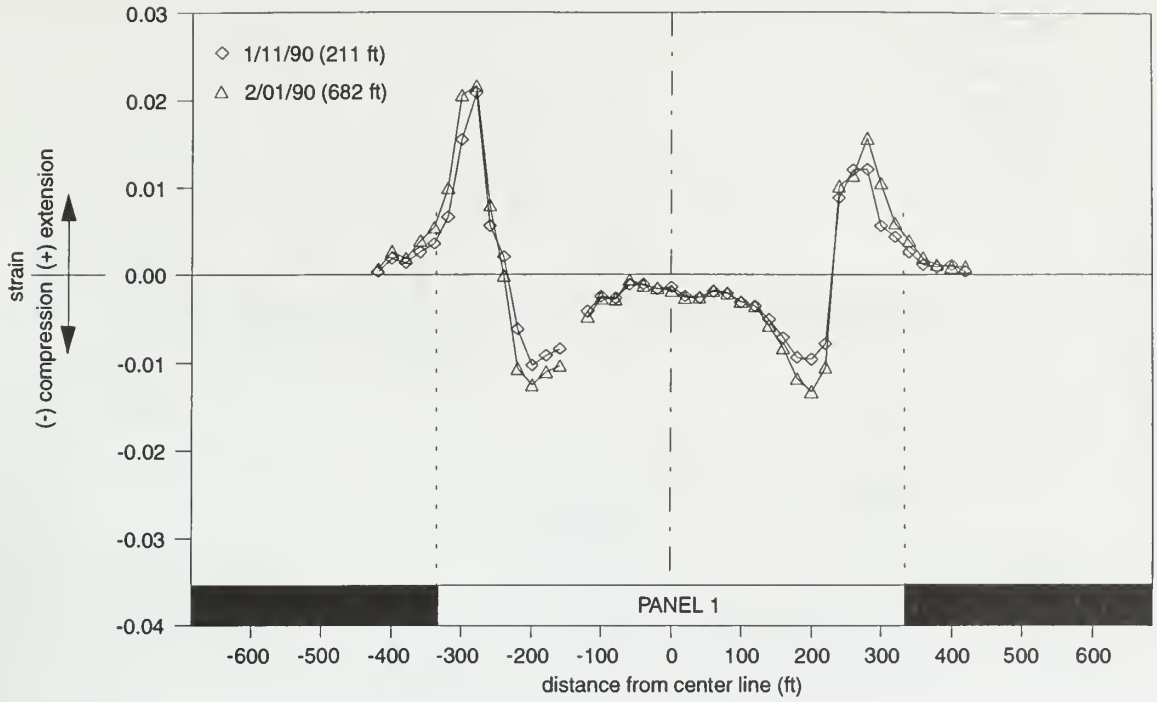

Figure 21 Panel 1 transverse strain profile for 1/11/1990 and 2/1/1990.

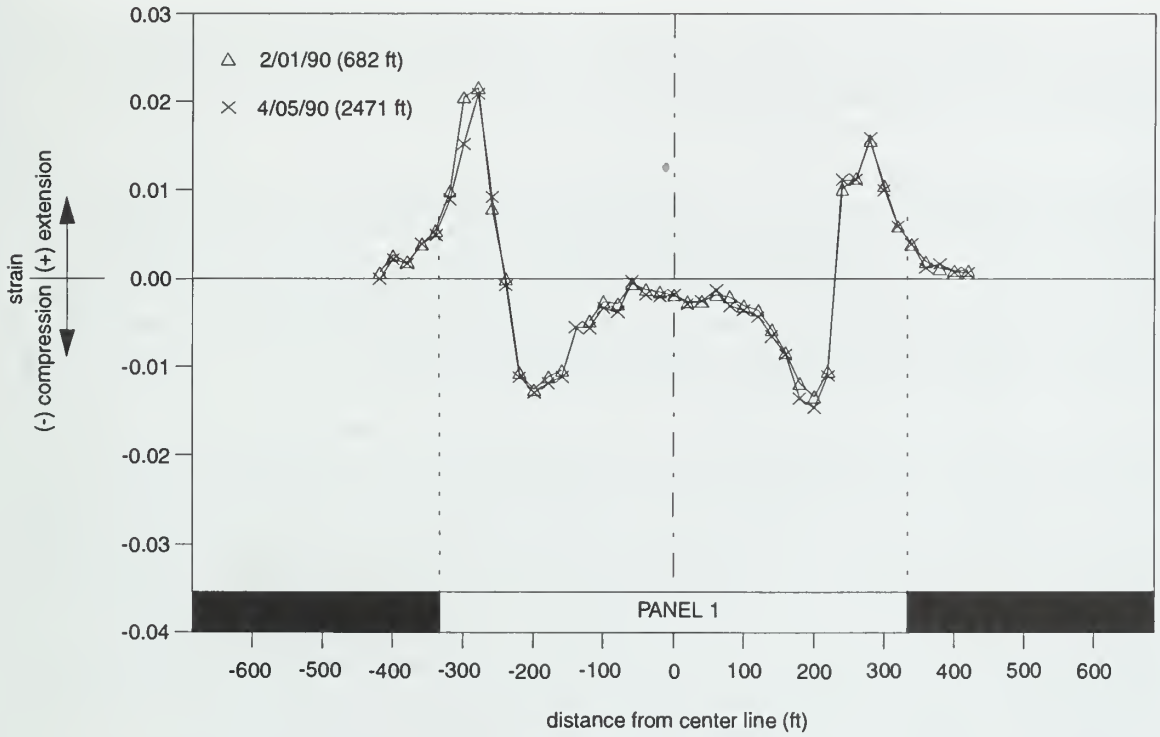

Figure 22 Panel 1 transverse strain profile for 2/1/1990 and 4/5/1990.

station. No substantial changes were observed for the last two sets of readings when the face was located at distances of 682 and 2,471 feet past the transverse line. The differences in horizontal strains between these two sets of readings were within 0.5% (figs. 19, 20, 21, and 22). Therefore, it is assumed that the effect on horizontal movements by active mining ceased when the face was between 211 and 682 feet past an area.

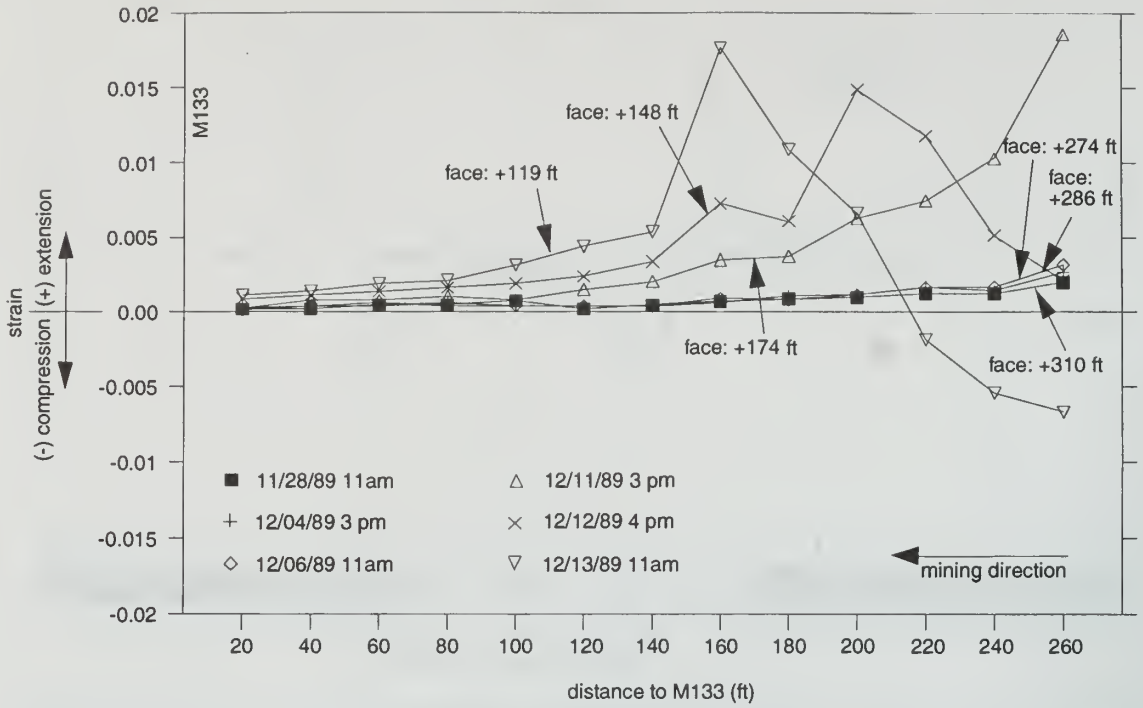

Figure 23 Panel 1 longitudinal strain profile for dates from 11/1989 to 12/1989 (+ approaching, - past).

For the transverse profiles, the maximum extensional strains were consistently found at a distance of about 54 feet inside the panel edge, whereas maximum compressional strains were generally located about 134 feet inside the panel edge. The corresponding ratios of distance from edge divided by depth were 0.135 and 0.335, respectively.

The last set of transverse readings taken immediately after the completion of the panel indicated a maximum extensional strain of 2.1% on the north side of the panel and 1.6% on the south side. In addition, a maximum compressional strain of 1.3% on the north side and 1.5% on the south side was determined. Changes in horizontal strains near the panel centerline were negligible because of a symmetrical loading condition with respect to the panel centerline. Within the extension zone, most of the strains were absorbed in the form of longitudinal cracks that reached apertures as much as a few inches. The length of these cracks extended from several feet up to several hundreds of feet; their depths were not directly measured.

A 260-foot longitudinal line at the centerline of panel 1 was also monitored during the same period of readings taken along the transverse line. The longitudinal line was composed of 16 survey monuments installed every 20 feet; its purpose was to provide the dynamic longitudinal strain profile. Such a profile presents the distribution of the temporary changes in surface horizontal strains parallel to the mining direction. Longitudinal extensional displacements started about 200 to 250 feet ahead of the panel face. This initial strain, which remained practically constant and negligible, had a magnitude of less than 0.1% up to a distance of 120 to 160 feet away from the face; it then started to increase with decreasing distance to the face, without any linear relationship (fig. 23). Maximum dynamic extensional strains between 1.2% and 1.8% developed at a distance ranging from 20 to 80 feet behind the panel face (figs. 23, 24). Far behind, at a distance of 80 to 130 feet, the changes in longitudinal strains approached zero. Maximum dynamic compressional strains of 1.3% to 1.4% were then induced at a distance of 130 to 170 feet behind the face. For distances exceeding 350 to 450 feet behind the face, the strains approached and remained close to zero, reflecting the dynamic character of the subsidence wave (fig. 25).

Tiltplates Dynamic slope changes were monitored with three tiltplates installed along the centerline of panel 1. Tiltplates TP172, TP174, and TP176 were placed at distances of 100, 140, and 180 feet east of the transverse line, respectively. Readings started on November 8, 1989, when the panel face was 657, 617, and 577 feet away from tiltplates TP172, TP174, and TP176, respectively.

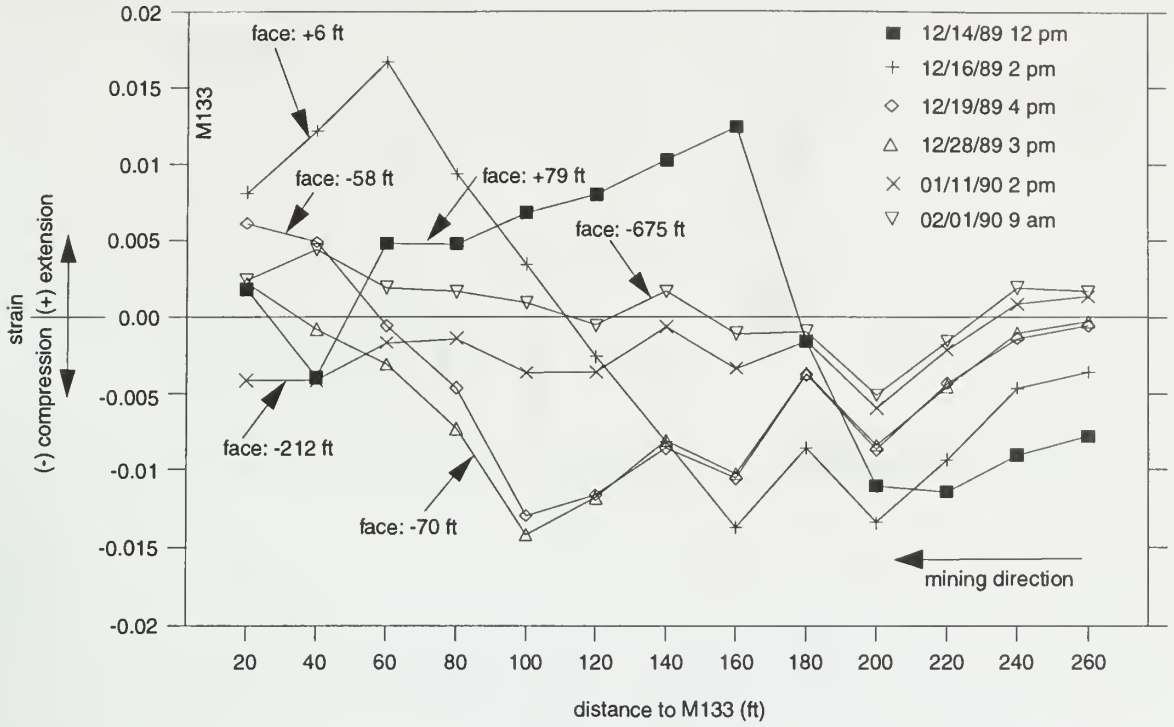

Figure 24 Panel 1 longitudinal strain profile for dates from 12/1989 to 2/1990 (+ approaching, -past).

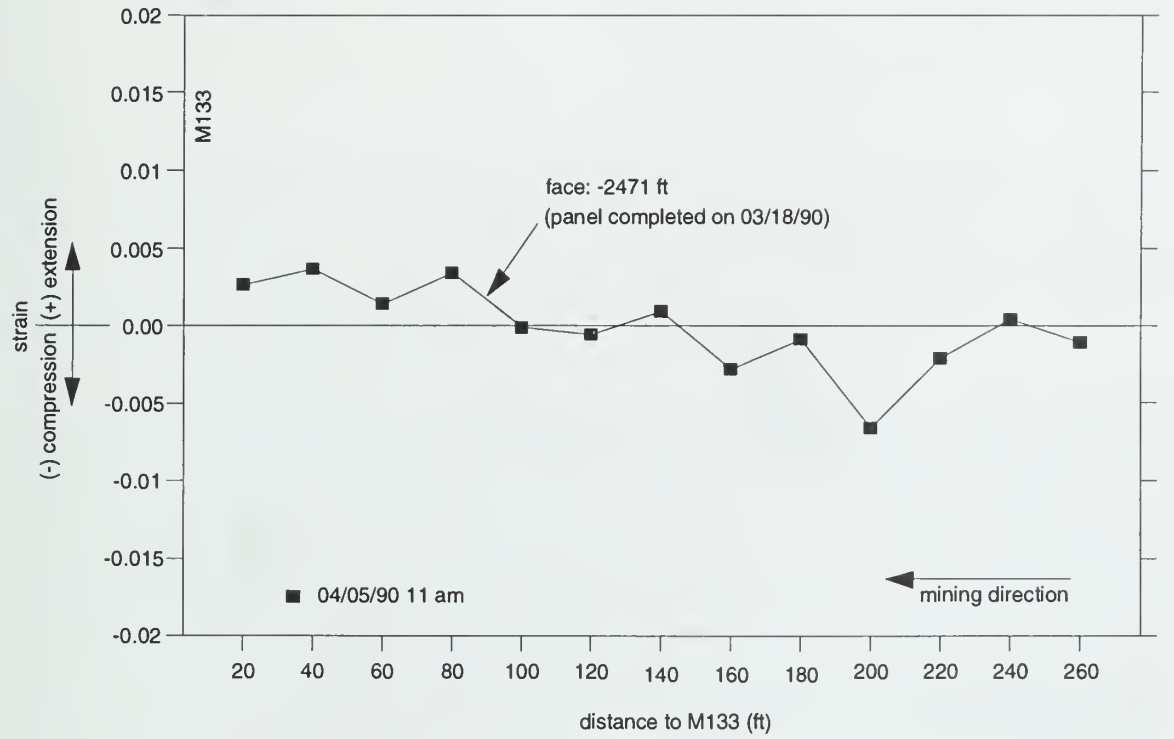

Figure 25 Panel 1 longitudinal strain profile for 4/5/1990 (+ approaching, - past).

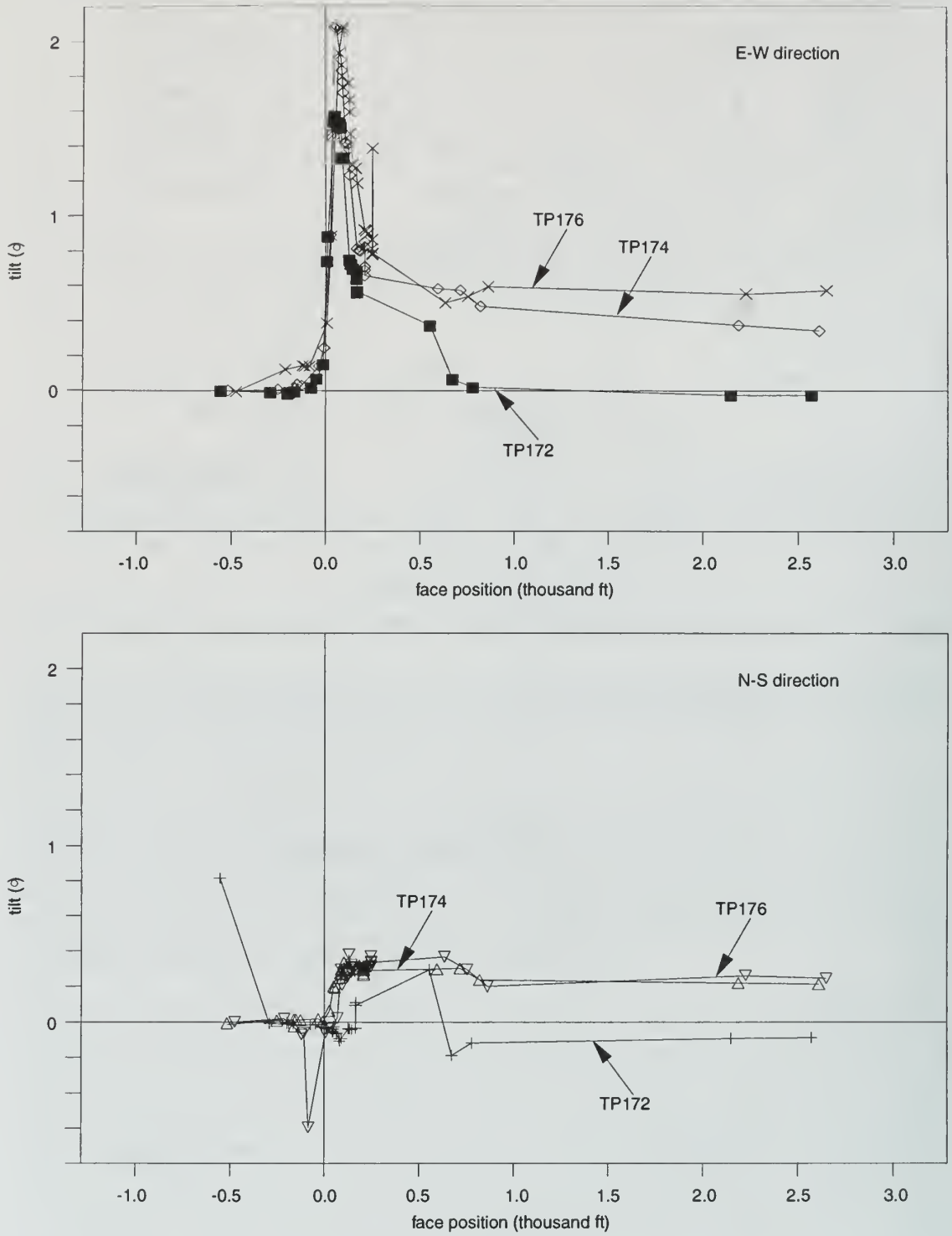

Figure 26 Development of tilt with face advance for panel 1.

Tilt changes started when the face was about 200 feet from the instruments (fig. 26); this position is close to the start of subsidence as well as surface extensional strains in the mining direction. The magnitude of tilt increased continuously within the dynamic extensional zone, which was located between 200 feet ahead of and 70 to 100 feet behind the mine face. A maximum tilt of about 2.5° was measured at the transition between the extension and compression zones, and it coincided with the minimal surface strains found at the inflection point. The corresponding value of subsidence at this point was 2 to 2.5 feet (fig. 27). Within the compression zone, located

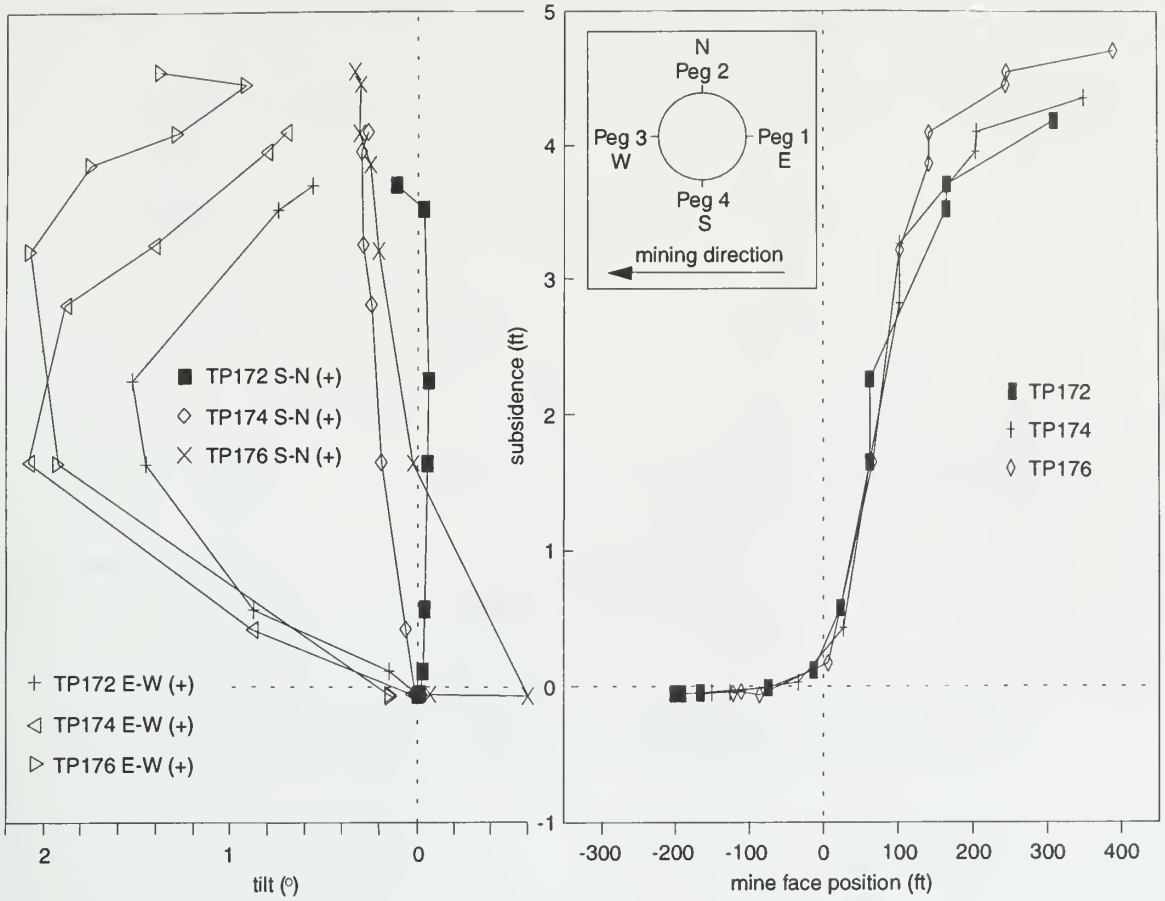

Figure 27 Subsidence, tilt, and curvature for panel 1, along the longitudinal line.

between 70 and about 500 feet behind the mine face, the magnitude of tilt started to decrease continuously to less than 0.5°. Time-dependent changes in tilt measured during the 3 months after undermining were lower than 0.1° (fig. 28). The transverse tilt perpendicular to the mining direction initiated simultaneously with the start of longitudinal tilt; it increased slightly as the face approached the tiltplates and reached a maximum value of about 0.5° at the end of the longitudinal extension zone. It then remained practically unchanged during the following period of readings. Tiltplate data are presented in appendix D.

Grid results A 60-foot-square grid was placed within the static tensile zone at the south edge of panel 2 to monitor the changes in maximum and minimum principal strains induced at the ground surface. Previous research indicated that the most complex surface movements would occur at this location and that the ratio of horizontal to vertical displacements would be at a maximum here. The westernmost grid row perpendicular to the mining direction coincided with the alignment of the transverse line (fig. 29). The grid was composed of nine 20-foot-square surface elements distributed 3 by 3. A total of 16 survey monuments was installed at the corners of these surface elements. In addition, four inclinometers were installed in 20-foot-deep boreholes at the corners of the grid to document the distribution of horizontal displacements, both parallel and perpendicular to the mining direction, with depth. The northeast and northwest inclinometers were 60 feet closer to the panel centerline than were the southeast and southwest inclinometers. Eight sets of readings were taken during a 2-month period, starting on September 22, 1990, when the panel face was 31 feet past the transverse line. The last set of readings was obtained on November 29, 1990, when the face was 2,328 feet past the transverse line. The face passed the grid between September 20 and 21, 1990; the panel was completed on November 27, 1990.

As the panel face advanced towards the grid, the ground surface initially moved northeast. Initial tilts measured on September 22 were small in magnitude (0.007–0.01 foot/foot, or 0.40°–0.57°) and limited to the northeast corner of the grid. The gradual and continuous increase in surface displacements, under the effect of the face advance, occurred simultaneously with the progressive

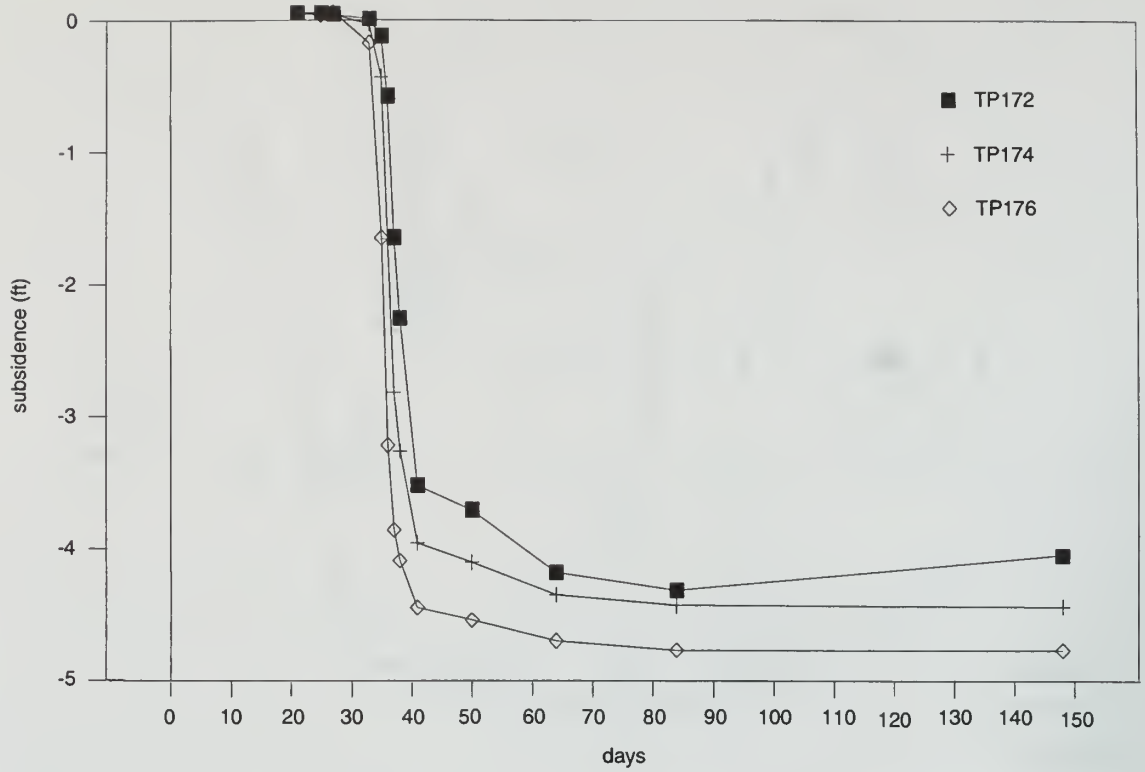

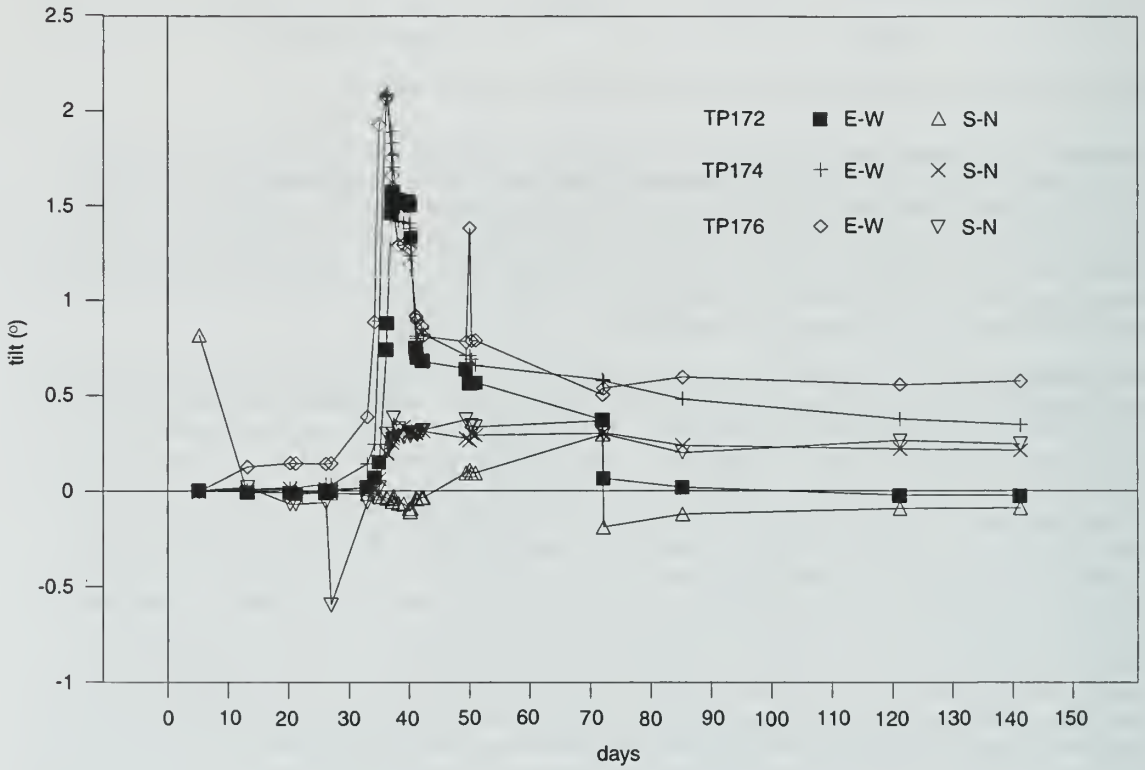

Figure 28 Development of subsidence and tilt over time for panel 1.

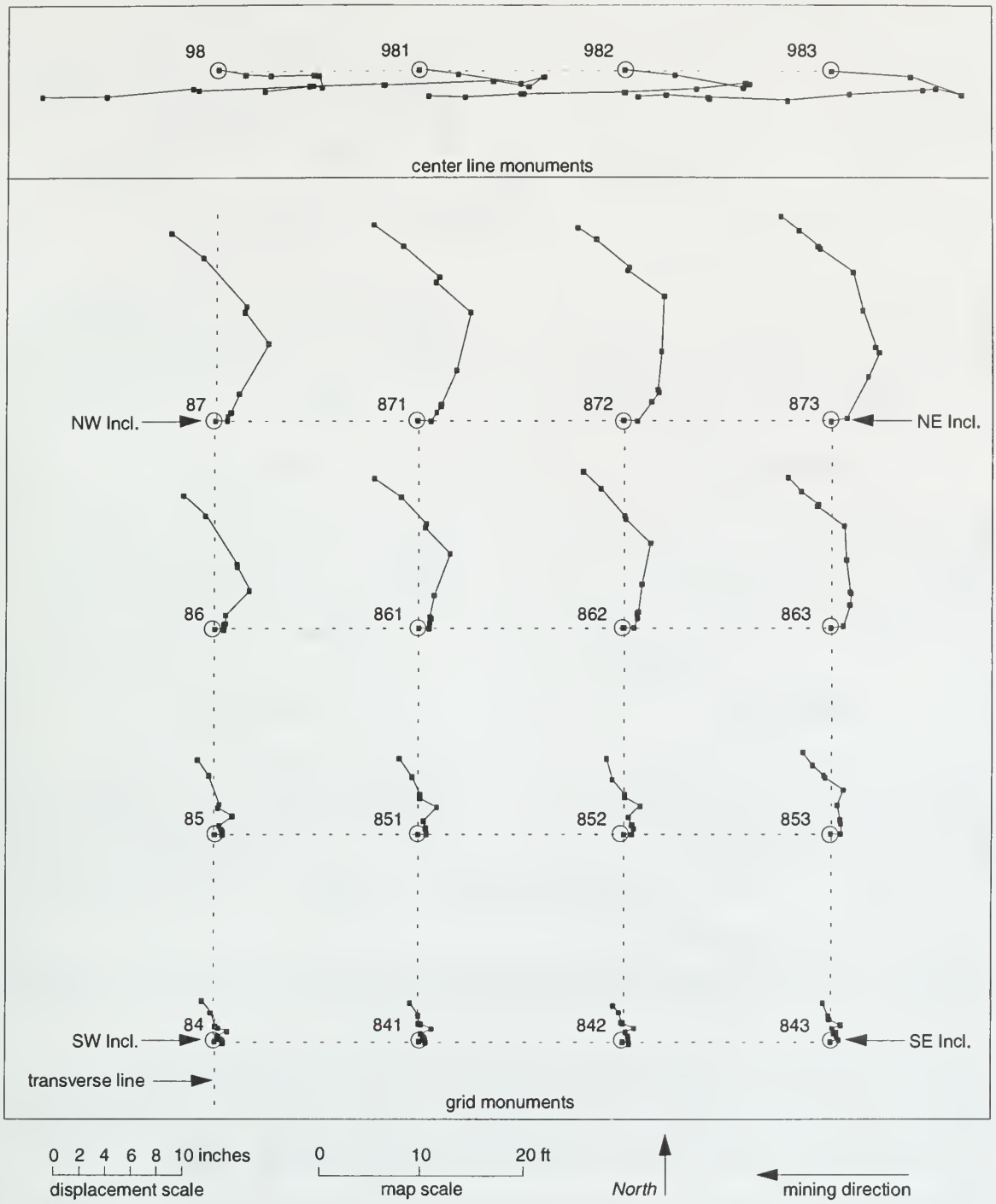

Figure 29 Panel 2 center line and grid surface horizontal displacements.

change in the direction of the displacements from the northeast to the north (fig. 30). Maximum displacements of up to 15 inches were measured at the northernmost monuments. Maximum horizontal extensional strains (maximum principal strains) of as much as 2.7% occurred when the face was about 300 feet past the grid (fig. 31). These values are slightly larger than the maximum tensile strain of 2.1% obtained within the static tensile zone on the transverse profile of panel 1. The largest compressive strain (minimum principal strain) determined within the grid was 0.7%, which is about one-half of the maximum compressive strain of 1.5% obtained in the static compressive zone along the transverse profile of panel 1. The maximum ratio of horizontal to vertical displacements was as high as 1.2 in the three southernmost grid rows (table 1); this ratio decreased to 0.87 in the northernmost grid row. The resultant of the northward and westward

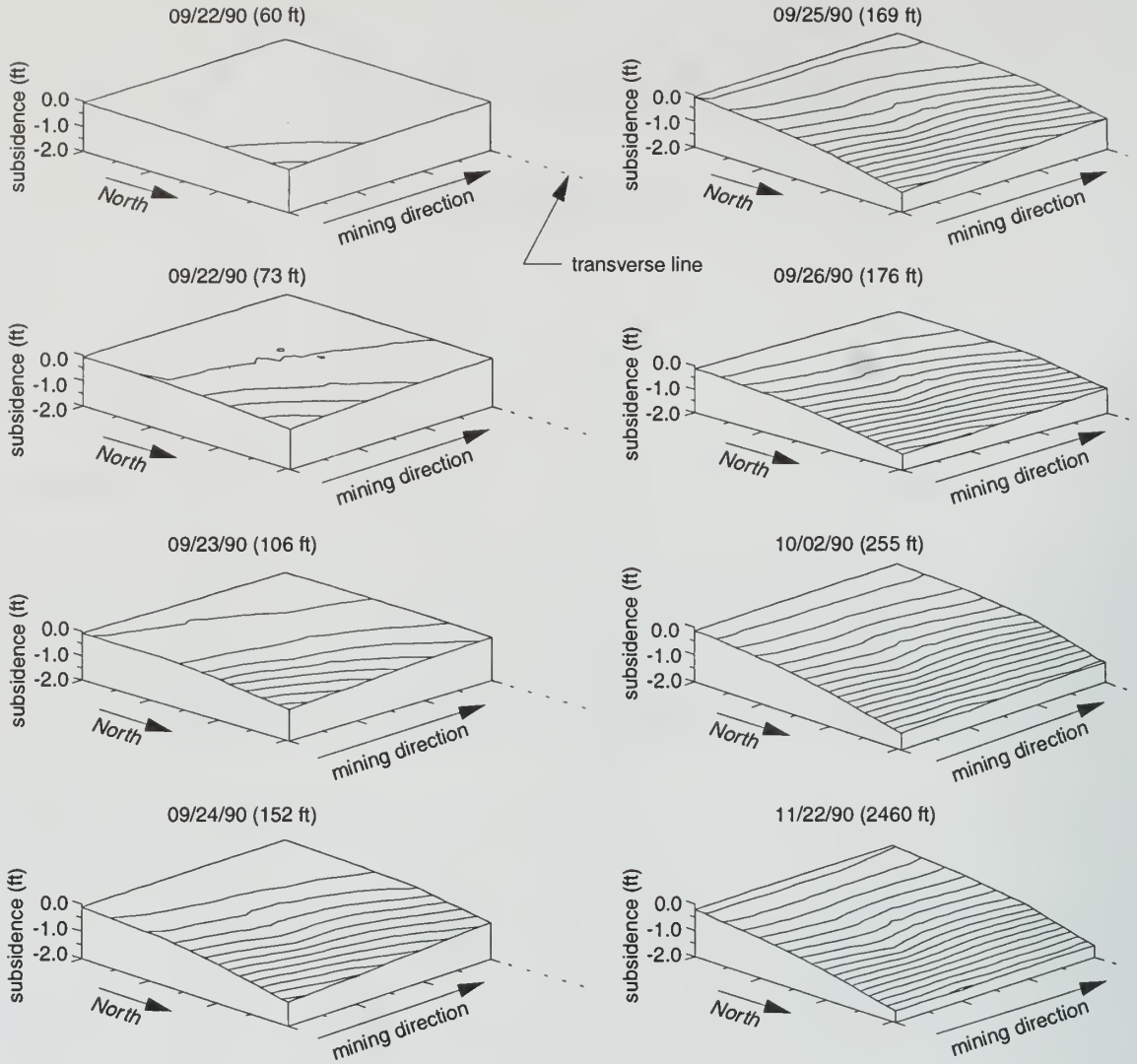

Note: Face position in relation to transverse line.

Figure 30 Three-dimensional plots showing the development of subsidence in the panel 2 grid. Each contour line equals 1 inch of vertical displacement (view is to the southwest).

components of displacements was considered in the computation of the displacement ratio. At the panel centerline, the maximum displacement ratio was about 0.25, which corresponded to a value of approximately one-fourth of that determined at the grid site located in the tensile zone of the panel. Final tilt values as large as 0.036 foot/foot (2.1°) were measured in the northern row of the grid. Tensile cracks started under a maximum principal strain of 0.6% to 0.9%.

Inclinometer readings followed the trends observed in the grid monuments: higher horizontal displacements were measured in the northeast and northwest inclinometers, which were closer to the panel centerline. Displacements of as much as 13.5 inches to the north were measured at a depth of 2 feet when the panel face was about 300 feet past the instruments (fig. 32). This face position was selected for subsequent displacement comparisons in the north direction because it indicated the end of the effect of the active mining on ground displacements. At this position, a remarkable decrease in the rate of displacements was registered for all inclinometers. For example, the rate of northward displacement in the northeast inclinometer decreased about 210 times from 4.2 inches/day to 0.02 inches/day. The corresponding northward displacements in the southeast and southwest inclinometers were about 1.8 inches (fig. 33). The resulting net horizontal displacement perpendicular to the mining direction was 11.7 inches over a length of 60 feet. Therefore, the average change in horizontal strain in the north direction at a depth of 2 feet was 1.63%. There was an indication that the effect of active mining predominated during the initial 5 days

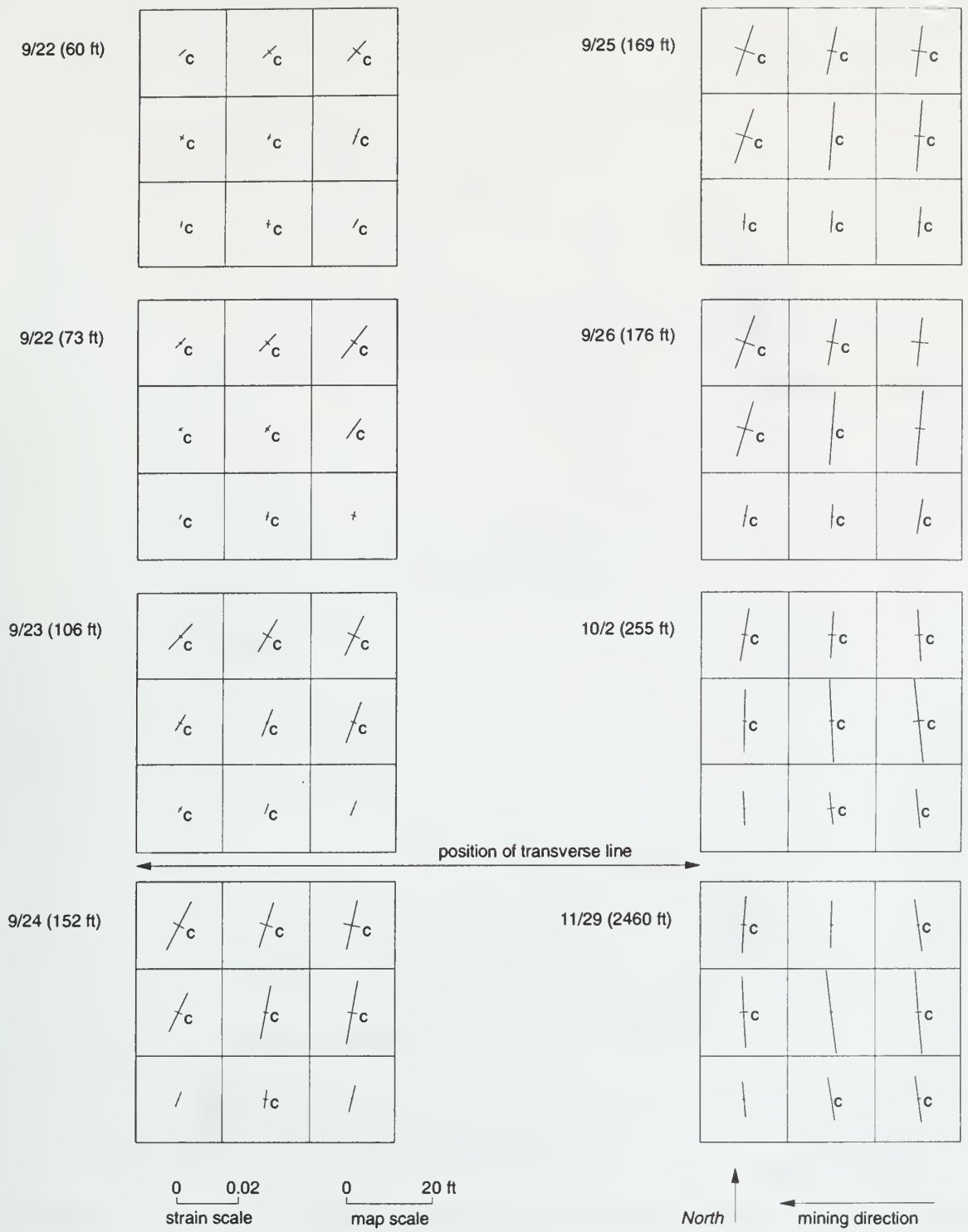

Figure 31 Principal strains calculated within each grid element for panel 2.

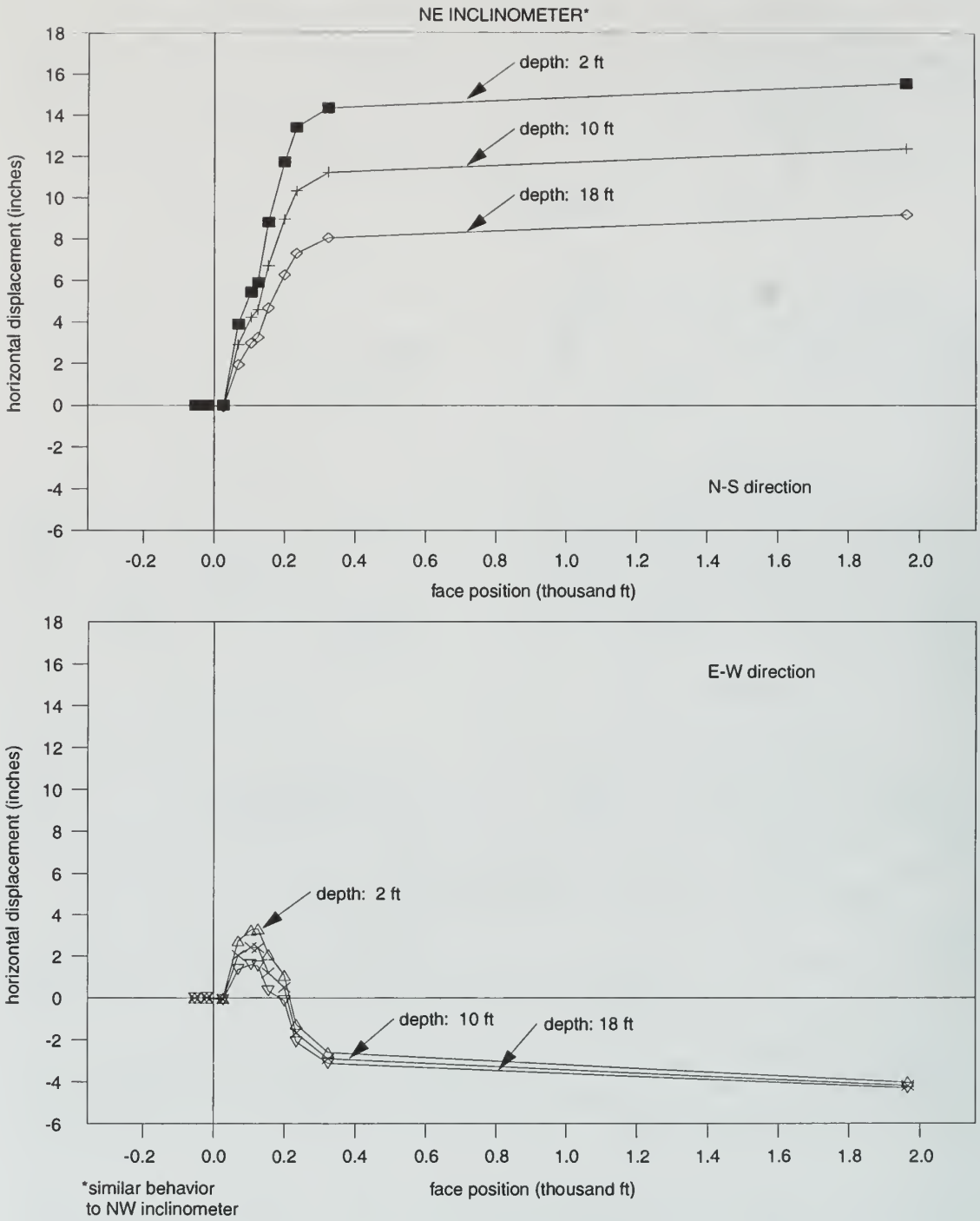

Figure 32 Horizontal displacements at northeast grid corner inclinometer for panel 2.

after the panel face passed the northeast and northwest inclinometers, and during the first 3 days for the southeast and southwest inclinometers. The development of time-dependent horizontal displacements was apparent in the last set of readings, taken 71 days after the panel face passed the instruments; the magnitude of displacements at a depth of 2 feet increased to as much as 16.0 inches in the northeast and northwest inclinometers and to as much as 3.0 inches in the southeast and southwest inclinometers. In general, displacements to the north decreased almost linearly with depth (figs. 34, 35). Given such a "linear" relationship within the drift, the horizontal displacements would decrease to zero at a depth of about 40 feet (Van Roosendaal et al. 1991).

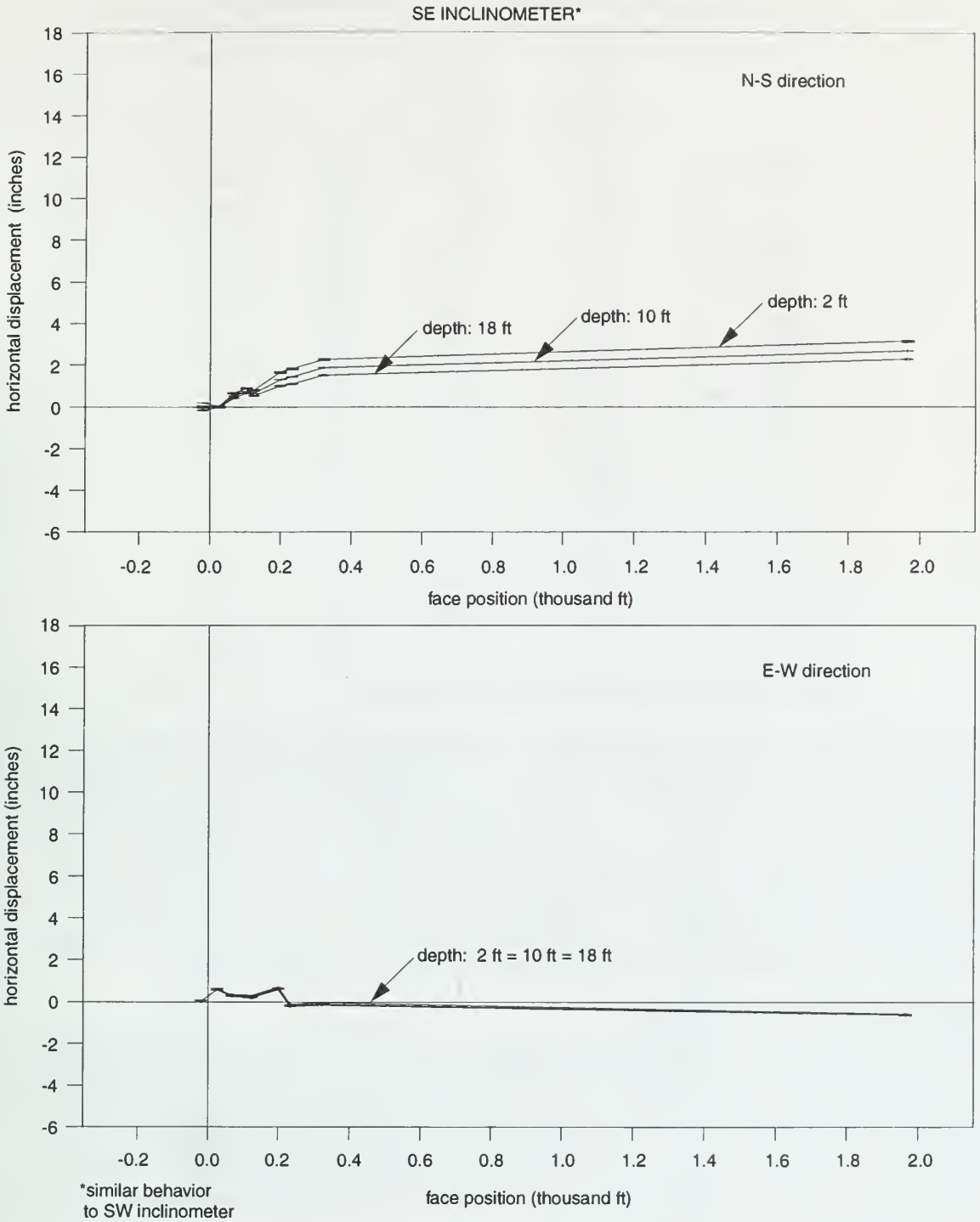

Figure 33 Horizontal displacements at southeast grid corner inclinometer for panel 2.

The magnitude of displacements towards the east direction was smaller and did not exceed 3.5 inches at a depth of 2 feet in the northeast and northwest inclinometers (fig. 32); eastward displacements started as the panel face reached the inclinometers and achieved the maximum value when the face was about 100 to 150 feet past them. The maximum displacements in the southeast and southwest inclinometers were measured when the face was about 200 feet past them and were close to 1 inch (fig. 33). After the maximum values were reached in the east direction, the displacements shifted west. The northeast and northwest inclinometers moved back to their initial positions along the east–west alignment when the mine face was about 200 feet past

Table 1 Panel 2 grid and centerline ratio of horizontal to vertical displacements.

Monument no.	Resultant horizontal displacement (ft)	11/22/90 surface settlement (ft)	HD/VD*	Direction
POS CO 0084	0.289	-0.2395	1.205	NW
POS CO 0841	0.265	-0.205	1.293	NW
POS CO 0842	0.253	-0.225	1.126	NW
POS CO 0843	0.269	-0.232	1.160	NW
POS CO 0085	0.521	-0.4655	1.120	NW
POS CO 0851	0.530	-0.4845	1.094	NW
POS CO 0852	0.528	-0.4405	1.198	NW
POS CO 0853	0.588	-0.5265	1.117	NW
POS CO 0086	0.936	-0.8265	1.133	NW
POS CO 0861	1.067	-0.936	1.140	NW
POS CO 0862	1.110	-0.844	1.315	NW
POS CO 0863	1.062	-0.966	1.100	NW
POS CO 0087	1.327	-1.5475	0.858	NW
POS CO 0871	1.372	-1.562	0.879	NW
POS CO 0872	1.361	-1.611	0.845	NW
POS CO 0873	1.417	-1.5775	0.898	NW
POS CO 0098	1.134	-4.49	0.253	SW
POS CO 0981	1.031	-4.667	0.221	SW
POS CO 0982	1.249	-4.588	0.272	SW
POS CO 0983	1.236	-4.51	0.274	SW

* Ratio of horizonal displacement to vertical displacement.

them; the southeast and southwest inclinometers reached their initial positions when the face was 250 feet past them. The northeast and northwest inclinometers then continued to move westward, maintaining the same rate of displacements (about 1.1 inches/day and 0.6 inch/day, respectively) until the face was 250 feet past them. Further displacements occurred at considerably lower rates—0.021 inch/day for the northeast inclinometer and 0.036 inch/day for the northwest inclinometer. These values correspond to a decrease of about 53 and 17 times the previous rates, respectively. Postmining displacements increased the horizontal displacements as much as 4 inches towards the west in the northeast and northwest inclinometers, and as much as 1 inch in the southeast and southwest inclinometers. These values of horizontal displacement were observed in all monitored depths (figs. 34, 35). All grid data are presented in appendix E.

Overburden Characterization

Geotechnical core logs Although drilling through the overburden was more difficult after subsidence because of the loss of drilling fluid in fractures, core recovery was good to excellent before and after subsidence. A comparison of the presubsidence (GT1) core from the TDR borehole and the postsubsidence (GT2) core drilled nearby is shown in figure 36. The core recovery largely reflected drilling problems. The rock quality designation (RQD) shows small decreases into the 90% to 99% range for some intervals because of subsidence fracturing in the postsubsidence core. The RQD is not an especially sensitive indicator because the observed subsidence-induced fractures are generally not narrowly spaced.

There was a clear increase in fracturing due to subsidence when the presubsidence (GT1) and postsubsidence (GT2) core logs were compared. On a whole-core basis, the increase was from 0.38 fracture per foot (GT1) to 0.50 fracture per foot (GT2). When comparable depth ranges were matched, the increase was from 0.32 (GT1) to 0.50 fracture per foot (GT2).

The change in the nature of the fractures is also distinctive. No fractures or discontinuities of more than 45° dip, except those around nodules or on steepened bedding, occurred in GT1. After subsidence, however, many high-angled (65°–85°) fractures were found within shale, siltstone, and sandstone units. The interval of GT2 with the largest increase in fracturing (178–188 ft) was within the Trivoli Sandstone; this interval shows the predominantly high-angled fracturing associated with subsidence. The pre- and postsubsidence geotechnical core logs are presented in

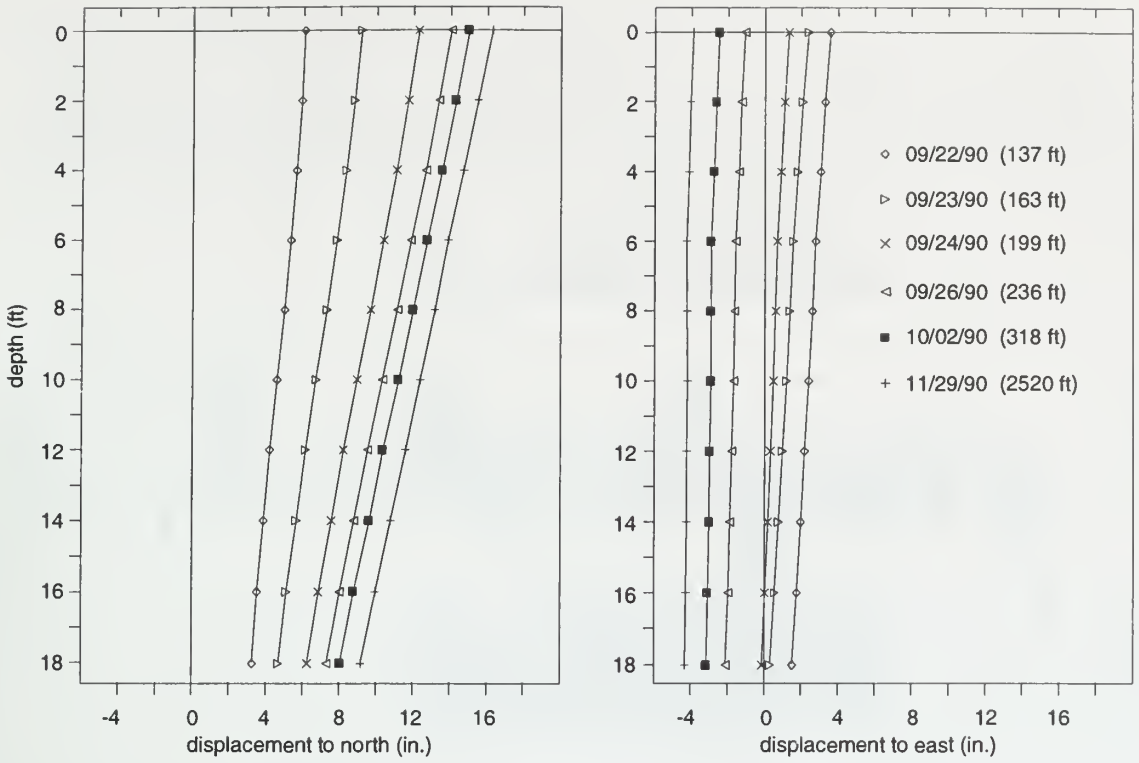

Figure 34 Displacement profiles for the inclinometer at northeast corner of the panel 2 grid.

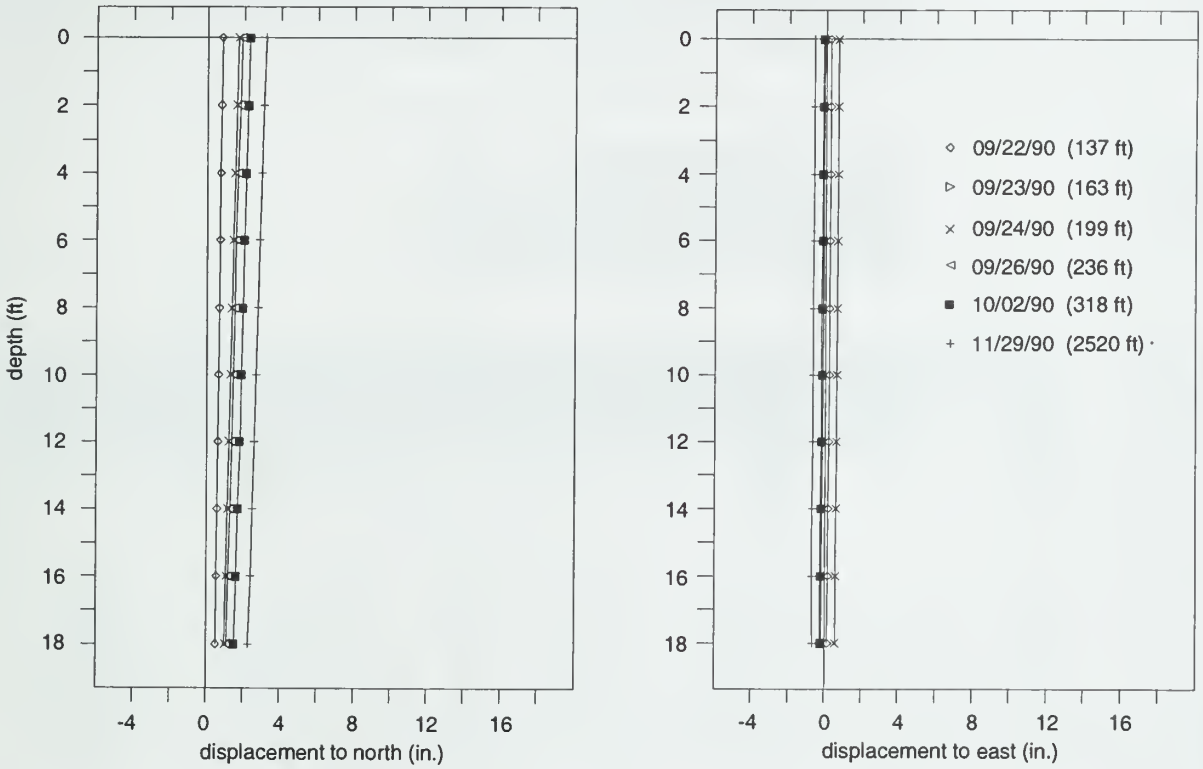

Figure 35 Displacement profiles for the inclinometer at the southeast corner of the panel 2 grid.

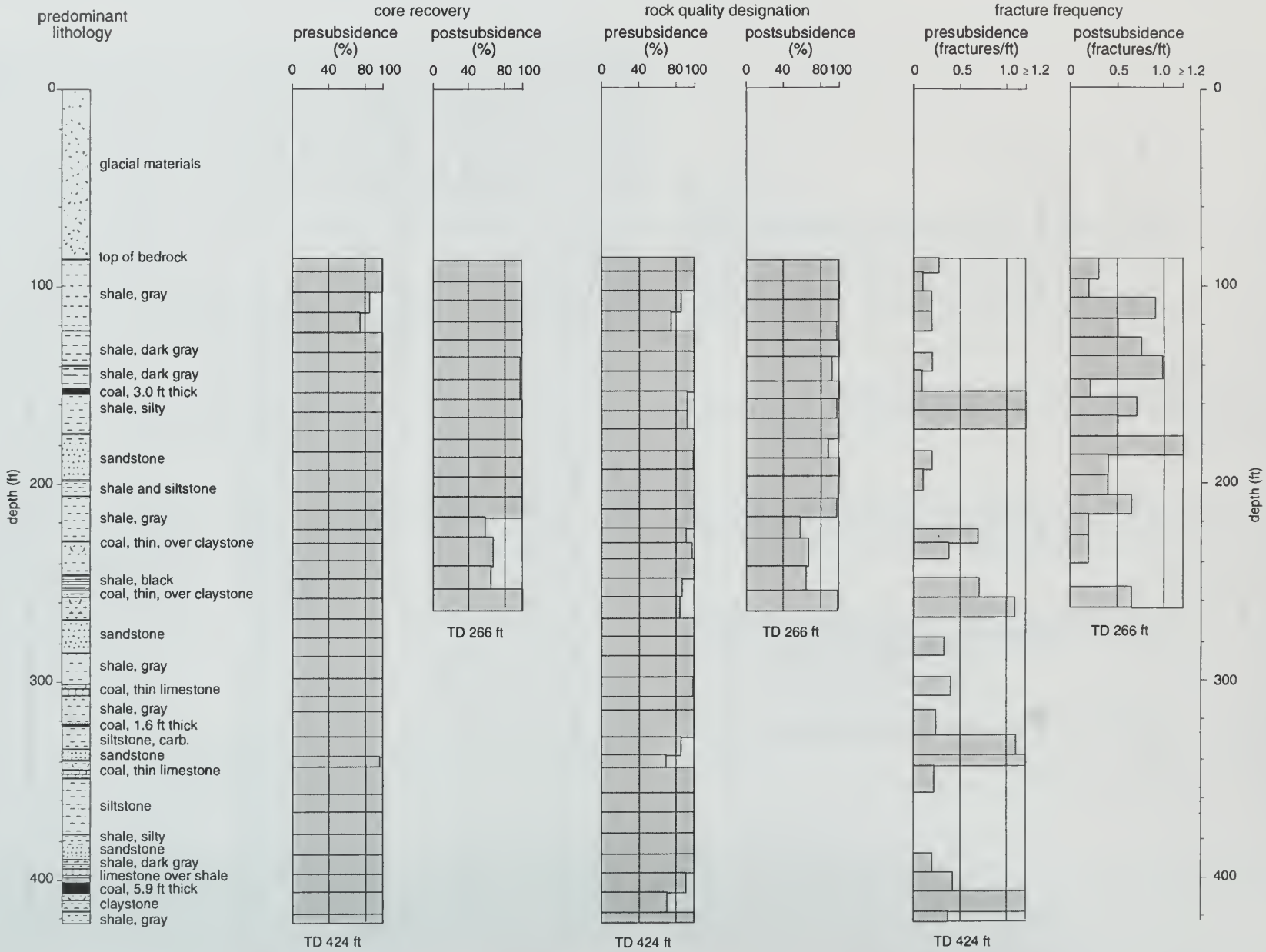

Figure 36 Comparison of pre- and postsubsidence geotechnical core logs.

appendix F. The GeoTechnical Graphics System software (1991) was used to combine all the field logging notes into a final core log.

Geophysical logs A comparison of downhole geophysical logs for pre- and postmining (figs. 37, 38) showed that the sandstone layers tend to exhibit a larger decrease in both shear and compressive wave velocities; a decrease as high as 35% was measured within a 25-foot-thick sandstone layer between the depths of 176 and 199 feet. This decrease reflected not only the

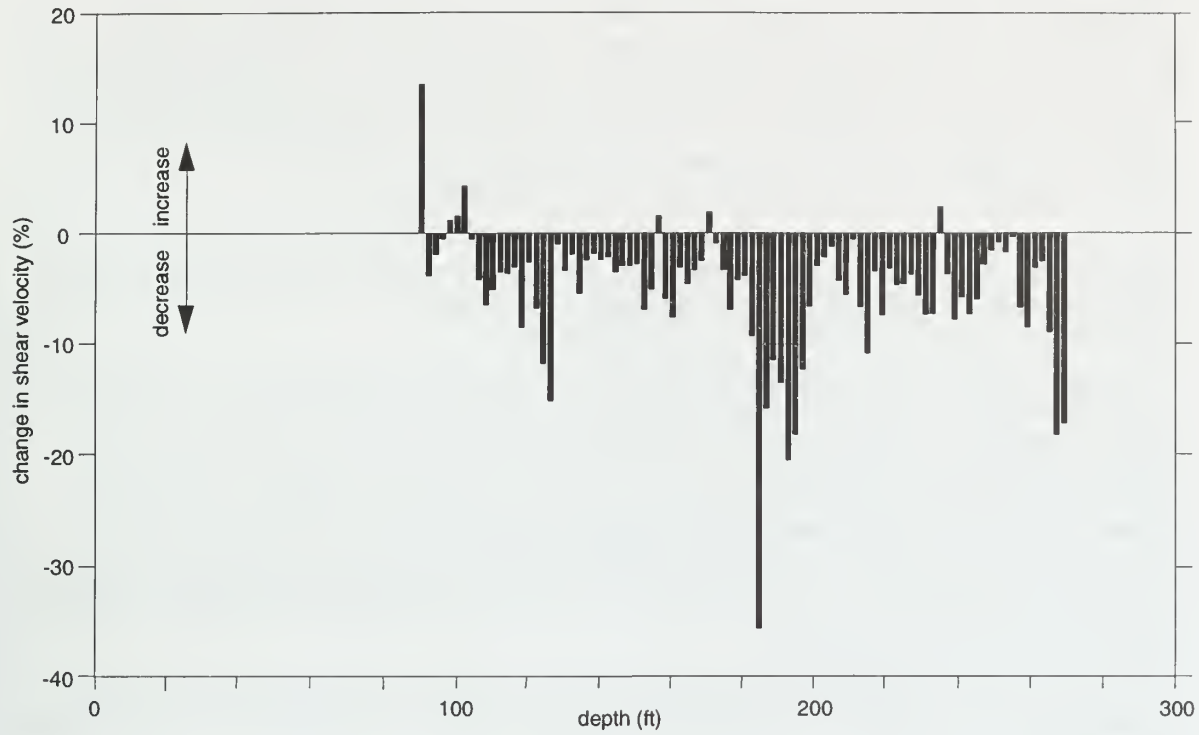

Figure 37 Changes in shear wave velocity (pre- and postsubsidence) for panel 1.

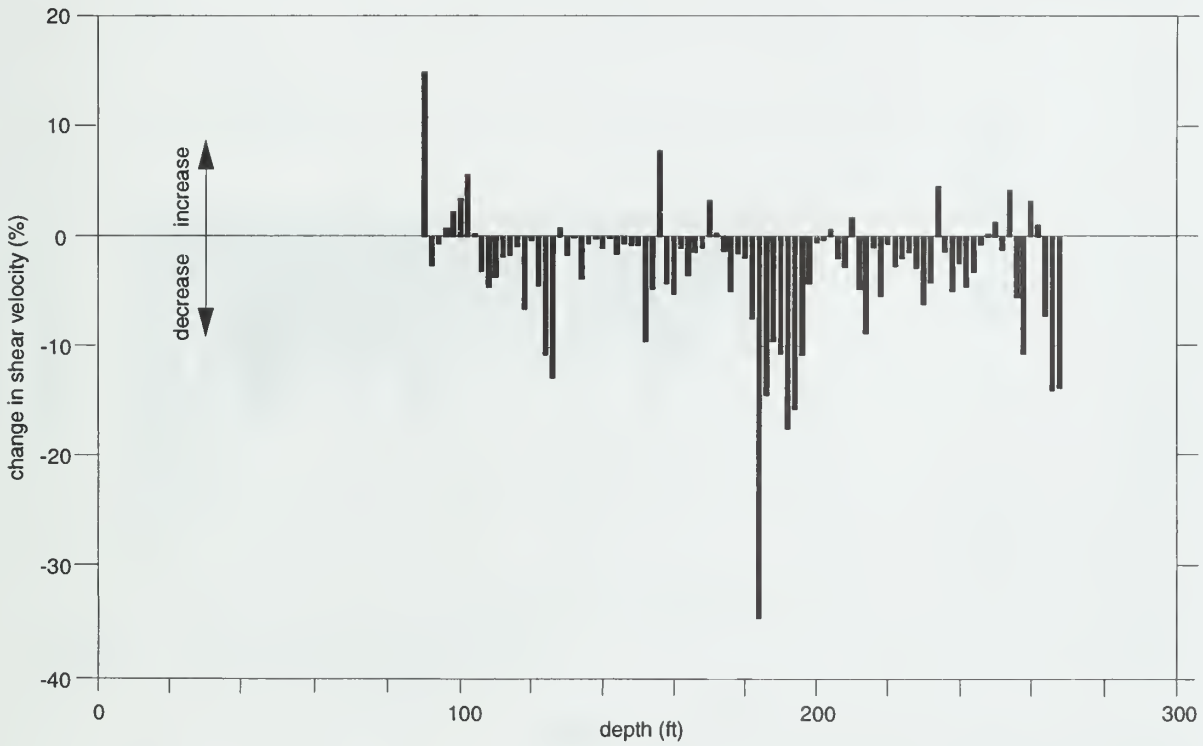

Figure 38 Changes in compressive wave velocity (pre- and postsubsidence) for panel 1.

development of more fractures in this more brittle layer with respect to other adjacent layers, but also the occurrence of bed separation. In another sandstone layer between the depths of 272 and 285 feet, shear and compressive wave velocities decreased 18% and 14%, respectively. For the remaining depths, decreases of 1% to 15% in shear wave velocity and decreases of 1% to 13% in compressive wave velocity were recorded; more often, the decreases in both velocities were less than 8%. The decreases in wave velocities were induced as a consequence of wave attenuation through a fractured medium filled with fluid.

The percentage change in bulk density was relatively smaller; the largest decrease, which occurred between the depths of 255 and 266 feet, did not exceed about 7% to 8% (fig. 39). At these depths, a layer of coal graded down to impure limestone and then to claystone at the base. It was apparent that the changes in bulk density were related to rocks less brittle than sandstone because the second larger decrease of 7% was measured in a shale layer located between the depths of 152 and 172 feet. The decreases in the remaining depths were smaller than 5%. Pre- and postsubsidence geophysical logs are presented in appendixes G and H.

Intact rock properties Postsubsidence rock strength properties data, obtained from laboratory testing, were compared with presubsidence data to evaluate possible changes in "intact" rock properties within the overburden. There was no clear indication that the rock properties changed under the effect of active mining (figs. 40, 41; tables 2, 3).

The typical response of the ground to the change in state of stress imposed by the face advance was the generation of differential displacements that resulted in fractures or cracks. It is known that, for a given rock mass, the frequency of these fractures depends on the magnitude of the change in stresses, which in turn depends on the ratio of width/depth of the panel, the stiffness of the rock mass, and the rate of face advance. Samples for laboratory testing were collected between fractures. Under this condition, the effect of fractures is eliminated in such a way that mining-induced micro-fractures were the only factor that could change the "intact" rock properties. The effect of the fractures on rock properties is dependent on the sample size, the ratio of fracture spacing to sample size, and the orientation of the fractures. There was no apparent effect of subsidence on intact rock strength.

The glacial drift located above the bedrock presented liquid limit, plastic limit, and natural water content values that ranged between 2% and 35%, 14% and 18%, and 20% and 26%, respectively (appendix I).

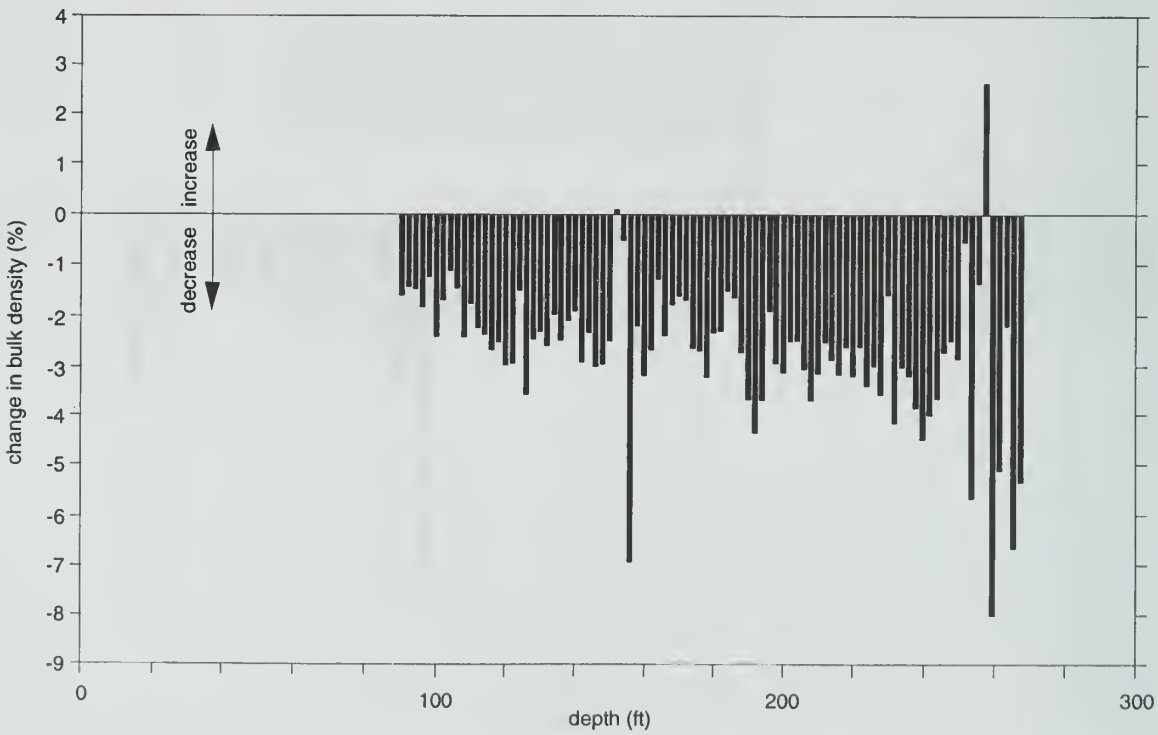

Figure 39 Change in bulk density (pre- and postsubsidence).

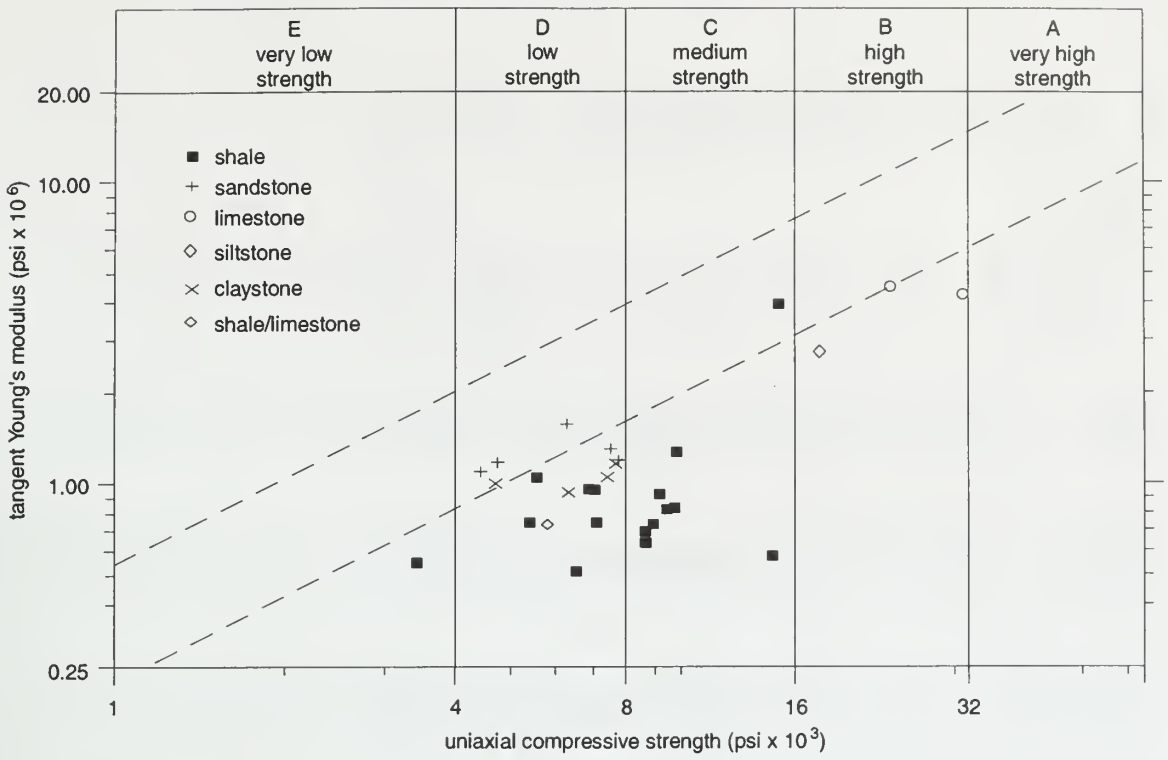

Figure 40 Presubsidence intact rock properties.

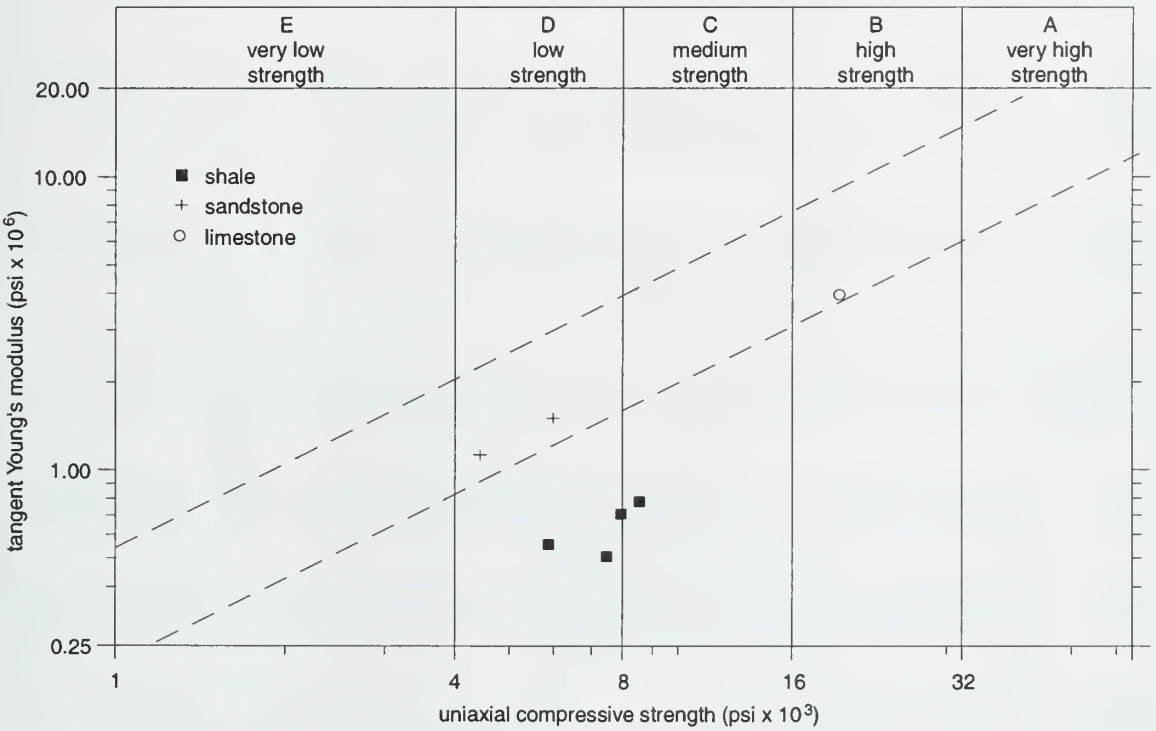

Figure 41 Postsubsidence intact rock properties.

Table 2 Rock properties for samples from the presubsidence borehole.

Sample ID depth (ft)	Rock type	qu (psi)	Height/ diameter ratio qu samples	Moisture content (@qu)(%)	Modulus (psi x 10*6)	Shore hardness	Average indirect tensile strength (psi)	Average axial point load index (psi)	Average T500 (MPa)	Compressive wave velocity (ft/sec)	
										Perpendicular to bedding	Parallel to bedding
126	SH/LS	17594	1.98	0.31	2.74	36	1568	2349	9.03	13323	16524
135	SH	6574	1.68	1.47	0.52	16	**	787	3.54	**	12420
147	SH	**	**	**	**	**	757	631	2.44	**	**
158	SH	9468	1.84	0.84	0.83	16	692	1459	6.4	8417	12513
166	SH	8972	1.75	1	0.74	15	705	1088	4.28	**	12427
175	SH	6855	1.93	1.14	**	17	875	1228	4.92	**	12223
179	SS	4454	1.96	0.15	1.1	17	342	652	2.55	7252	8486
197	SS	6323	1.96	0.21	1.58	14	444	703	2.77	**	9588
203	SH	7158	1.68	**	0.75	19	785	1105	3.69	**	13066
214	SH	8698	1.92	1.54	0.65	16	783	725	3.29	4549	12803
215	SH	3450	1.64	1.8	0.55	17	369	724	2.87	**	12629
228	SH	14355	1.95	2.11	0.62	18	608	672	2.53	**	12897
235	SH	9859	1.78	0.31	1.28	29	738	1824	6.82	**	12343
247	SH	9800	1.79	1.04	0.84	17	811	983	3.78	**	13487
261	CLST-SH	7430	1.97	0.73	1.05	15	427	867	3.34	9528	10817
266	CLST-SH	4759	1.71	0.84	0.99	22	458	781	2.81	**	**
277	SS	7560	1.87	0.23	1.31	21	509	922	3.33	**	**
286	SH	9195	1.88	1.28	0.93	14	881	1388	5.2	**	**
289	SH	7094	1.97	1.06	0.96	15	919	1620	6.37	**	**
307	LS	31293	1.75	0.24	4.24	44	2180	3567	13.65	**	**
313	SH	8664	1.93	1.35	0.7	18	944	1132	4.61	**	**
326	CLST	7606	1.87	0.82	1.17	19	1013	1501	5.83	**	**
327	CLST	6382	1.96	1.3	0.94	17	1077	1450	5.31	**	**
336	SS	4772	1.88	0.31	1.18	20	279	431	1.73	**	**
348	SLTST	**	2.04	**	**	**	506	1122	4.59	**	**
352	SH	5597	2.09	1.6	1.06	27	802	1216	4.7	**	**
362	SH	5439	2.09	1.7	0.75	15	815	371	1.42	**	**
371	SH	**	2.08	**	**	**	386	948	3.46	**	**
380	SLTST	5850	1.94	1.16	0.73	23	953	1286	5	**	**
389	SS	7801	1.75	0.64	1.2	25	747	1776	6.91	**	**
400	LS	23397	1.75	0.08	4.49	40	1667	2641	10.01	**	**
402	SH	14894	2.03	0.08	3.94	38	1569	2074	8.06	**	**
416	SH	6898	1.87	1	0.96	15	887	1099	4.51	**	**
420	LS	17471	1.79	0.32	**	42	858	1741	7.24	**	**

** No sample available

Table 3 Rock properties for samples from the postsubsidence borehole.

Sample ID depth (ft)	Rock type	qu (psi)	Height/ diameter ratio qu samples	Moisture content (@ qu) (%)	Modulus (psi x 10*6)	Shore hardness	Average indirect tensile strength (psi)	Average axial point load index (psi)	Average T500 (MPa)	Compressive wave velocity (ft/sec)	
										Perpendicular to bedding	Parallel to bedding
104	SH	8500	2.004	1.46	0.78	19	669	894	3.71	7136	11197
111	SH	**	**	**	**	**	630	914	3.82	6664	11848
118	SH	7452	1.976	1.72	0.51	21	**	**	**	**	12620
124	LS	19383	2.06	0.35	3.93	35	1139	2563	10.32	15739	16667
130	SH	**	**	**	**	**	**	774	**	7089	11891
146	SH	5844	1.853	1.28	0.56	18	**	1168	**	5842	13101
178A	SS	4437	2.106	2.04	1.12	13	337	599	3.17	6587	8004
178B	SS	5981	1.97	0.98	1.50	14	**	**	**	**	**
209	SH	7896	2.027	1.79	0.71	16	619	1123	4.46	8002	12257

** No sample available

Overburden Deformation Monitoring

Time-domain reflectometry A 0.5-inch (12.5-mm) diameter TDR cable was installed in a 425-foot-deep, angled borehole at the centerline of panel 1. Readings were taken for 8 months, starting on October 12, 1989, about 2 months before the instrument was undermined, at which time the panel face was located 1,334 feet away. The last reading was obtained on June 28, 1990, approximately 6½ months after the panel face had passed the instrument and 3½ months after the completion of the panel. The panel was terminated on March 18, 1990, at a distance of 2,564 feet past the TDR cable. Readings were taken up to five times daily during the active mining.

Subsidence-induced changes in the cable were predominantly differential shear displacements, as compared with extensional displacements. As one would expect, the frequency of displacements increased with the face advance towards the cable. The first differential shear displacement was recorded on November 28, 1989, when the mine face was about 208 feet away from the instrument (fig. 42). A shear plane was detected at a depth of 173 feet within a layer of slightly silty and slightly fissile shale close to the contact with an underlying sandstone layer. The generation of this differential shear displacement could be ascribed to the slight difference in stiffness between the two rocks at that depth. The presubsidence values for Young's modulus obtained in intact samples of shale and sandstone collected close to this contact were 0.8×10^6 psi and 1.1×10^6 psi, respectively.

On December 11, 1989, when the panel face was located 79 feet away, the differential displacement along this first shear plane increased and progressed to a break in the cable at about a depth of 173 feet. No subsequent information was available for the units below the cable break. At the same time, the cable was subjected to an extensional displacement between the depths of 152 and 155 feet, where a thin coal layer separated shale layers.

Two days later (December 13, 1989) at 4:00 p.m., three new differential shear displacements at the depths of 101, 117, and 141 feet were measured within a slightly silty and slightly fissile shale layer located between the depths of 86 and 176.2 feet; the mine face was only 11 feet from the instrument. This shale was well indurated between the depths of 86 and 103.5 feet and also between the depths of 123.5 and 132.5 feet. The value of Young's modulus determined in an intact sample of well indurated shale was 2.7×10^6 psi, about three times higher than those values obtained in nonindurated shales. Such contrasting stiffness in the shale layer tended to control the location of the shear planes. All three shear planes were located within 8.5 feet of the contact between the well indurated and nonindurated shales. In addition, an increase in the thickness of that tensile zone from the depths of 152 and 155 feet to the depths of 150 and 160 feet was detected on December 11. At 9:00 p.m. on December 13, an extensional displacement was recorded within the glacial drift between the depths of 52 and 55 feet, where a standard penetration test (SPT) was refused. The indication of a vertical extension in glacial drift was in accordance with the surface subsidence monitoring data and with the shallow MPBX readings. The next day, at 9:00 a.m., when the mine face was 18 feet past the instrument, a cable break was recorded at a depth of 141 feet; an extensional displacement was also detected at a depth of 76 feet. The reading taken 3 hours later (11:45 a.m.) indicated that the cable underwent a shear break at a depth of 101 feet. On December 15, 1989, the first reading of the day (taken at 10:30 a.m.) showed that the cable had broken at a depth of 76 feet. The mine face at that time was located approximately 63 feet past the instrument. After this cable breakage within the glacial drift, displacement data for the rock mass were not available.

Over the next 6½ months of readings, only the upper portion of the glacial drift, where the TDR cable remained unbroken, could be monitored. Minor differential shear displacements that were insufficient to generate any cable breakage were recorded during this period. On December 27, 1989, when the mine face was 160 feet past the cable, differential shear displacements were registered at the depths of 32.5, 54.5, and 74.5 feet. Two more time-dependent differential shear displacements were detected later when the panel mining had already been completed: one on April 19, 1990, at a depth of 36 feet and another on May 23, 1990, at a depth of 12.5 feet. Differential shear displacements tended to form at depths with lower SPT values. SPT values ranged from 6 to 49 blows per foot; more often, they were higher than 15 blows per foot. The penetration of a split-spoon sampler met refusal at a depth of about 50 feet.

Unfortunately, the TDR cable readings did not reflect the overall behavior of the overburden rock mass during and after active mining because of several cable breakages. A TDR cable with a diameter of 12.7 mm, the type installed in panel 1, could not support a shear displacement higher

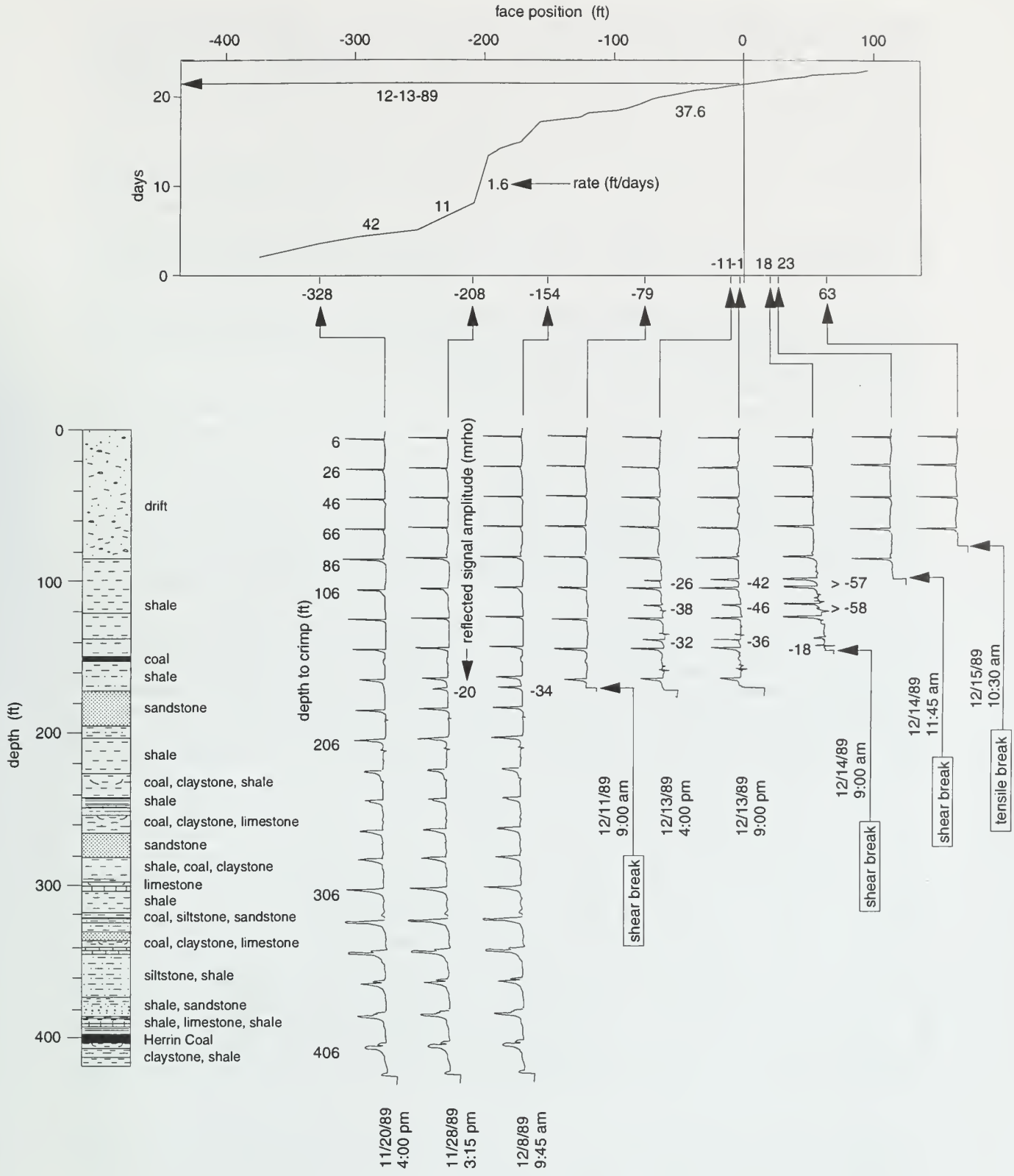

Figure 42 Progression of TDR cable deformation at the centerline of panel 1.

than 10 mm (0.5 in.) or a tensile displacement more than 20 mm (1.0 in.) (Bauer et al. 1991). Because the rock mass over the panel experienced displacements larger than those that could be resisted by the TDR cable, cable breakages were inevitable. The breakages of the TDR cable indicated, however, the most stressed region along the intact cable at the moment of the readings. Such a region was usually located near a contact between two layers with contrasting stiffness. Most often, the displacements were induced through the weak layer.

Multiple-position borehole extensometer Vertical deformation in the overburden was determined by monitoring two six-anchor multi-position borehole extensometers (MPBX) installed at the centerline of panel 1. MPBX readings were taken for 5 months, starting on November 8, 1989, when the panel face was about 700 feet from the borehole extensometers. The last set of readings was obtained on March 29, 1990, when the face was about 2,500 feet past the instruments. The anchor displacements were measured up to four times daily during active mining.

Because the shallow and the deep MPBXs were located along the panel centerline and were only 31 feet apart, the anchor displacements in these two extensometers were analyzed together. In addition, they were correlated with the subsidence data obtained at the top of boreholes and the results were used to determine the total anchor displacements (fig. 43).

Most of the displacements occurred during a period of 5 days, between December 15 and December 19, 1989. Large displacements began when the face was within 30 feet of the extensometers, continued while the face paused, and then advanced 150 feet past them. The anchor rods settled between 3.6 and 3.9 feet at the end of this 5-day period. This period coincided with the period when the surface subsidence monuments underwent the most rapid rate of subsidence of about 0.25 foot per day. Initially, differential displacements between the ground surface and the shallowest anchor at a depth of 120 feet were very small. As the mine face advanced and the magnitude of settlements increased, however, extensional differential displacements between these two points became as much as 0.5 foot. Increase in differential displacements as the face advanced was the general tendency that predominated between most of the anchors. Most of the extension was induced within the glacial drift, which extended to a depth of 80 feet. In addition, a differential extension of 0.15 foot was measured on December 19 between the depths of 200 and 220 feet. The description for this hole showed that, at a depth of 200 feet, there was a geological contact between a 25-foot-thick sandstone layer and an underlying 30-foot-thick shale layer. The extensional behavior may be associated with the difference in relative stiffness and subsequent bridging between these two rocks and, more importantly, with the relative position between them. The Young's modulus of the sandstone averaged 1.3 x 10^6 psi and that of the shale averaged less

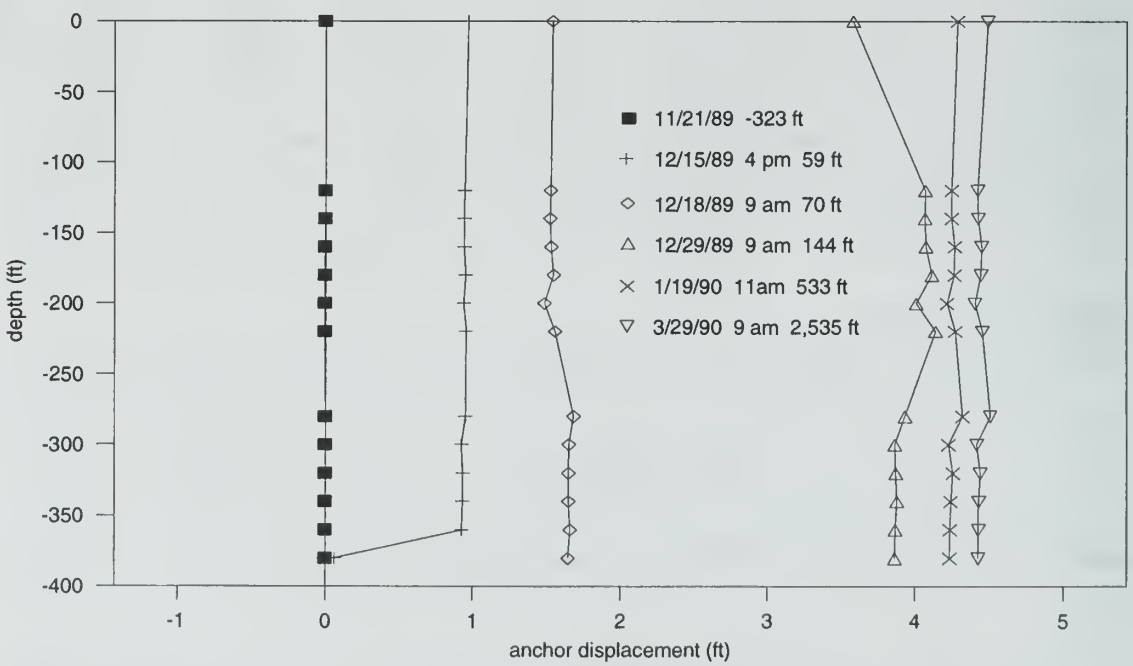

Figure 43 Distribution of vertical displacements with depth for panel 1.

than 0.6 x 10^6 psi (table 2). Comparison of measurements taken at depths of 220 and 280 feet suggests that the rock mass, composed mainly of shale, experienced a differential settlement of about 0.15 foot. The magnitude of differential displacements between other anchors was consistently lower than 0.10 foot during this period.

The rock mass, which was located between the depths of 80 and 175 feet and composed mainly of shales overlying a sandstone layer, behaved as a rigid slab or beam during the period of large displacements. A similar "beam" performance was observed between the depths of 300 and 385 feet where the rock mass was composed of several layers of limestone, shale, claystone, and sandstone. Each of these lithologic units averaged less than 10 feet in thickness.

Additional settlements were measured for 3 weeks after the undermining when the panel face progressed from 150 to 300 feet past the extensometers. The maximum cumulative settlement measured at the end of this period was close to 4.4 feet for all of the anchors. The change from a more irregular distribution of displacements with depth, as observed at the end of the previous period, to a new, practically uniform displacement pattern indicated the accommodation of the rock mass with the closure of fractures or bedding separations. Subsequent extensometer readings taken during a period of about 3.5 months after the undermining showed very small increases in displacements, which were usually less than 0.1 foot. There was no evidence that any anchor rods broke during active mining. Appendix K contains the data collected from both the shallow and deep MPBXs.

Hydrogeologic Response to Subsidence

Appendix J contains a full set of drift and bedrock hydrographs, which have drop line data integrated with the continuous recorder data, and a table of piezometer characteristics. The hydrographs were edited for data that suggested a pressure transducer failure as compared with other nearby piezometer data; hydrographs were terminated if the transducer stopped functioning or the piezometer was damaged.

Drift water level response Drift piezometers 1, 2, and 3, and the drift control piezometer were located adjacent to panel 1 (fig. 7). Their maximum depth within the drift ranged from 53 to 76 feet (appendix J). Drift water levels showed substantial changes during and after mining. Factors influencing the changes in water levels included proximity of mining to the piezometer, the rate of and pauses in longwall face advance, and seasonal patterns of precipitation and evapotranspiration. The hydrograph for drift piezometer 3 (DP3) is used to illustrate these trends (fig. 44).

Drift piezometers 1, 2, and 3 all showed similar patterns of response to mining, but the drift control piezometer (DPC) showed only a slight response to nearby mining and then was in a flowing artesian condition for much of the study period. DP1, DP2, and DP3 all showed generally rising levels in the late fall and an upward spike in early December 1989. The spike may have been due to the "Noordbergum" effect (Verruijt 1969), which is a short-term dynamic effect caused by ambient stress from lowered water pressure in units below the piezometer. Piezometers DP2 and DP3 showed slight drops in early December, which may have been a result of the projected influence of the maximum tensile zone behind the approaching longwall face, still 250 feet away. It is impossible to separate the seasonal rise in the late fall from a likely gradual rise due to the Noordbergum effect (A.M. Curtiss, NIU, pers. comm. 1994); however, the strong upward spike on the DP1 hydrograph around December 10 probably was the Noordbergum effect alone. All three piezometers showed a rapid drop of 8 to 11 feet related to the start of the maximum tensile period produced by the passing of the mine face beneath each piezometer. DP1, DP2, and DP3 also all reflected the upward spike in mid-January, which may have been produced by the compressive event following soon after the passing of the face. After the spike, the decline continued until early February 1990. There was then a recovery until May, which was followed by another decline.

Mining of panel 2 on September 2, 1990, produced a decline in DP2 and DP3 that continued for nearly 1 month, but there was a negligible response in DP1, which was 600 feet from the mining. Piezometers DP2 and DP3 reacted to the tensile and compressive wave from the mining of panel 2. After October 1990, the curves seemed to respond primarily to seasonal precipitation patterns (fig. 45). The mining of panel 3 (which passed the piezometers on April 21, 1991) seemed to have had little effect on the three piezometers.

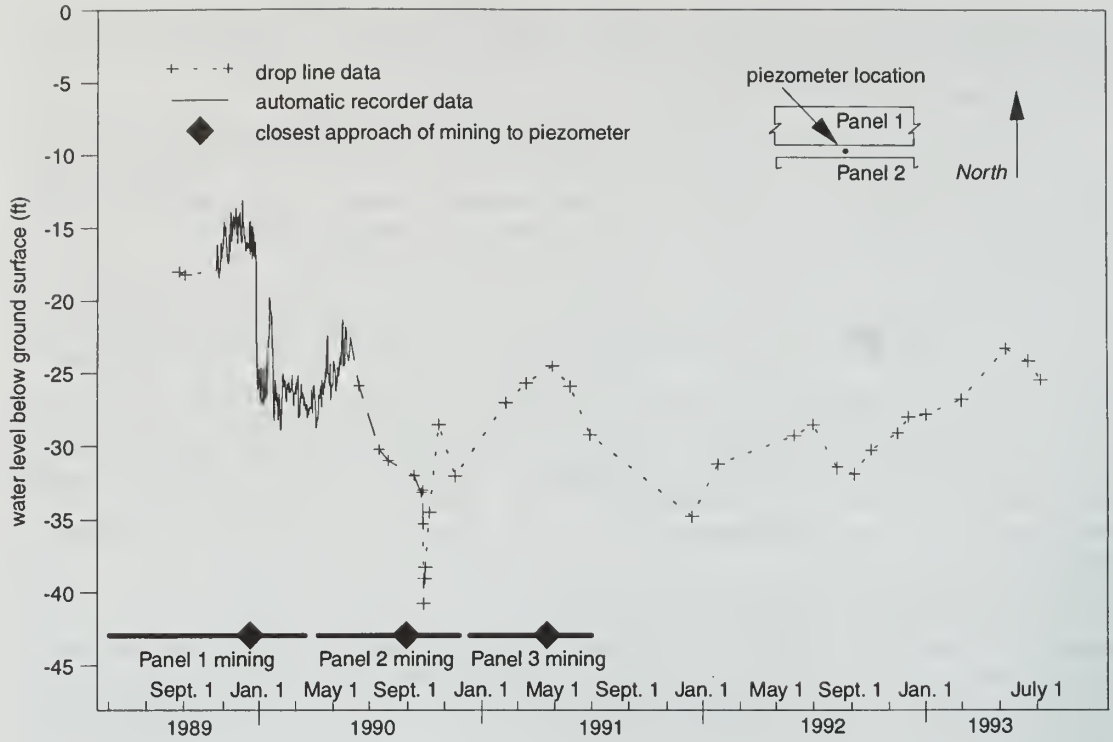

Figure 44 Response of drift piezometer 3 (DP3) to periods of mining.

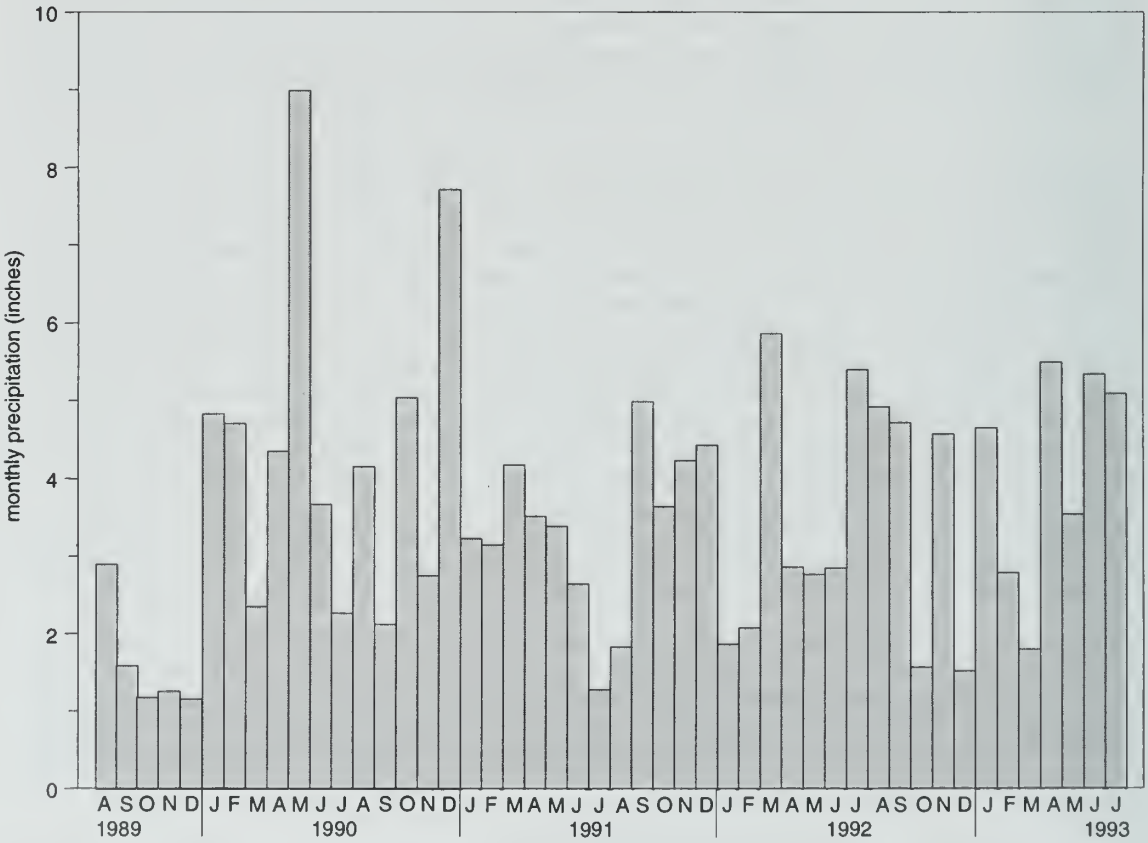

Figure 45 Monthly precipitation near the study site.

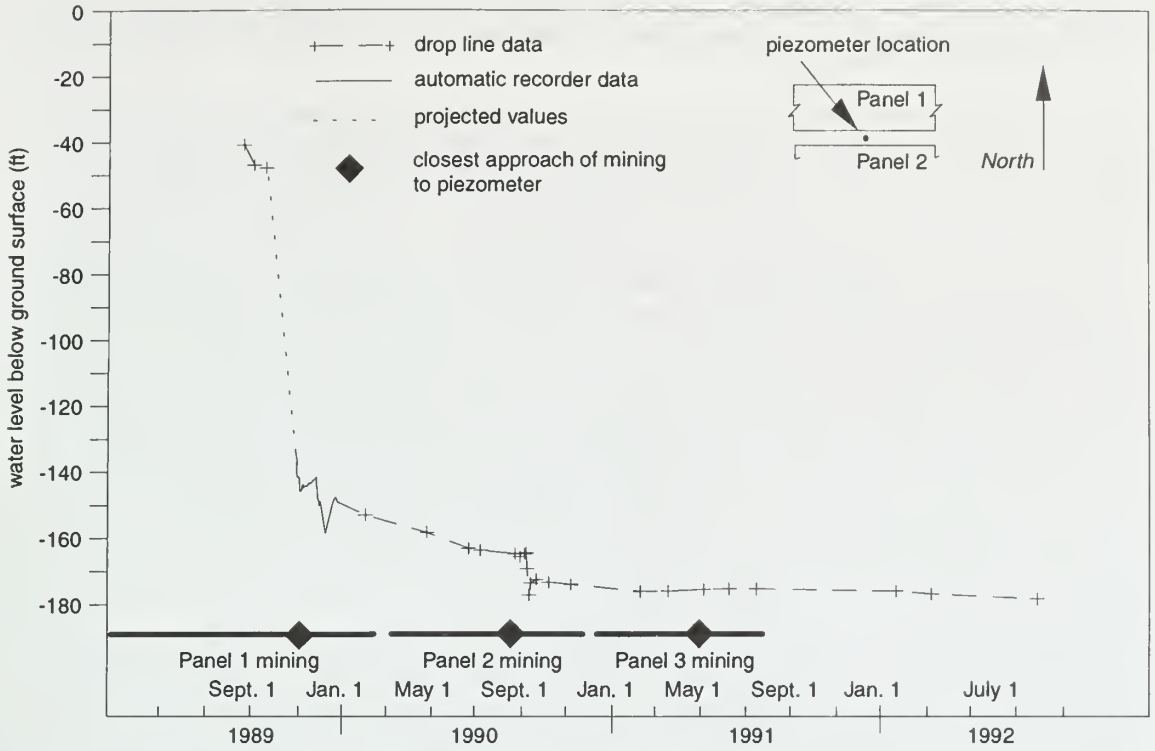

Figure 46 Response of bedrock piezometer 7 (BP7) to periods of mining.

The low summer water levels in the drift for 1991 and 1992 were probably accentuated by relatively low annual precipitation for these 2 years. Monitoring ceased 3.6 years after the piezometers were undermined.

The range of influence on drift piezometers ahead of mining can only be estimated due to the scarcity of early data. The effects of mining panel 2, which was adjacent to panel 1 instruments, were seen at 300 feet away, but no response was seen at 600 feet away. Because of the high conductivity and transmissivity of the drift aquifers, the earliest mining-induced changes may have been below the sensitivity of the transducers. Upward spikes seen in several drift hydrographs just before piezometer undermining have been attributed to the Noordbergum effect.

Bedrock water level response The bedrock piezometers, with the exception of BP4, were all placed in the Trivoli Sandstone. BP4 was placed in the underlying Gimlet Sandstone, 70 feet below the Trivoli Sandstone. These two sandstone units are separated from each other and from the bedrock surface by aquitards. The Trivoli Sandstone is continuous in the area and was noticeably argillaceous only at the bedrock control piezometer (BPC). The Gimlet Sandstone is also continuous in the area, but it is generally thinner. Bedrock water levels showed substantial changes during and after mining. Because recharge is very slow and seasonal precipitation doesn't influence them noticeably, the primary factor influencing bedrock water levels was the change in rock mass properties in proximity to mining. Each undamaged bedrock piezometer showed similar patterns, but most of the bedrock piezometers over panel 1 were damaged within 6 weeks of being undermined (appendix J). The hydrograph for bedrock piezometer 7 (BP7) is used to illustrate these patterns (fig. 46).

The easternmost piezometers (BP1 and BP2) were installed only a short time ahead of mining influences; BP1 showed fairly even water levels before the large drop, whereas BP2 showed a rise not due to rainfall before the large drop. Both piezometers were damaged as the mine face passed beneath them. Water levels probably dropped below both piezometers, judging from indications from piezometers farther west.

The next piezometer undermined, BP4, was the easternmost of the centerline cluster of instruments and the only piezometer in the deeper aquifer, the Gimlet Sandstone. BP4 also showed an early rise, followed by a decline ahead of undermining. During the steep decline in water level

(more than 110 ft), there was a decrease in slope in late November–early December, probably related to slow face advance. The level in BP4 dropped below the transducer, and soon thereafter the transducer stopped functioning.

BP3 was 100 feet north of the centerline instrument cluster and was set in the Trivoli Sandstone; it had a steep drop in level, similar to the other piezometers over the panel. The graphs of BP3 and a postsubsidence bedrock piezometer (BPPS) have been combined because they were constructed at the same depth range within the aquifer and are located near each other.

BP5, BP6, and BP7, all in the Trivoli Sandstone, were the only piezometers that were adjacent to mining and for which data records are relatively complete, reflecting the full initial drop. There are more than 2 years of postsubsidence water level measurements for BP7. BP5 and BP6 both showed abrupt 120-foot drops in the water level caused by undermining, and both show a decrease in slope during the drop caused by a pause in mining in late November. Less than 1 day after undermining the instrument cluster and monument line, longwall mining slowed to negligible advance for the 2 weeks during the Christmas/New Year's period (fig. 47). During this period, water in BP5 and BP6 rebounded 25 feet and 8 feet, respectively, but the levels dropped sharply again in early January when mining resumed apace. BP6, for example, recovered at the rate of 0.4 foot per day from December 19 to January 7 when mining averaged 1.0 foot per day, but then the water level dropped at a rate of 3 feet per day when rapid mining resumed. By mid-January, when the face was 300 feet beyond the piezometers, the water levels began to stabilize and rise slightly.

Bedrock piezometer 7 was placed over the chain pillars between panels 1 and 2. The details of the steep 100-foot drop in head were not recorded, but the hydrograph shows the same pattern of events as do the hydrographs for BP5 and BP6 in the period from mid-December to early February. BP7 water levels recovered at the rate of 0.23 foot per day from December 19 to January 7, but dropped at 2.2 feet per day when rapid mining resumed. From January 23 to 31, with the face 500 to 650 feet away from the piezometer, BP7 recovered at the rate of 0.84 foot per day as the face advanced at an average of 8.5 feet per day. This recovery suggests that, after the mining of panel 1, the range of influence for BP7 was less than 500 feet. Another 10-foot drop occurred in September 1990 as the second longwall panel passed less than 100 feet away; the water level stabilized soon after, at about 175 feet below ground surface. The bedrock control piezometer

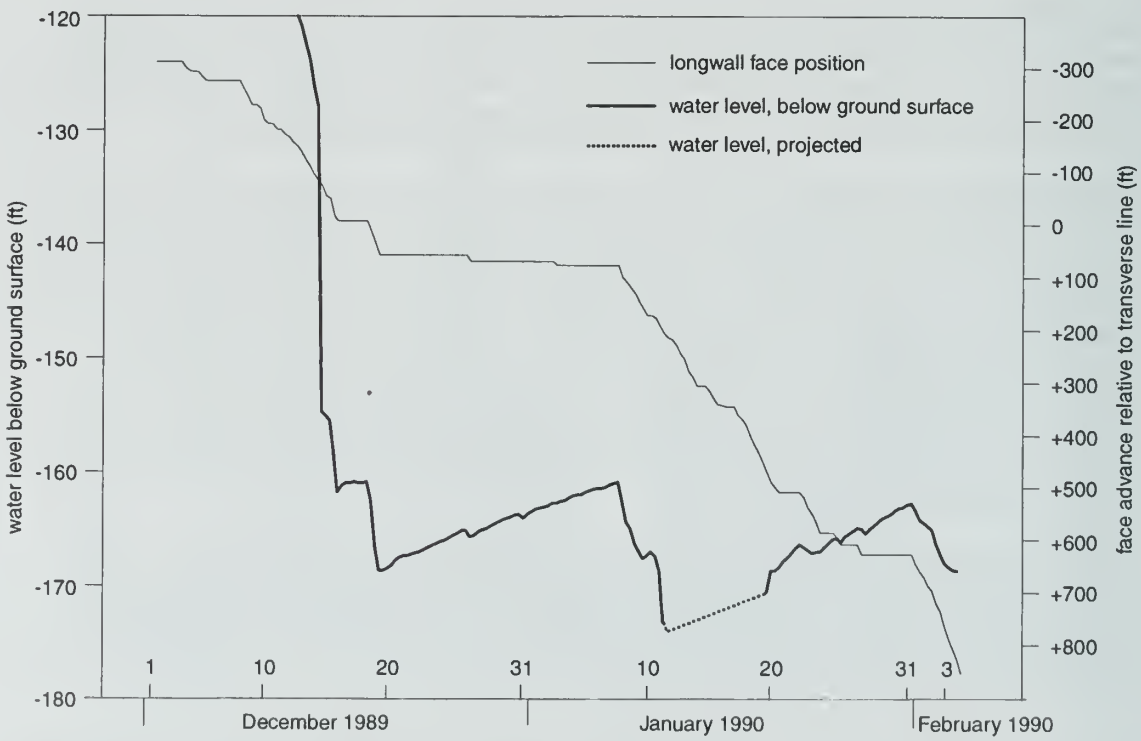

Figure 47 Detailed response of BP6 to the mine face advance.

(BPC) located north of panel 1 showed an initial drop of 60 feet as panel 1 passed, and it then showed a gradual decline until the spring of 1992, when it stabilized at about 130 feet below ground surface.

These piezometric drops associated with mining are produced by increased secondary porosity that is caused by the opening of new fractures and the widening of existing fractures associated with the tensile portion of the subsidence wave. After the ground surface goes through maximum slope change, the compressive part of the subsidence wave passes, partially closing the fractures. As the longwall face advance slows, reduced fracturing of the bedrock allows a limited rebound of the water level. While the compressive event may mark the beginning of water level stabilization in a general sense, levels may continue to decline below the center of the subsidence trough and possibly elsewhere (even away from the trough, as at BPC). This gentle decline is probably the result of continued (although increasingly distant) mining activity, which remains a source of drainage in the groundwater system. Examination of combined results suggests that the initial, mining-induced water-level drop within the panel was consistently greater than 120 feet. Furthermore, BPPS values were stabilized at about 170 feet below ground surface in 1992–1993, and the net drop in head was about 130 feet. There was no trend toward further recovery shown. The initial drop over the chain pillars (BP7) was 10 to 15 feet less, but a similar net drop of about 130 feet occurred after the second longwall panel was mined.

The range of influence ahead of mining for bedrock piezometers was considerably greater than was the case for drift piezometers. In the Trivoli Sandstone, declines in water levels occurred with the face at least 2,800 feet away. The greater sensitivity of the Trivoli Sandstone in the study area is apparently due to its relatively high conductivity and continuity combined with its relative thinness.

Aquifer characteristics Multiple methods were used to evaluate hydraulic properties of the drift and bedrock in general and the Trivoli and Gimlet Sandstones in particular. Straddle-packer tests were performed in the bedrock before and after subsidence, but there were substantial problems in comparing data from these two tests. Multiple slug and pump tests were performed in piezometers and the pump well; these tests were concentrated during and after, but not before, subsidence. Despite these problems, a general sense of the changes in hydraulic properties was obtained (table 4).

Table 4 Hydraulic conductivity values for study site piezometers (from A.M. Curtiss, Northern Illinois University, unpublished data).

Piezometer	Type of test	Date	Timing relative to mining of panels	Conductivity value (cm/s)	Unit
BPC	Slug	1/4/93	after 2	7.88×10^{-7}	Trivoli Ss
BP3	Slug	12/14/89	during 1	2.51×10^{-5}	Trivoli Ss
BPPS	Slug	3/11/91	after 1	2.72×10^{-5}	Trivoli Ss
BP4	Slug	8/25/89	before 1	4.82×10^{-5}	Gimlet Ss
BP4	Slug	11/8/89	before 1	4.01×10^{-5}	Gimlet Ss
BP6	Slug	8/25/89	before 1	4.70×10^{-5}	Trivoli Ss
BP6	Slug	11/8/89	before 1	4.65×10^{-5}	Trivoli Ss
BP6	Slug	12/14/89	during 1	4.56×10^{-5}	Trivoli Ss
BP7	Slug	12/14/89	during 1	2.33×10^{-5}	Trivoli Ss
BP7	Slug	5/23/90	after 1	3.55×10^{-5}	Trivoli Ss
BP7	Slug	3/11/91	after 2	6.35×10^{-5}	Trivoli Ss
DP1	Slug	3/11/91	after 2	3.34×10^{-4}	drift
DP1	Slug	1/2/93	after 2	8.69×10^{-4}	drift
DP2	Slug	1/2/93	after 2	2.33×10^{-3}	drift
DP2	Slug	1/5/93	after 2	1.50×10^{-3}	drift
DP3	Slug	1/2/93	after 2	2.26×10^{-3}	drift
PW1	Recovery	10/13/89	before 1	3.34×10^{-5}	Trivoli Ss
PW1	Recovery	10/14/89	before 1	4.27×10^{-5}	Trivoli Ss

The evaluation of the hydraulic properties of the drift was hindered by lack of presubsidence data. The postsubsidence conductivity values varied from 3×10^{-4} to 2×10^{-3} cm/s; values obtained from DP1 varied unexpectedly. It was unclear how the surface fractures that accompanied the advance of the subsidence wave would affect the long-term conductivity of the drift as a unit. The narrow subvertical openings seen at the surface extend at least 14 feet into the drift (Van Roosendaal et al. 1992a, b), increasing vertical water movement through increased dilatancy. In areas of maximum tension, fracturing may have increased vertical flow at the till/bedrock interface as well. From the sharp, short-term drop in water levels shown by the three drift piezometers over the panel, it seems likely that water moved downward in this manner between the initial surface fracturing and the substantial closure of the fractures at depth during the compressional event. The period these vertical pathways are open at depth is typically only 1 week (Van Roosendaal et al. 1992a, b). The continued rebound of DP1 and DP2 from the spring of 1990 onward indicates that little permanent change occurred to the drift aquifer.

Results of packer tests run in bedrock boreholes at the center of the panel before and after subsidence are discussed briefly in Booth and Spande (1991). The presubsidence borehole was so tight that it would not accept any take of water at typical test pressures. An apparent hydraulic conductivity of 6×10^{-6} cm/s for the fine grained upper portion of the Trivoli Sandstone was not maintained, and the authors suggest that this is a localized effect of the test. However, the medium grained lower portion of the Trivoli Sandstone and the upper half of the Gimlet Sandstone showed no uptake in presubsidence testing, suggesting that there may have been local mud caking or equipment problems as well. The conductivity of the shale-dominated intervals that act as aquitards is estimated to be less than 1×10^{-8} cm/s before subsidence.

Postsubsidence testing shows that conductivity values remained at about 1×10^{-6} cm/s for the Trivoli Sandstone. Shale units above the Trivoli Sandstone showed uptake at about 1×10^{-7} cm/s at higher pressures. This is clear evidence of fracturing because these units would not take any flow in the presubsidence tests.

Bedrock slug and pump tests were concentrated during and after mining (table 4); only six of these values were obtained before the mining of panel 1. A review of the presubsidence conductivity values for the Trivoli Sandstone over the panel shows a narrow range of values, from 3×10^{-5} to 5×10^{-5} cm/s. The low value of 8×10^{-8} cm/s at the control site north of the panel represents a siltstone-rich facies of the Trivoli Sandstone (A.M. Curtiss, NIU, unpublished data).

Comparative data for the same piezometer before and after mining exist only for BP7, located over the chain pillars between panels 1 and 2. Conductivity increased about 50% from the mining of panel 1 to after mining of panel 1. After mining of panel 2, the conductivity increased by an additional 80%. Conductivity was certainly lower before panel 1 was mined, so the total increase in conductivity might well have been 300% to 400% (table 4). It seems likely that greater increases in hydraulic conductivity occurred within the panel area, but these were probably not as high as conductivity values reported in the Jefferson County IMSRP study (Mehnert et al. 1994), in which conductivities increased a full order of magnitude in a sandstone aquifer.

BP4 was the only piezometer in the Gimlet Sandstone aquifer, about 70 feet below the Trivoli Sandstone. Because the piezometer was damaged during subsidence, no comparison was possible. Its initial conductivity was about 4×10^{-5} cm/s, similar to that of the Trivoli Sandstone, so similar increases due to subsidence would be expected.

The increased hydraulic conductivity in the mass of subsided bedrock was caused by at least two factors: (1) regularly distributed void space resulting from extension acting on existing joints and bedding planes (dilation of rock mass), and (2) development of new tensional and shear fractures.

The primary change to the two bedrock aquifers was an opening up of existing discontinuities, with development of new tensional and shear fracturing caused by the passing extensional wave. These changes significantly increased the bedrock's storativity, which accounts for the substantial water level drops in the upper bedrock registered by the piezometers.

INTEGRATION OF OBSERVATIONS

Active mining caused surface displacements that, independent of displacement direction, started when the panel face approached 250 feet away from any displacement-monitoring instruments and stopped after the face progressed 500 feet past the instruments. These conditions generated

a dynamic subsidence wave with a length of 750 feet. The panel roof was located at a depth of about 400 feet, and the ratio of wave length to panel depth was 1.875. About 85% of the total displacements were induced when the panel face was located between 100 feet away and 250 feet past the instruments. Subsidence, which developed at the centerlines of panels 1 and 2, ranged between 4.4 and 4.7 feet. At the edge of these panels, which were located 334 feet and 309 feet from the respective panel centerlines, the corresponding subsidences were 0.13 foot and 0.11 foot. Subsidence of 0.08 foot was recorded at the centerline of the chain pillar between panels 1 and 2; subsidence was 0.03 foot at the centerline between panels 2 and 3. Both centerlines were 66 feet from any panel edge.

The angle of draw was consistently 20°, for an average panel depth of 400 feet; the extent of the ground surface beyond the projection of the panel edge affected by the subsidence larger than 0.03 foot was less than 150 feet. Given the 150-foot limit and the fact that chain pillars cover a width of 132 feet between panels, it was concluded that only the first 18 feet from the panel edge experienced the effect of subsidence caused by the mining at an adjacent panel. A set of readings taken 71 days after the face of panel 2 had passed the monitoring station indicated that additional subsidence of 0.12 and 0.13 foot had developed at the edge of panel 1 and at the centerline of the chain pillars located between panels 1 and 2, respectively; there was no indication of any additional subsidence at the centerline of panel 1 or at the opposite edge of panel 1. Similarly, the effect of the mining of panel 3 on panel 2 resulted in an additional subsidence of 0.18 foot at the edge of panel 2 and 0.2 foot at the centerline of the chain pillars between panels 2 and 3. If it is assumed that the panel centerlines were not affected by the mining at adjacent panels, time-dependent subsidence of 0.11 foot occurred at panel 1 over a period of 18 months and subsidence of 0.12 foot occurred at panel 2 over a period of about 6 months.

Extensional changes in horizontal strains parallel to the mine direction at the ground surface were observed for the first 350 feet of the subsidence wave (i.e., 47% of the wave length); compressional changes in strains were recorded for the remaining 400 feet of the wave. The maximum extensional changes in strains (1.2% to 1.8%) and compressional changes (1.3% to 1.4%) occurred about 50 and 150 feet behind the mine face, respectively. At a distance of about 100 feet behind the mine face, where a transition zone between the extensional and compressional changes in strains was located (inflection point), a maximum longitudinal tilt of 2.5°, or 0.044 foot per foot, was measured. The corresponding change in strains at this point was zero.

Transverse to the mine direction, a symmetrical strain profile with respect to the panel centerline was recorded. At panel 1, extensional strains were measured to 86 feet outside of the panel edge. Extensional changes in strains were induced for the outer 180 feet of the strain profile, whereas the development of compressional changes in strains were recorded from the panel centerline to 240 feet past it. Maximum extensional increments in strains of 1.6% to 2.1% were generated at a distance of 54 feet inside of the panel edge, and maximum compressional changes of 1.3% to 1.5% were recorded at a distance of 134 feet. As would be expected, changes in horizontal strains approached zero at the panel centerline, which was also the axis of symmetry. At the extension zone, most of the changes in strains resulted in cracks with apertures of up to a few inches. Maximum tilt recorded on the transverse profile was 2.1° over panel 2.

The overburden rock mass ahead of the face remained intact up to the time when the panel face reached a distance of about 50 feet away from the MPBXs and TDR cable installed at the panel centerline. At this time, the corresponding vertical displacement at this location was approximately 1 foot. The development of fractures predominantly in shear then began and continued during the entire period of high rates of vertical displacements. The mine-induced fractures induced slight differential vertical settlements (extension) of as much as 0.15 foot. These differential settlements decreased to negligible values as the fractures closed as the panel face progressed to a distance of 500 feet past the instruments. Fractures were generated close to the contact between units with contrasting stiffness magnitude; the fractures detected by the TDR cable were more often located in the more flexible layer. Within the upper 86 feet of rock mass, five fractures were recorded by TDR cable, resulting in an average of one fracture every 17 feet. This mean value represents the lower limit of the number of fractures because more fractures probably developed after the TDR cable broke. During the period of high rates of subsidence, the minimum aperture of extensional fractures detected by the TDR cable was 20 mm (the instant of TDR cable breakage). Extensional fractures effectively control the changes in hydrogeologic characteristics of the overburden rock mass. There was an indication that compressional changes in vertical strains as high as 0.5% were induced in stiffer units, namely the Trivoli Sandstone and the Gimlet Sandstone,

which were located at depths of 172 to 195 feet and 265 to 282 feet, respectively. Predominantly shale units located between the two sandstone units and an 86-foot-thick drift experienced extensional changes in vertical strains of as much as 0.7% during the same period. The remaining units located over the panel showed no vertical strain development. Vertical strains decreased with time.

Drift water levels over the panel generally trended downward just ahead of undermining. The exact timing of water level changes due to mining is difficult to determine, however, because of a scarcity of reference water levels, the high variability of the drift water levels in general, and the presence of an upward spike on some hydrographs. Several of the hydrographs from piezometers over the panel showed an upward spike about 1 week before undermining, possibly due to the Noordbergum effect. The control drift piezometer showed no clear premining changes and little response to undermining; it was then in flowing artesian condition due to local factors for much of the study period.

All three drift piezometers over or adjacent to the panel showed a rapid drop of 8 to 11 feet related to the passing of the mine face. The compressional event caused temporary rises of water levels in the drift piezometers, but consistent recovery of water levels was not underway until 6 weeks after undermining. Mining of panel 2 demonstrated the limited range of water level changes in the drift; a piezometer 600 feet away did not respond, whereas those piezometers within 300 feet of panel 2 showed reactions to both tensile and compressional dynamic events. After subsidence effects finished, water level recovery continued but was strongly influenced by precipitation. Because of the high in situ hydraulic conductivity and transmissivity of the drift aquifers, the earliest changes induced by mining may have been below the sensitivity of the transducers.

Bedrock piezometer water levels declined well ahead of mining. In the Trivoli Sandstone, a decline in water levels, based on readings from the piezometer near the transverse line and confirmed by a similar pattern observed in other bedrock piezometers, occurred with the face at least 2,800 feet away (A.M. Curtiss, NIU, unpublished data). The likely reason for this high sensitivity of the Trivoli Sandstone is that it has high in situ hydraulic conductivity and is a thin, continuous unit. Transmissivity within the Trivoli is such that a small head loss will be evident because of slow lateral recharge.

SUMMARY AND CONCLUSIONS

By the time the mine face had advanced 500 feet past the monitoring station, the ratio of subsidence to mined-out height at the centerline of panel 1 had reached 70.5%; 18 months later, this ratio had increased slightly to 71.8%. The ratio was 66.3% when the face was about 1,900 feet past panel 2; additional subsidence in the next 6 months increased this ratio to 68.1%. In comparison, the ratio was 63% about 3 months after the undermining of panel 3 at the Jefferson County IMSRP overburden research site, which had a mined-out thickness of 8 to 9 feet. The ratio reached 70% about 36 months later. Both of the panels at the Saline County site were 400 feet deep; their width-to-depth ratios ranged from 1.55 to 1.67. Panel 3 in Jefferson County, however, was 617 feet wide and 720 feet deep, resulting in a width-to-depth ratio of 0.86.

Maximum dynamic horizontal tensile strains of about 0.018 foot per foot were generated at the ground surface 50 feet behind the panel face. This maximum change in strains was associated with a slope of 0.017 foot per foot. The maximum static horizontal tensile strains of 0.02 foot per foot and a corresponding slope of 0.037 foot per foot were induced 54 feet inside the panel edge.

Maximum changes in longitudinal dynamic slopes of about 2.5° (0.044 ft/ft) occurred at the centerline of panel 1 at an average distance of 85 feet behind the mine face. Maximum changes in transverse static slopes of about 2.4° (0.041 ft/ft) were generated at an average distance of 95 feet inside the edge of the panel.

A maximum rate of subsidence of 0.031 foot per hour (0.755 ft/day), under a rate of face advance of 1.4 feet per hour (33.5 ft/day), was measured at the centerline of panel 1 during the period in which the panel face advanced from 100 feet before to 250 feet past the transverse line. The transverse subsidence profile reflected this effect of rapid progressive subsidence by showing an asymmetric shape with respect to the panel centerline, as illustrated in figure 17 (face at +70 ft); this asymmetric subsidence is due to ongoing subsidence during the 3-hour survey of the transverse line.

The drift piezometers all showed a slight rise, due to the Noordbergum effect, as mining approached, followed by significant drops related to the period of maximum tensile strain resulting from undermining. Following these drops, the hydrographs exhibited small compressional rises (spikes). All of the drift piezometers were rebounding within 2 months of undermining. When monitoring ceased (3.6 years after the piezometers were undermined), levels had recovered to near premining levels and were expected to rise somewhat further.

The bedrock piezometers over the panel all showed initial water level drops of more than 120 feet. The rates of decline of piezometer levels respond closely with the rate of face advance. The bedrock piezometer over the chain pillars (between panels) did not initially decline as much (after the first panel was mined), but it dropped to a similar level when the adjacent panel was mined. The control bedrock piezometer showed a water level drop of 60 feet in response to the mining of the first panel but then showed further declines as the second and third panels were mined. These piezometric drops are produced by increased secondary porosity lower in the bedrock resulting from the opening of new fractures and the widening of existing fractures.

The lateral range of influence ahead of the advancing face for drift piezometers, as determined using hydrographs from continuous data, is more than 300 but less than 600 feet. The range of influence ahead of mining for bedrock piezometers was considerably farther than that for the drift piezometers. In the Trivoli Sandstone, declines in water levels occurred with the face at least 2,800 feet away. The greater sensitivity of the Trivoli Sandstone in the study area is apparently due to its relatively high conductivity and continuity combined with its relative thinness.

The evaluation of the hydraulic properties of the drift was hindered by a lack of presubsidence values, but the postsubsidence conductivity ranged from 3×10^{-4} to 2×10^{-3} cm/s. Short-term drops in water levels in the drift occurred in the period between tensional fracturing and compressional sealing, but little permanent change to the drift aquifer is thought to have occurred.

There were indications that substantial subsidence-induced increases in the hydraulic conductivity were produced in the bedrock units, despite the limited comparative data available because of damaged piezometers. Net increases in bedrock hydraulic conductivity resulting from the mining of multiple panels are thought to be on the order of 300% to 400%, but they may be somewhat higher. The increased hydraulic conductivity in the mass of subsided bedrock is caused by the dilation of the rock mass along existing joints and bedding planes as well as the development of new tensional and shear fractures. These changes significantly increased bedrock storativity, which accounts for the substantial water level drops registered by the piezometers in the upper bedrock.

RECOMMENDATIONS

This investigation at Saline County was the last of three overburden monitoring studies funded under the IMSRP contract. These studies provided valuable experience concerning useful data collection and performance of instrumentation within ground subsiding over high-extraction coal mining operations. These findings should be useful to other programs planned for similar settings.

Monuments and Benchmarks

Multiple benchmarks for control of the surveys should be placed in settings similar to the survey monuments. Also, the benchmarks should be constructed of the same materials and to the same dimensions as the survey monuments. These practices minimize the differential impacts of changing groundwater levels and weather conditions on benchmarks. In this study, total station surveys were used to document the three-dimensional changes in position of monuments or other instrumentation, but they were not used for precision level surveys for subsidence profile information.

Instrumentation that passes through the glacial overburden (soil) to monitor bedrock conditions should not be grouted with cement in the soil. A flexible bentonite grout should be used so that subsidence-induced movements do not damage instruments between the bedrock/soil interface and the ground surface.

Extensometer Readings

Both fiberglass and metal rod extensometers performed very well in characterizing the vertical strains associated with large subsidence movements. A sondex installation around the largest

inclinometer casing available produced vertical and horizontal readings until shear so deformed the instrumentation that no sondes could be lowered below a certain depth. Thus, the top of the casing must be used as a fixed reference. Coordinates of the top of the casing need to be taken with the total station survey every time the inclinometer is read.

Piezometers

Piezometers with automated data acquisition units allowed the documentation of extreme changes in the rate of water level fluctuations, which would have been missed by using a dropline. Also, these automated units documented water-level responses to short-term planned stoppage of mining. For a similar study, one should plan to redrill boreholes after subsidence and set new piezometers because many will break when large subsidence movements occur.

Time-domain Reflectometry Cable

TDR cables helped to document fracture locations and movement types (tensile versus shear) in the subsiding bedrock. The TDR data should be used along with extensometer and inclinometer/ sondex readings to produce a detailed picture of the rock mass response to subsidence.

Mined-out Height

The subsidence profile generated at the ground surface is very sensitive to the mined-out height (void) produced at the mine level. Accurate vertical measurements of the mined-out height are needed below subsidence monitoring lines. It is not accurate to use only coal thickness because the mining operations are not fixed in height, and additional roof rock is usually brought down during the mining operation.

Pre- and Postsubsidence Rock Mass Characterization

Bedrock characteristics were documented by using core logging as well as fracture descriptions, geophysical logs with in situ borehole seismic velocity measurements, laboratory rock strength testing, and in situ hydraulic conductivity testing through straddle-packer testing. Postsubsidence values were recorded in newly cored boreholes in the overburden. These boreholes were limited in depth because fracturing of the bedrock restricted drilling to less than the full depth of the previous boreholes. Pre- and postsubsidence boreholes should be located within 25% of the overburden thickness and aligned parallel to the mining direction to provide a reliable comparison of the core logs and testing data.

Tiltplates

Tiltplates provided measurements of angular distortions in three dimensions. These measurements have been shown to be consistent with measurements from survey monuments. Tiltplate data can be collected and analyzed more quickly than survey data. Both data should be used to supply backup information for the data interpretation.

ACKNOWLEDGMENTS

This report was prepared by the Engineering Geology Section of the Illinois State Geological Survey, Champaign, Illinois under USBM Cooperative Agreement CO267001. The Cooperative Agreement was initiated under the Illinois Mine Subsidence Research Program (IMSRP). It was administered under the technical direction of the U.S. Bureau of Mines, Twin Cities Research Center, with Larry Powell acting as Technical Project Officer. Kent Charles and Jose Martinez were the contract administrators for the Bureau of Mines. This report is a summary of the work completed as part of this contract during the period October 1, 1986, to September 30, 1993, and submitted to the USBM in August 1994.

The authors acknowledge the work of David F. Brutcher, Joseph T. Kelleher, and Christine E. Ovanic for their assistance in the field; Billy A. Trent assisted with manuscript preparation. The authors would also like to thank the landowners (Fanno and Rose Bledig, Carl Gates, Greg and Stephen Oglesby) and the mining company for their assistance and cooperation.

In addition to funding from the U.S. Bureau of Mines, the IMSRP also received funding from the Illinois Coal Development Board, under the administration of the Illinois Department of Natural Resources, Office of Coal Development and Marketing.

APPENDIXES

Available upon request as Open File Series 1997-9

REFERENCES

American Society for Testing and Materials, 1988, Annual Book of Standards, Section 4 Construction, Vol. 04.08 Soil and Rock, Building Stones, Geotextiles, 951 p.

Bauer, R.A., C.H. Dowding, D.J. Van Roosendaal, B.B. Mehnert, M.B. Su, and K. O'Connor, 1991, Application of Time Domain Reflectometry to Subsidence Monitoring: Final report to Office of Surface Mining, 48 p.; NTIS PB91-228411.

Bauer, R.A., and D.J. Van Roosendaal, 1992, Monitoring problems: Are we really measuring coal mine subsidence? *in* S.S. Peng, editor, Proceedings, Third Workshop on Surface Subsidence due to Underground Mining: West Virginia University, Morgantown, p. 332–338.

Booth, C.J., 1986, Strata-movement concepts and the hydrogeological impact of underground coal mining: Ground Water, v. 24, p. 507–515.

Booth, C.J., and E.D. Spande, 1991, Changes in hydraulic properties of strata over active longwall mining, Illinois, USA, *in* Proceedings, Fourth International Mine Water Congress, Pörtschach, Austria/Lubljana, Slovenia, September 1991, 12 p.

Booth, C.J., 1992, Hydrogeologic impacts of underground (longwall) mining in the Illinois Basin, *in* S.S. Peng, editor, Proceedings, Third Workshop on Surface Subsidence due to Underground Mining: West Virginia University, Morgantown, p. 222–227.

BPB Instruments, 1982, Field Instrumentation, Subsurface N.1, DD1, Dual Density, Gamma Ray, Caliper, Sonde, technical leaflet.

Brook, N., 1980, Technical note—Size correction for point load testing: International Journal of Rock Mechanics and Mining Sciences & Geomechanics Abstracts, v. 17, p. 231–235.

Brown, E.T., editor, 1981, Rock Characterization Testing and Monitoring: ISRM Suggested Methods. Commission on Testing Methods: International Society for Rock Mechanics: Pergamon Press, Oxford, New York, 211 p.

Cartwright, K., and C.S. Hunt, 1978, Hydrogeology of underground coal mines in Illinois: Illinois State Geological Survey reprint 1978-N, Reprinted from Proceedings, International Symposium on Water in Mining and Underground Works, Granada, Spain, September 17–22, 1978, 20 p.

Coe, C.J., and S.M. Stowe, 1984, Evaluating the impact of longwall coal mining on the hydrologic balance, *in* D.H. Graves, editor, Proceedings, 1984 Symposium on Surface Mining, Hydrology, Sedimentology, and Reclamation, December 2–7, 1984: University of Kentucky, Lexington, p. 395–403.

Conroy, P.J., 1980, Longwall coal mining: Dames and Moore Engineering Bulletin 52, p. 13–26.

Dowding, C.H., M.B. Su, and K. O'Connor, 1988, Principles of time domain reflectometry applied to measurement of rock mass deformation: International Journal of Rock Mechanics and Mining Sciences & Geomechanics Abstracts, v. 25, p. 287–297.

Dowding, C.H., M.B. Su, and K. O'Connor, 1989, Measurement of rock mass deformation with grouted coaxial antenna cables: Rock Mechanics and Rock Engineering, v. 22, p. 1–23.

Duigon, M.T., and M.J. Smigaj, 1985, First Report on the Hydrologic Effects of Underground Coal Mining in Southern Garrett County, Maryland: Maryland Geological Survey, Report of Investigations 41, 99 p.

Federal Geodetic Control Committee, 1984, Standards and Specifications for Geodetic Control Networks: Federal Geodetic Control Committee Rockville, MD, 34 p.

Forster, A., and D.M. McCann, 1979, Use of geophysical logging techniques in the determination of in-situ geotechnical parameters: Transactions of the 6th European Symposium of SPWLA, Paper G, 19 p.

Frye, J.C., A.B. Leonard, H.B. Willman, and H.D. Glass, 1972, Geology and Paleontology of Late Pleistocene Lake Saline, Southeastern Illinois: Illinois State Geological Survey Circular 471, 44 p.

Garritty, P., 1982, Water percolation into fully caved longwall faces, *in* Proceedings of the Symposium on Strata Mechanics, Newcastle-upon-Tyne: Developments in Geotechnical Engineering, v. 32, p. 25–29.

GeoTechnical Graphics, 1991, GeoTechnical Graphics System (GTGS) Software (version 3.1): Berkeley, CA.

Horberg, C.L., 1950, Bedrock Topography of Illinois: Illinois State Geological Survey Bulletin 73, 111 p.

Illinois State Water Survey, 1957, Potential Water Resources of Southern Illinois: Illinois State Water Survey, Report of Investigations 31, 97 p.

International Society for Rock Mechanics, 1985, Commission of Testing Methods, J.A. Franklin, coordinator: International Journal of Rock Mechanics and Mining Sciences & Geomechanics Abstracts, v. 22, p. 51–60.

Janes, J.R., 1983, A Demonstration of Longwall Mining—Final Report: Contract Report No. J0333949, U.S. Bureau of Mines, 105 p.

Leighton, M.M., G.E. Ekblaw, and C.L. Horberg, 1948, Physiographic Divisions of Illinois: Illinois State Geological Survey, Report of Investigations 129, 19 p.

Lynch, E.J., 1962, Formation Evaluation: Harper & Row, New York, 422 p.

MacClintock, P., 1929, Physiographic Divisions of the Area Covered by the Illinoian Driftsheet in Southern Illinois: Illinois State Geological Survey, Report of Investigations 19, 57 p.

Mehnert, B.B., D.J. Van Roosendaal, R.A. Bauer, P.J. DeMaris, and N. Kawamura, 1994, Final Report of Subsidence Investigations at the Rend Lake Site, Jefferson County, Illinois: Bureau of Mines, U.S. Department of the Interior, 237 p.

Ming-Gao, C., 1982, A study of the behavior of overlying strata in longwall mining and its application to strata control, *in* I.W. Farmer, editor, Proceedings of the Symposium on Strata Mechanics: Elsevier, New York, p. 13–17.

Nelson, W.J., and H.F. Krausse, 1981, The Cottage Grove Fault System in Southern Illinois: Illinois State Geological Survey Circular 522, 65 p.

New South Wales Coal Association, 1989, Mine Subsidence: A Community Information Booklet: Jointly published by New South Wales Coal Association, Department of Minerals and Energy, and the Mine Subsidence Board of Australia, September 1989, 32 p.

Nieto, A.S., 1979, Evaluation of damage potential to earth dam by subsurface coal mining at Rend Lake, Illinois, *in* Ohio River Valley Soils Seminar, Geotechnics of Mining: University of Kentucky, Lexington, October 5, 1979, p. 9–18.

Owili-Eger, A.S., 1983, Geohydrologic and hydrogeochemical impacts of longwall coal mining on local aquifers: Society of Mining Engineers of AIME Fall Meeting, Salt Lake City, UT, preprint No. 83-376, 16 p.

Pauvlik, C.M., and S.P. Esling, 1987, The effects of longwall mining subsidence on the groundwater conditions of a shallow, unconfined aquitard in southern Illinois, *in* Proceedings, National Symposium on Mining, Hydrology, Sedimentology, and Reclamation, Lexington, Kentucky, December 7–11, 1987, p. 189–195.

Peng, S.S., and H.S. Chiang, 1984, Longwall Mining: John Wiley, New York, 708 p.

Pennington, D., J.G. Hill, G.J. Burgdorf, and D.R. Price, 1984, Effects of Longwall Mine Subsidence on Overlying Aquifers in Western Pennsylvania: U.S. Bureau of Mines OFR 142-84, 129 p.

Pryor, W.A., 1956, Groundwater Geology in Southern Illinois—A Preliminary Geologic Report: Illinois State Geological Survey Circular 212, 25 p.

Seils, D.E., R.G. Darmody, and F.W. Simmons, 1992, The effects of coal mine subsidence on soil macroporosity and water flow, *in* R.E. Dunker, R.I. Barnhisel, and R.G. Darmody, editors, Proceedings, National Symposium on Prime Farmland Reclamation, Aug. 10–14: Department of Agronomy, University of Illinois at Urbana–Champaign, p. 137–145.

Sloan, P., and R.C. Warner, 1984, A case study of groundwater impact caused by underground mining, *in* D.H. Graves, editor, Proceedings, 1984 Symposium on Surface Mining, Hydrology, Sedimentology, and Reclamation, December 2–7, 1984, University of Kentucky, Lexington, p. 113–120.

Soil Conservation Service of the U.S. Department of Agriculture, 1978, Soil Survey of Saline County, Illinois: 94 p. plus 60 plates.

Soil Conservation Service of the U.S. Department of Agriculture, 1988, Soil Survey of Perry County, Illinois: 1988, 172 p. plus 66 plates.

Tandanand, S., and T. Triplett, 1987, New approach for determining ground tilt and strain due to subsidence, *in* Proceedings, National Symposium on Mining, Hydrology, Sedimentology, and Reclamation, University of Kentucky, p. 217–221.

Van Roosendaal, D.J., D.F. Brutcher, B.B. Mehnert, J.T. Kelleher, and R.A. Bauer, 1990, Overburden deformation and hydrologic changes due to longwall mine subsidence in Illinois, *in* Y.P. Chugh, editor, Proceedings of 3rd Conference on Ground Control Problems in the Illinois Coal Basin: Southern Illinois University at Carbondale, p. 73–82.

Van Roosendaal, D.J., B.B. Mehnert, J.T. Kelleher, and C.E. Ovanic, 1991, Three dimensional ground movements associated with longwall mine subsidence in Illinois, *in* Proceedings, Association of Engineering Geologists 34th Annual Meeting, Chicago, IL, 1991, p. 815–826.

Van Roosendaal, D.J., P.J. Carpenter, B.B. Mehnert, M.A. Johnston, and J.T. Kelleher, 1992a, Longwall mine subsidence of farmland in southern Illinois: near-surface fracturing and associated hydrogeological effects, *in* R.E. Dunker, R.I. Barnhisel, and R.G. Darmody, editors, Proceedings, National Symposium on Prime Farmland Reclamation, Aug. 10–14, Department of Agronomy, University of Illinois at Urbana–Champaign, p. 147–158.

Van Roosendaal, D.J., B.B. Mehnert, and R.A. Bauer, 1992b, Three-dimensional ground movements during dynamic subsidence of a longwall mine in Illinois, *in* S.S. Peng, editor, Proceedings, Third Workshop on Surface Subsidence due to Underground Mining, June 1–4, Department of Mining Engineering, West Virginia University, Morgantown, p. 290–298.

Verruijt, A., 1969, Flow through porous media: Chapter 8 in R.J.M. DeWiest, editor, Elastic Storage of Aquifers, Academic Press, New York, p. 331–376.

Whittaker, B.N., and D.J. Reddish, 1989, Subsidence: Occurrence, Prediction and Control: Developments in Geotechnical Engineering, 56: Elsevier, New York, 528 p.

Whitworth, K.R., 1982, Induced changes in permeability of coal measure strata as an indicator of the mechanics of rock deformation above a longwall coal face, *in* I.W. Farmer, editor, Proceedings of the Symposium on Strata Mechanics: Elsevier, New York, p. 18–24.